Title
Understanding the Roles of Non-Coding Sequences in Heterochromatin Assembly in Fission Yeast

Permalink
https://escholarship.org/uc/item/7t9119v8

Author
Marina, Diana Bahrani

Publication Date
2012

Peer reviewed|Thesis/dissertation

**Understanding the Roles of Non-Coding Sequences in
Heterochromatin Assembly in Fission Yeast**

by

Diana Bahrani Marina

DISSERTATION

Submitted in partial satisfaction of the requirements for the degree of

DOCTOR OF PHILOSOPHY

in

Biochemistry and Molecular Biology

in the

GRADUATE DIVISION

of the

UNIVERSITY OF CALIFORNIA, SAN FRANCISCO

Acknowledgments

This work would not have been possible without the support of many people. I would like to thank my thesis advisor, Hiten Madhani, for all of his scientific support and guidance in the course of this study. I very much appreciate the thoughtful feedback, comments and advice given by members of my thesis committee: Geeta Narlikar and Barbara Panning. I would also like to thank the current and past members of the Madhani Lab for their professional and personal support. I am indebted to my wonderful parents and siblings for their continuous support and everlasting love. Finally, I would like to thank my husband, Bernd, who has been nothing but patient, caring and supportive through my ups and downs in graduate school.

Understanding the Roles of Non-Coding Sequences in Heterochromatin

Assembly in Fission Yeast

by

Diana Bahrani Marina

ABSTRACT

In eukaryotic cells, genomic DNA is packaged with histones to form chromatin. While euchromatin is found in gene-rich regions of the genome, heterochromatin is associated with centromeres and telomeres that are gene-poor, transcriptionally less active and contain high densities of repetitive non-coding DNA sequences. The structural component of heterochromatin consists of unique proteins that bind to distinct histone tail modifications. This structure serves important cellular functions that include regulating gene expression and maintaining chromosomal integrity. Despite extensive research, there remain many unanswered questions about how heterochromatic structures are assembled.

The overall goal of this study is to gain a better understanding of how heterochromatin assembles in fission yeast. More specifically, we are interested in the basic question: what determines where heterochromatin forms? We hypothesized that non-coding DNA sequences embedded in heterochromatin play crucial roles in specifying where heterochromatin forms. To test this hypothesis, we dissected these non-coding sequences and we investigated the roles of some protein factors bound to them. The findings of this study are

divided into 3 chapters.

Chapter II of this dissertation describes a systematic study to identify DNA sequences that are sufficient to nucleate heterochromatin. In this study, we developed an ectopic heterochromatic reporter construct to dissect heterochromatic sequences and to test their capability in inducing heterochromatin formation at a given locus. Using this construct, we found that several large DNA fragments from pericentromeric regions are able to induce ectopic heterochromatin formation. Furthermore, we found a unique hexameric DNA motif that is necessary but not sufficient for heterochromatin formation.

In chapter III, we describe a novel protein player in heterochromatin assembly. This protein, Seb1, binds specifically to non-coding RNAs that are transcribed from heterochromatic regions. Using genetic and biochemical tools, we demonstrate that Seb1 directs heterochromatin formation by recruiting several chromatin-modifying enzymes to heterochromatic regions.

Finally, in chapter IV we describe the role of heterochromatic transcript polyadenylation in heterochromatin assembly. By investigating the functions of a poly(A)-binding protein and a putative deadenylase, we found that polyadenylation of heterochromatic transcripts inhibits heterochromatin formation. Together, the results of this study shed new light on mechanisms of heterochromatin assembly.

Table of Contents

List of Tables

List of Figures

Chapter I: General Introduction

In eukaryotic cells, long strands of genomic DNA need to fit into a very small nucleus. At the same time, the DNA has to be easily accessible for critical cellular processes such as replication and transcription. Therefore, genomic DNA needs to be tightly compacted in an orderly fashion inside the nucleus. To achieve this specialized form of packaging, the cell utilizes unique DNA-compacting proteins called histones. Approximately 146 bp of DNA is wrapped around an octamer of histones consisting of 4 pairs of core histones (histones H2A, H2B, H3 and H4) (Luger, Mader, Richmond, Sargent, & Richmond, 1997). This basic unit of DNA-protein packaging is called the nucleosome. Nucleosomes form the elemental repeating units of chromatin, a complex association of genomic DNA and proteins.

Heterochromatin and its characteristics

In the 1920's, a German botanist named Emil Heitz who studied chromosomes of moss plants first described the 2 distinct forms of chromatin based on their different cytological staining characteristics (Passarge, 1979). Heitz coined the terms: euchromatin and heterochromatin to refer to these 2 types of chromatin. Euchromatin is lightly stained and is not compacted during interphase while heterochromatin is darkly stained and remains highly condensed throughout the cell cycle (Passarge, 1979). Subsequent studies revealed that euchromatin is highly transcribed and is associated with gene-rich

regions of the genome. On the other hand, heterochromatin is transcriptionally less active and is mostly found at gene-poor centromeres and telomeres that consist of high densities of repetitive DNA sequences and transposable elements (Grewal & Jia, 2007).

Although first identified cytologically, euchromatin and heterochromatin are now characterized by their distinct histone tail modifications. Euchromatin is associated with hyperacetylated histone tails while hallmarks of heterochromatin include hypoacetylation of histone tails and methylation of histone H3 at lysine 9 (H3K9Me) (Grewal & Jia, 2007). The H3K9 methyl mark serves as a binding platform for the conserved family of HP1 proteins that make up the structural component of heterochromatin (Bannister et al., 2001; Lachner, O'Carroll, Rea, Mechtler, & Jenuwein, 2001; Nakayama, Rice, Strahl, Allis, & Grewal, 2001). These histone tail modifications are carried out by chromatin-modifying enzymes that include histone acetyltransferases (HATs), histone deacetylases (HDACs) and histone methyltransferases (HMTs). Both HDACs and HMTs are recruited to the heterochromatic loci of the genome by various mechanisms involving DNA- and RNA-binding proteins described below (Grewal & Jia, 2007).

While initially viewed as a region with 'junk' DNA without significant biological function, it is now apparent that heterochromatin serves several important roles in the cell. For example, at centromeres heterochromatin is required to ensure proper segregation of chromosomes during cell division

(Henikoff, 2000). At telomeres, heterochromatin prevents chromosome degradation and aberrant chromosomal fusion (Buhler & Gasser, 2009). Heterochromatin also serves to repress transcription and to suppress recombination of repetitive, non-coding DNA sequences (Henikoff, 2000). Additionally, heterochromatin also regulates gene expression. Active genes inserted in or near heterochromatic regions are transcriptionally repressed or silenced (Allshire, Javerzat, Redhead, & Cranston, 1994). Interestingly, the silent state of these genes is clonally inherited. This gene silencing phenomenon is called the Position Effect Variegation (PEV) (Buhler & Gasser, 2009). PEV is universally conserved across eukaryotes but it was first reported in 1930 by Hermann Muller who studied radiation-induced chromosomal rearrangement in *Drosophila*.

Given that heterochromatin is required for critical functions in the cell, it is not surprising that numerous human diseases such as cancer and heart disease are associated with aberrant heterochromatin (Henikoff, 2000). It is therefore crucial to have a good understanding of how heterochromatin formation occurs in the cell. The overall goal of this dissertation study is to gain a better understanding of heterochromatin assembly process. More specifically, this study addresses the basic question: What specifies where heterochromatin forms? We hypothesized that non-coding DNA sequences embedded in heterochromatin play crucial roles in recruiting chromatin-modifying enzymes to specify heterochromatin. To test this hypothesis, we employed 2 different strategies:

First, we dissected the non-coding sequences embedded in heterochromatin and determined minimum sequences necessary for heterochromatin assembly. Second, we investigated the roles of several proteins that bind specifically to these non-coding sequences in heterochromatin formation.

Heterochromatin formation in the fission yeast *Schizosaccharomyces pombe*

In this study, the fission yeast *Schizosaccharomyces pombe (S. pombe)* is used as a model organism to understand the complex and multistep process of heterochromatin assembly. *S. pombe* is a good model system for this purpose due to several reasons: First, *S. pombe* is easy to grow and it is genetically tractable. Second, there are conserved pathways of heterochromatin formation between *S. pombe* and higher eukaryotes including human (Grewal & Jia, 2007). Additionally, despite having a relatively small genome with only 3 chromosomes, *S. pombe* has large regions in its genome that are associated with heterochromatin. The main heterochromatic regions of *S. pombe* are the pericentromeric repeats, the subtelomeric regions and the silent mating-type locus (Grewal & Jia, 2007).

Heterochromatic regions of *S. pombe*

The centromeres of *S. pombe* consist of a central core (*cnt*) domain surrounded by large arrays of non-coding, inverted repeats called the innermost repeats (*imr)* and the outer repeats (*otr*) (Wood et al., 2002). Heterochromatic

marks are found in the entire *otr* region and in a small part of the *imr* region (Cam et al., 2005). While the sequence of the *imr* region is unique to each of the 3 centromeres, the *otr* region can be further divided into the *dg* and *dh* repeats that are found in all 3 centromeres (Wood et al., 2002). The copy number of the *dg* and *dh* repeats varies between centromeres and between laboratory isolates (Steiner, Hahnenberger, & Clarke, 1993). For example, in the most common laboratory isolate of *S. pombe,* the smallest centromere (*cenI*) has 2 copies of *dg* and *dh*, while the largest centromere (*cenIII*) has 6 copies of each repeat (Wood et al., 2002). The *otr* regions are flanked by tRNA genes and IRC inverted repeats that serve as boundary elements separating heterochromatic pericentromeres from the surrounding euchromatic domains (Grewal & Jia, 2007).

The mating-type locus of *S. pombe* is located on chromosome II. It contains 3 genes: *mat1, mat2* and *mat3.* While *mat1* gene is transcriptionally active and determines the mating type of the cell, *mat2* and *mat3* genes are silenced by heterochromatic marks that coat the entire 20-kb domain surrounded by inverted repeat (IR) boundaries (Noma, Allis, & Grewal, 2001). Between *mat2* and *mat3* genes, there is a DNA sequence called the *cenH* element. This element is 4.3-kb long and it shares sequence homology with the pericentromeric *dg* and *dh* repeats (Grewal & Klar, 1997). Between *cenH* and *mat3* loci, there is another DNA element called *REIII* that also contributes to heterochromatin nucleation. The *REIII* element contains 2 ATGACGT heptamers that serve as

binding sites for stress-activated transcription factors Atf1 and Pcr1, which recruit chromatin-modifying enzymes to this locus (Jia, Noma, & Grewal, 2004).

Heterochromatic marks are also found in the subtelomeric regions of *S. pombe.* Interestingly, the subtelomeric regions of chromosomes I and II contain open reading frames (ORFs) of putative helicase genes *tlh1+* and *tlh2+*. These helicases are members of the conserved RecQ family and their ORFs are homologous to the *dh* repeats found in the *otr* region of pericentromeres (Mandell, Goodrich, Bahler, & Cech, 2005). Therefore, all heterochromatic domains in *S. pombe* share a common sequence that contains the *dg* and *dh* repeats. Studies have shown that these repeats are sufficient to form heterochromatin at ectopic loci (Partridge, Scott, Bannister, Kouzarides, & Allshire, 2002).

Chapter II of this dissertation describes a systematic analysis of the *dg* and *dh* repeats of centromere I to identify sequences sufficient to induce heterochromatin at an ectopic location. We found that several large fragments (approximately 2-3 kb in length) derived from both *dg* and *dh* repeats are sufficient to cause heterochromatic silencing at the endogenous *ura4+* locus. The heterochromatic silencing induced by these fragments is gradually lost as larger regions are deleted, suggesting the existence of numerous, weak distributed signals required for silencing. Furthermore, we demonstrate that the *REIII* element of the silent mating-type locus is able to induce heterochromatic

silencing at the *ura4+* locus when combined with small fragments (as small as 200 bp) from the pericentromeric *dh* repeats that are too small to induce silencing on their own. We also identified a unique hexameric AAYATG motif that is necessary to induce heterochromatic silencing at the *ura4+* locus. The AAYATG sequence is present as tandem repeats in the *dh* region. It is currently unknown how this sequence motif contributes to heterochromatin assembly. We postulate that it serves as a binding site for protein factors required for heterochromatin formation.

Mechanisms of heterochromatin nucleation in *S. pombe*

In *S. pombe,* multiple pathways of heterochromatin formation have been described (Grewal & Jia, 2007; Reyes-Turcu & Grewal, 2012). All pathways ultimately lead to the recruitment of HDACs and HMTs to heterochromatic loci to deacetylate and methylate histone tails, respectively. These pathways can be grouped into 2 main categories: DNA-dependent and RNA-dependent pathways of heterochromatin assembly. The DNA-dependent pathways are mediated by DNA-binding proteins that can further recruit chromatin-modifying enzymes to nucleate heterochromatin. These DNA-binding factors function by recognizing specific sequence motifs at heterochromatic loci. The RNA-dependent pathways of heterochromatin assembly are mediated by non-coding RNAs (ncRNAs) transcribed from the *dg* and *dh* repeats. The most studied RNA-dependent pathway is mediated by RNA interference (RNAi). The RNAi machinery processes the *dg* and *dh* ncRNAs to generate small interfering RNAs (siRNAs)

that induce post-transcriptional silencing of the *dg* and *dh* ncRNAs when bound

by the Argonaute protein Ago1 (Lejeune & Allshire, 2011; Verdel, Vavasseur, Le

Gorrec, & Touat-Todeschini, 2009). siRNAs bound by Ago1 also mediate the

recruitment of chromatin-modifying enzymes to assemble heterochromatin at the

dg and *dh* repeats, thereby inducing transcriptional silencing at these repeats

(Bayne et al., 2010; Verdel et al., 2004).

Heterochromatin nucleation by DNA-binding proteins

Examples of DNA-binding factors that nucleate heterochromatin can be

found at the silent mating-type locus. Here, two transcription factors, Atf1 and

Pcr1, bind to two ATGACGT heptamers that are present at the *REIII* element (Jia

et al., 2004). These factors further recruit the HDAC Clr3 to the silent mating-type

locus (Yamada, Fischle, Sugiyama, Allis, & Grewal, 2005). Clr3 is required to

deacetylate histone H3 at lysine 14 (H3K14) (Nakayama et al., 2001). H3K14

deacetylation by Clr3 is necessary to promote H3K9Me by Clr4, the only H3K9

methyltransferase in *S. pombe* (Nakayama et al., 2001)*.* Clr3 also functions to

limit RNA Polymerase II (PolII) occupancy at heterochromatin (Sugiyama et al.,

2007).

Another example of DNA-based mechanisms of heterochromatin

assembly is observed at subtelomeric regions. The telomeric DNA-binding

protein Taz1 also recruits Clr3 to subtelomeric regions by recognizing a specific

DNA motif (Buhler & Gasser, 2009; Kanoh, Sadaie, Urano, & Ishikawa, 2005;

Sugiyama et al., 2007). Both DNA-dependent pathways at the silent mating-type locus and at subtelomeres function redundantly with RNAi-based mechanism (described below) to nucleate heterochromatin at these loci.

At pericentromeres, 3 DNA-binding proteins (Abp1, Cbh1 and Cbh2) that are homologous to human CENP-B protein contribute to heterochromatin assembly by recruiting Swi6, the *S. pombe* HP1 homolog (Nakagawa et al., 2002). In human, CENP-B is a sequence-specific DNA-binding protein that binds to a specific motif present at the inner centromere (Masumoto, Masukata, Muro, Nozaki, & Okazaki, 1989; Muro et al., 1992; Yoda, Kitagawa, Masumoto, Muro, & Okazaki, 1992). The binding of CENP-B dimers to centromeres is required for proper kinetochore formation (Masumoto et al., 1989; Muro et al., 1992; Yoda et al., 1992). It is postulated that these CENP-B homologs recruit HDACs and HMTs to their binding sites (Nakagawa et al., 2002) but the exact mechanism by which these DNA-binding proteins promote heterochromatin assembly is still obscure.

Heterochromatin assembly by RNA-dependent mechanisms

In addition to DNA-binding factors, heterochromatin assembly in *S. pombe* also requires RNAs and RNA processing factors (Reyes-Turcu & Grewal, 2012). These RNAs are generated by transcription of the *dg* and *dh* repeats by RNA Polymerase II (PolII) in the S phase of the cell cycle (Chen et al., 2008; Djupedal et al., 2005; Kato et al., 2005; Kloc, Zaratiegui, Nora, & Martienssen, 2008). The

non-coding *dg* and *dh* transcripts become substrates for the RNA-interference

(RNAi) machinery that produces small interfering RNAs (siRNAs) by the

combined action of Dicer (Dcr1) and the RNA-directed RNA Polymerase complex

(RDRC) (Lejeune & Allshire, 2011; Verdel et al., 2009). The siRNAs are bound

by Argonaute (Ago1), a subunit of the RNA- induced transcriptional silencing

(RITS) complex (Verdel et al., 2004). The RITS complex promotes both post-

transcriptional degradation of the *dg* and *dh* transcripts and transcriptional

silencing by recruiting the Clr4 methyltransferase complex (CLRC) (Bayne et al.,

2010; Noma et al., 2004). A protein scaffold called Stc1 mediates the interaction

between the RITS and CLRC complexes, thereby coupling RNAi to

heterochromatin (Bayne et al., 2010). Clr4 is the only HMT that catalyzes the

methylation of histone H3 at lysine 9 (H3K9Me), a distinct hallmark of

heterochromatin (Nakayama et al., 2001; Zhang, Mosch, Fischle, & Grewal,

2008). This methyl mark is bound by chromodomains of HP1 proteins, Swi6 and

Chp2 (Bannister et al., 2001; Fischer et al., 2009; Thon & Verhein-Hansen,

2000). Both proteins further recruit the histone deacetylase Clr3 to hypoacetylate

histone tails (Sadaie et al., 2008; Sugiyama et al., 2007). Clr3 functions in a

chromatin-modifying complex called SHREC (Snf2-HDAC repressor complex)

(Sugiyama et al., 2007). In addition to Clr3, this complex includes silencing

factors Clr1 and Clr2 and the putative chromatin-remodeling enzyme Mit1

(Sugiyama et al., 2007). SHREC limits PolII occupancy at heterochromatin,

thereby contributing to transcriptional silencing (Sugiyama et al., 2007). Since the

dg and *dh* repeats serve as substrates for RNAi, it is not surprising that the RNAi-

dependent pathway of heterochromatin formation is observed at all three

heterochromatic loci in *S. pombe* that contain these repeats. Despite active

research, the exact sequence of RNAi-dependent events that lead to

heterochromatin assembly is still obscure.

Although RNAi plays a major role in heterochromatin assembly, mutations

in the RNAi pathway do not completely abolish H3K9Me indicating the existence

of RNAi-independent pathways (Sadaie, Iida, Urano, & Nakayama, 2004). A

recent study has uncovered an RNAi-independent pathway in heterochromatin

assembly that involves RNA processing factors Mlo3 and Cid14 (Reyes-Turcu,

Zhang, Zofall, Chen, & Grewal, 2011). Cells lacking these factors are able to

assemble functional pericentromeric heterochromatin in the absence of RNAi

(Reyes-Turcu et al., 2011). Mlo3 is involved in both mRNP biogenesis and RNA

quality control with Cid14 (Zhang et al., 2011). Cid14 is a non-canonical poly(A)

polymerase that belongs to the TRAMP complex (Buhler, Haas, Gygi, & Moazed,

2007). TRAMP functions primarily in the nuclear RNA quality control by

recognizing aberrant RNAs and channels them to the exosome for degradation

(Houseley, LaCava, & Tollervey, 2006; LaCava et al., 2005). While the exact

mechanism of this pathway is still unknown, it is postulated that in the absence of

both RNAi and Mlo3-TRAMP, the unprocessed ncRNAs might form specific RNA

structures that can be recognized by CLRC, the H3K9 methyltransferase

complex (Reyes-Turcu & Grewal, 2012).

Chapter III of this dissertation describes a novel RNAi-independent but RNA-dependent pathway in heterochromatin nucleation at pericentromeres. This pathway is mediated by a conserved ncRNA-binding protein called Seb1. We demonstrate that Seb1 binds to pericentromeric *dg* and *dh* ncRNAs and it recruits the chromatin-modifying complex, SHREC to pericentromeres. We postulate that Seb1 recognizes a specific sequence motif overrepresented in the *dg* and *dh* ncRNAs and it acts as a specificity factor that triggers heterochromatin formation.

Chapter IV of this dissertation describes the role of pericentromeric transcript polyadenylation in heterochromatic silencing. More specifically, in this chapter, we describe and test a model for pericentromeric transcript recognition by 2 competing RNA-processing machineries: RNAi and the nuclear exosome. We hypothesize that Pab2, a poly(A)-binding protein and Dfs1, a putative deadenylase play major roles in targeting pericentromeric transcripts to each RNA-processing pathway. Pab2 is a nuclear poly(A)-binding protein that functions with the nuclear exosome to process non-coding snoRNAs (Lemay et al., 2010). We demonstrate that cells lacking Pab2 have increased heterochromatic silencing. We postulate that Pab2 binds to polyadenylated pericentromeric transcripts and targets these transcripts to the nuclear exosome thereby limiting the processing of these transcripts by RNAi. On the other hand, deletion of *dfs1+* causes loss of heterochromatic silencing. We hypothesize that deadenylation of pericentromeric transcripts by Dfs1 is required for processing of

these transcripts by RNAi. In this chapter, we present and discuss several experimental results that are supportive of this model. Overall, results obtained in this dissertation study shed new light on the mechanisms of heterochromatin assembly in *S. pombe.*

Summary for a Lay Audience

The nucleus of a cell is a very crowded place. In human cells for example, the average nucleus is less than 2 micrometers in diameter. However, it contains more than 3.4 billion base pairs of DNA, which would extend close to 2 meters if stretched out in a line. This extremely tight packaging of DNA inside the nucleus is made possible by the association of DNA with specialized proteins to form a structure called chromatin. The term 'chromatin' meaning 'stainable material' was first coined by German biologist Walther Flemming who studied cell division in the middle of the 19th century. Over 50 years later in the 1920's, a botanist named Emil Heitz recognized that there are 2 types of chromatin that show different characteristics when stained with an appropriate dye. Heitz named these 2 forms of chromatin: euchromatin and heterochromatin. Euchromatin refers to the lightly stained and less condensed part of chromatin while heterochromatin represents the darkly stained and highly compacted part. Numerous studies in the next few decades revealed that euchromatin is associated with gene-rich regions in the genome while heterochromatin is mostly gene-poor. Because heterochromatin lacks genes, it was initially thought to contain 'junk' DNA and to have little biological significance. However, after

decades of study, it is now apparent that heterochromatin has a number of critical functions in the cell. For example, heterochromatin is required to maintain the structural integrity of chromosomes. It also plays a pivotal role in regulating gene expression, i.e. controlling how genes are turned ON or OFF. Misregulation of gene expression can lead to various diseases. In fact, numerous human diseases such as cancer and heart diseases are associated with abnormal heterochromatin. Therefore, it is crucial to have a good understanding of how heterochromatin assembles in the nucleus.

For my doctoral dissertation research, I studied how heterochromatin forms inside the nucleus of the fission yeast *Schizosaccharomyces pombe* (*S. pombe*). Yeast is a microscopic, single-celled organism that is commonly used to make bread and beer. The fission yeast is a good model organism to study because it is easy to grow and cultivate and it is possible to create mutations in its genome. Moreover, many of yeast cellular processes including heterochromatin assembly resemble processes observed in human cells. This study investigated the role of the so-called 'junk' DNA embedded within heterochromatin in recruiting proteins that are required for its assembly. This study also identified new protein players that have important roles in heterochromatin formation. The hope is that the basic knowledge gained in this study contributes to the greater understanding of how cells work. This understanding is crucial in the advancement of diagnosis, treatment and prevention of human diseases.

REFERENCES

Allshire, R. C., Javerzat, J. P., Redhead, N. J., & Cranston, G. (1994). Position effect variegation at fission yeast centromeres. [Research Support, Non-U.S. Gov't

Research Support, U.S. Gov't, P.H.S.]. *Cell, 76*(1), 157-169.

Bannister, A. J., Zegerman, P., Partridge, J. F., Miska, E. A., Thomas, J. O., Allshire, R. C., & Kouzarides, T. (2001). Selective recognition of methylated lysine 9 on histone H3 by the HP1 chromo domain. *Nature, 410*(6824), 120-124.

Bayne, E. H., White, S. A., Kagansky, A., Bijos, D. A., Sanchez-Pulido, L., Hoe, K. L., . . . Allshire, R. C. (2010). Stc1: a critical link between RNAi and chromatin modification required for heterochromatin integrity. [Research Support, Non-U.S. Gov't]. *Cell, 140*(5), 666-677. doi: S0092-8674(10)00073-5 [pii]

10.1016/j.cell.2010.01.038

Buhler, M., & Gasser, S. M. (2009). Silent chromatin at the middle and ends: lessons from yeasts. [Review]. *EMBO J, 28*(15), 2149-2161. doi: 10.1038/emboj.2009.185

Buhler, M., Haas, W., Gygi, S. P., & Moazed, D. (2007). RNAi-dependent and -independent RNA turnover mechanisms contribute to heterochromatic gene silencing. *Cell, 129*(4), 707-721. doi: S0092-8674(07)00454-0 [pii]

10.1016/j.cell.2007.03.038

Cam, H. P., Sugiyama, T., Chen, E. S., Chen, X., FitzGerald, P. C., & Grewal, S. I. (2005). Comprehensive analysis of heterochromatin- and RNAi-mediated epigenetic control of the fission yeast genome. *Nat Genet, 37*(8), 809-819. doi: 10.1038/ng1602

Chen, E. S., Zhang, K., Nicolas, E., Cam, H. P., Zofall, M., & Grewal, S. I. (2008). Cell cycle control of centromeric repeat transcription and heterochromatin assembly. *Nature, 451*(7179), 734-737. doi: nature06561 [pii]

10.1038/nature06561

Djupedal, I., Portoso, M., Spahr, H., Bonilla, C., Gustafsson, C. M., Allshire, R. C., & Ekwall, K. (2005). RNA Pol II subunit Rpb7 promotes centromeric transcription and RNAi-directed chromatin silencing. *Genes Dev, 19*(19), 2301-2306. doi: 19/19/2301 [pii]

10.1101/gad.344205

Fischer, T., Cui, B., Dhakshnamoorthy, J., Zhou, M., Rubin, C., Zofall, M., . . . Grewal, S. I. (2009). Diverse roles of HP1 proteins in heterochromatin assembly and functions in fission yeast. [Research Support, N.I.H., Intramural]. *Proc Natl Acad Sci U S A, 106*(22), 8998-9003. doi: 10.1073/pnas.0813063106

Grewal, S. I., & Jia, S. (2007). Heterochromatin revisited. [Research Support, N.I.H., Intramural

Review]. *Nat Rev Genet, 8*(1), 35-46. doi: 10.1038/nrg2008

Grewal, S. I., & Klar, A. J. (1997). A recombinationally repressed region between mat2 and mat3 loci shares homology to centromeric repeats and regulates directionality of mating-type switching in fission yeast. [Comparative Study Research Support, U.S. Gov't, P.H.S.]. *Genetics, 146*(4), 1221-1238.

Henikoff, S. (2000). Heterochromatin function in complex genomes. [Review]. *Biochim Biophys Acta, 1470*(1), O1-8.

Houseley, J., LaCava, J., & Tollervey, D. (2006). RNA-quality control by the exosome. [Review]. *Nat Rev Mol Cell Biol, 7*(7), 529-539. doi: 10.1038/nrm1964

Jia, S., Noma, K., & Grewal, S. I. (2004). RNAi-independent heterochromatin nucleation by the stress-activated ATF/CREB family proteins. *Science, 304*(5679), 1971-1976.

Kanoh, J., Sadaie, M., Urano, T., & Ishikawa, F. (2005). Telomere binding protein Taz1 establishes Swi6 heterochromatin independently of RNAi at telomeres. *Curr Biol, 15*(20), 1808-1819.

Kato, H., Goto, D. B., Martienssen, R. A., Urano, T., Furukawa, K., & Murakami, Y. (2005). RNA polymerase II is required for RNAi-dependent heterochromatin assembly. *Science, 309*(5733), 467-469. doi: 1114955 [pii]
10.1126/science.1114955

Kloc, A., Zaratiegui, M., Nora, E., & Martienssen, R. (2008). RNA interference guides histone modification during the S phase of chromosomal replication. *Curr Biol, 18*(7), 490-495. doi: S0960-9822(08)00316-3 [pii]
10.1016/j.cub.2008.03.016

LaCava, J., Houseley, J., Saveanu, C., Petfalski, E., Thompson, E., Jacquier, A., & Tollervey, D. (2005). RNA degradation by the exosome is promoted by a nuclear polyadenylation complex. [Research Support, Non-U.S. Gov't]. *Cell, 121*(5), 713-724. doi: 10.1016/j.cell.2005.04.029

Lachner, M., O'Carroll, D., Rea, S., Mechtler, K., & Jenuwein, T. (2001). Methylation of histone H3 lysine 9 creates a binding site for HP1 proteins. *Nature, 410*(6824), 116-120.

Lejeune, E., & Allshire, R. C. (2011). Common ground: small RNA programming and chromatin modifications. *Curr Opin Cell Biol, 23*(3), 258-265. doi: S0955-0674(11)00022-6 [pii]
10.1016/j.ceb.2011.03.005

Lemay, J. F., D'Amours, A., Lemieux, C., Lackner, D. H., St-Sauveur, V. G., Bahler, J., & Bachand, F. (2010). The nuclear poly(A)-binding protein interacts with the exosome to promote synthesis of noncoding small nucleolar RNAs. [Research Support, Non-U.S. Gov't]. *Mol Cell, 37*(1), 34-45. doi: 10.1016/j.molcel.2009.12.019

Luger, K., Mader, A. W., Richmond, R. K., Sargent, D. F., & Richmond, T. J. (1997). Crystal structure of the nucleosome core particle at 2.8 A resolution. [Research Support, Non-U.S. Gov't]. *Nature, 389*(6648), 251-260. doi: 10.1038/38444

Mandell, J. G., Goodrich, K. J., Bahler, J., & Cech, T. R. (2005). Expression of a RecQ helicase homolog affects progression through crisis in fission yeast

lacking telomerase. [Research Support, U.S. Gov't, P.H.S.]. *J Biol Chem, 280*(7), 5249-5257. doi: 10.1074/jbc.M412756200

Masumoto, H., Masukata, H., Muro, Y., Nozaki, N., & Okazaki, T. (1989). A human centromere antigen (CENP-B) interacts with a short specific sequence in alphoid DNA, a human centromeric satellite. [Comparative Study

Research Support, Non-U.S. Gov't]. *J Cell Biol, 109*(5), 1963-1973.

Muro, Y., Masumoto, H., Yoda, K., Nozaki, N., Ohashi, M., & Okazaki, T. (1992). Centromere protein B assembles human centromeric alpha-satellite DNA at the 17-bp sequence, CENP-B box. [Research Support, Non-U.S. Gov't]. *J Cell Biol, 116*(3), 585-596.

Nakagawa, H., Lee, J. K., Hurwitz, J., Allshire, R. C., Nakayama, J., Grewal, S. I., . . . Murakami, Y. (2002). Fission yeast CENP-B homologs nucleate centromeric heterochromatin by promoting heterochromatin-specific histone tail modifications. *Genes Dev, 16*(14), 1766-1778. doi: 10.1101/gad.997702

Nakayama, J., Rice, J. C., Strahl, B. D., Allis, C. D., & Grewal, S. I. (2001). Role of histone H3 lysine 9 methylation in epigenetic control of heterochromatin assembly. *Science, 292*(5514), 110-113.

Noma, K., Allis, C. D., & Grewal, S. I. (2001). Transitions in distinct histone H3 methylation patterns at the heterochromatin domain boundaries. [Research Support, Non-U.S. Gov't

Research Support, U.S. Gov't, P.H.S.]. *Science, 293*(5532), 1150-1155. doi: 10.1126/science.1064150

Noma, K., Sugiyama, T., Cam, H., Verdel, A., Zofall, M., Jia, S., . . . Grewal, S. I. (2004). RITS acts in cis to promote RNA interference-mediated transcriptional and post-transcriptional silencing. *Nat Genet, 36*(11), 1174-1180. doi: ng1452 [pii]

10.1038/ng1452

Partridge, J. F., Scott, K. S., Bannister, A. J., Kouzarides, T., & Allshire, R. C. (2002). cis-acting DNA from fission yeast centromeres mediates histone H3 methylation and recruitment of silencing factors and cohesin to an ectopic site. [Research Support, Non-U.S. Gov't

Research Support, U.S. Gov't, P.H.S.]. *Curr Biol, 12*(19), 1652-1660.

Passarge, E. (1979). Emil Heitz and the concept of heterochromatin: longitudinal chromosome differentiation was recognized fifty years ago. [Bibliography

Biography

Historical Article]. *Am J Hum Genet, 31*(2), 106-115.

Reyes-Turcu, F. E., & Grewal, S. I. (2012). Different means, same end-heterochromatin formation by RNAi and RNAi-independent RNA processing factors in fission yeast. [Research Support, N.I.H., Intramural

Review]. *Curr Opin Genet Dev, 22*(2), 156-163. doi: 10.1016/j.gde.2011.12.004

Reyes-Turcu, F. E., Zhang, K., Zofall, M., Chen, E., & Grewal, S. I. (2011). Defects in RNA quality control factors reveal RNAi-independent nucleation of heterochromatin. [Research Support, N.I.H., Intramural]. *Nat Struct Mol Biol, 18*(10), 1132-1138. doi: 10.1038/nsmb.2122

Sadaie, M., Iida, T., Urano, T., & Nakayama, J. (2004). A chromodomain protein, Chp1, is required for the establishment of heterochromatin in fission yeast. *Embo J, 23*(19), 3825-3835.

Sadaie, M., Kawaguchi, R., Ohtani, Y., Arisaka, F., Tanaka, K., Shirahige, K., & Nakayama, J. (2008). Balance between distinct HP1 family proteins controls heterochromatin assembly in fission yeast. *Mol Cell Biol, 28*(23), 6973-6988. doi: MCB.00791-08 [pii]

10.1128/MCB.00791-08

Steiner, N. C., Hahnenberger, K. M., & Clarke, L. (1993). Centromeres of the fission yeast Schizosaccharomyces pombe are highly variable genetic loci. [Research Support, U.S. Gov't, Non-P.H.S.

Research Support, U.S. Gov't, P.H.S.]. *Mol Cell Biol, 13*(8), 4578-4587.

Sugiyama, T., Cam, H. P., Sugiyama, R., Noma, K., Zofall, M., Kobayashi, R., & Grewal, S. I. (2007). SHREC, an effector complex for heterochromatic transcriptional silencing. *Cell, 128*(3), 491-504. doi: S0092-8674(07)00059-1 [pii]

10.1016/j.cell.2006.12.035

Thon, G., & Verhein-Hansen, J. (2000). Four chromo-domain proteins of Schizosaccharomyces pombe differentially repress transcription at various chromosomal locations. [Research Support, Non-U.S. Gov't]. *Genetics, 155*(2), 551-568.

Verdel, A., Jia, S., Gerber, S., Sugiyama, T., Gygi, S., Grewal, S. I., & Moazed, D. (2004). RNAi-mediated targeting of heterochromatin by the RITS complex. *Science, 303*(5658), 672-676. doi: 10.1126/science.1093686

1093686 [pii]

Verdel, A., Vavasseur, A., Le Gorrec, M., & Touat-Todeschini, L. (2009). Common themes in siRNA-mediated epigenetic silencing pathways. *Int J Dev Biol, 53*(2-3), 245-257. doi: 082691av [pii]

10.1387/ijdb.082691av

Wood, V., Gwilliam, R., Rajandream, M. A., Lyne, M., Lyne, R., Stewart, A., . . . Nurse, P. (2002). The genome sequence of Schizosaccharomyces pombe. [Research Support, Non-U.S. Gov't]. *Nature, 415*(6874), 871-880. doi: 10.1038/nature724

Yamada, T., Fischle, W., Sugiyama, T., Allis, C. D., & Grewal, S. I. (2005). The nucleation and maintenance of heterochromatin by a histone deacetylase in fission yeast. [Research Support, N.I.H., Extramural

Research Support, N.I.H., Intramural

Research Support, Non-U.S. Gov't]. *Mol Cell, 20*(2), 173-185. doi: 10.1016/j.molcel.2005.10.002

Yoda, K., Kitagawa, K., Masumoto, H., Muro, Y., & Okazaki, T. (1992). A human centromere protein, CENP-B, has a DNA binding domain containing four potential alpha helices at the NH2 terminus, which is separable from dimerizing activity. [Comparative Study

Research Support, Non-U.S. Gov't]. *J Cell Biol, 119*(6), 1413-1427.

Zhang, K., Fischer, T., Porter, R. L., Dhakshnamoorthy, J., Zofall, M., Zhou, M., . . . Grewal, S. I. (2011). Clr4/Suv39 and RNA quality control factors

cooperate to trigger RNAi and suppress antisense RNA. *Science, 331*(6024), 1624-1627. doi: 331/6024/1624 [pii]

10.1126/science.1198712

Zhang, K., Mosch, K., Fischle, W., & Grewal, S. I. (2008). Roles of the Clr4 methyltransferase complex in nucleation, spreading and maintenance of heterochromatin. *Nat Struct Mol Biol, 15*(4), 381-388. doi: nsmb.1406 [pii]

10.1038/nsmb.1406

Chapter II: Systematic sequence analysis of the *dg* and *dh* repeats of

centromere I

Diana B. Marina, Smita Shankar and Hiten D. Madhani

Author contributions:

Diana Marina performed the experiments shown in Figures 7-18 and wrote this

chapter. Smita Shankar performed the experiments shown in Figures 1-6. Hiten

Madhani supervised this work. All authors wrote a manuscript in which parts of

this chapter are described.

INTRODUCTION

In *S. pombe,* heterochromatin is found in the pericentromeric regions of all

3 chromosomes (Grewal & Jia, 2007). The repressive H3K9Me mark coats a

small portion of the inner repeat (*imr)* regions and the entire outer repeat (*otr*)

regions of the centromeres (Cam et al., 2005). Consequently, reporter genes

inserted into these repeat regions are epigenetically silenced (Allshire, Javerzat,

Redhead, & Cranston, 1994). While the *imr* regions are unique to each

centromere, the *otr* regions consist of the *dg* and *dh* repeats that can be found in

all centromeres (Wood et al., 2002). However, the copy number of these repeats

varies between different centromeres (Steiner, Hahnenberger, & Clarke, 1993).

These repeats are also found in subtelomeric regions and at the silent mating-

type locus of *S. pombe* (Grewal & Jia, 2007)*.*

Studies have shown that the *dg* and *dh* repeats are transcribed by RNA Polymerase II (PolII) exclusively in the S phase of the cell cycle (Chen et al., 2008; Kloc, Zaratiegui, Nora, & Martienssen, 2008). It is hypothesized that PolII gains access to heterochromatin during S phase when repressive heterochromatic marks are partially lost due to chromosome duplication. Transcription of these repeats is required to trigger the RNAi-dependent pathway of heterochromatin assembly (Grewal, 2010). The *dg* and *dh* transcripts become substrates for the RNAi machinery to generate small interfering RNAs (siRNAs) (Lejeune & Allshire, 2011; Verdel, Vavasseur, Le Gorrec, & Touat-Todeschini, 2009). siRNAs bound by the Argonaute protein (Ago1) mediate both transcriptional and post-transcriptional silencing of the *dg* and *dh* repeats. Post-transcriptional silencing of the repeats occurs through the base-pairing of siRNAs with the corresponding *dg* and *dh* transcripts that guides Ago1 to slice these transcripts (Noma et al., 2004; Verdel et al., 2004). Transcriptional silencing mediated by Ago1-bound siRNAs is achieved by the recruitment of the CLRC methyltransferase complex to the *dg* and *dh* repeats (Bayne et al., 2010; Noma et al., 2004). CLRC catalyzes the methylation of H3K9 (Nakayama, Rice, Strahl, Allis, & Grewal, 2001; Zhang, Mosch, Fischle, & Grewal, 2008) and this methyl mark is bound by the repressive HP1 proteins such as Swi6 and Chp2 (Bannister et al., 2001; Fischer et al., 2009; Thon & Verhein-Hansen, 2000). The HP1 proteins recruit other chromatin-modifying enzymes such as the HDAC Clr3 to prevent PolII from transcribing the heterochromatic regions outside of S phase (Grewal, 2010; Sadaie et al., 2008; Sugiyama et al., 2007)

In addition to mediating the RNAi-dependent pathway of heterochromatin assembly, the *dg* and *dh* repeats also play a role in recruiting a conserved ncRNA-binding protein called Seb1 to trigger the RNAi-independent but RNA-dependent pathway of heterochromatin assembly. Seb1 binds to *dg* and *dh* non-coding RNAs and functions in parallel to the RNAi pathway by recruiting the chromatin-modifying complex SHREC to the *dg* and *dh* repeats. This novel mechanism is described in chapter III of this dissertation. Given the importance of the *dg* and *dh* repeats in triggering RNA-dependent pathways of heterochromatin formation, we systematically dissected them in order to identify sequences sufficient to induce heterochromatin assembly. In this study, we report that large fragments derived from the *dg* and *dh* repeats are capable of inducing heterochromatic silencing at the endogenous *ura4+* locus. Additionally, we demonstrate that several RNAi-independent sequence elements can induce heterochromatic silencing synergistically with smaller fragments derived from the *dg* and *dh* repeats. Finally, we found a hexameric sequence motif present at the *dg* and *dh* repeats that is necessary but not sufficient to induce heterochromatic silencing.

RESULTS AND DISCUSSION

Development of an ectopic heterochromatic silencing reporter

To identify sequences sufficient to nucleate heterochromatin at an ectopic locus, we developed an ectopic heterochromatic reporter construct at the *ura4+*

locus. This reporter construct consists of a strong promoter (*adh1+* promoter)

driving transcription of inserted fragments (described below), a bidirectional

terminator to ensure proper transcription termination, the *B-box* boundary

element to prevent the spread of heterochromatin and the *natR* cassette used as

a selective marker (Figure 1). We inserted this reporter construct at a site that is

1026 bp downstream of the termination codon of the endogenous *ura4+* gene.

We chose this locus so that we can detect silencing of the *ura4+* gene by growth

assay on media containing a drug called 5-Fluoroorotic Acid (5-FOA). Cells that

express wild-type *ura4+* gene convert 5-FOA into the toxic substance 5'

Fluorouridine monophosphate. Therefore, only cells with silent or mutated *ura4+*

gene can grow on media containing 5-FOA.

Large fragments derived from *dg* and *dh* repeats can induce ectopic

heterochromatic silencing

      Since centromere I of *S. pombe* has the fewest copy number of *dg* and *dh*

repeats (1 copy of *dg* and *dh* on each centromere arm), we cloned 9 overlapping

segments of *dh* and *dg* repeats from centromere I (termed Fragments 1-9)

downstream of the strong *adh1+* promoter in both orientations (Figure 2). We

examined silencing of *ura4+* using 5-FOA media that selects for Ura- cells. Four

of the 18 constructs yielded a 5-FOA+ phenotype indicative of silencing of *ura4+*.

The silencing induced by these fragments is at least as strong as the silencing of

ura4+ gene that is placed in the *imr* region of centromere 1 (shown for

comparison). Fragments 1 and 2, which overlap by 1778 bp, promoted silencing,

but only in the "forward" orientation while Fragments 8 and 9, which overlap by

999 bp, promoted silencing, but only in the "reverse" orientation. The region of

overlap between Fragments 8 and 9 corresponds well to the L5 sequence of the

dg repeat identified previously as capable of inducing silencing at an ectopic site

(Figure 2) (Partridge, Scott, Bannister, Kouzarides, & Allshire, 2002).

To further characterize silencing induced by these fragments, we utilized

Fragment 1 as the representative fragment in testing the genetic requirements of

this ectopic silencing. Silencing by Fragment 1 requires the *S. pombe* Dicer

enzyme, Dcr1 and the H3K9 methyltransferase, Clr4 (Figure 3). It also requires

the presence of the *adh1+* promoter, indicating that it likely functions as a ncRNA

(Figure 3). Similar to silencing of reporter genes inserted in endogenous

heterochromatin, ectopic silencing by Fragment 1 also induces H3K9 methylation

at the *ura4+* locus (Figure 4) and a reduction of the *ura4+* transcript level (Figure

5).

Synergy silencing between *REIII* or a snoRNA gene and small fragments derived

from the *dh* repeat

We dissected the sequences required for silencing by deletion analysis of

a Fragment containing the overlap region between Fragments 1 and 2 and found

that silencing is gradually lost as larger regions are deleted, suggesting the

existence of numerous, weak distributed signals (Figure 6). Since RNAi-

independent mechanisms are known to cooperate with RNAi-dependent

mechanisms to induce heterochromatin formation (Jia, Noma, & Grewal, 2004),

we tested whether an element required for RNAi-independent silencing could act

synergistically with *dh* fragments too small to induce silencing on their own. For

these experiments, we used the *REIII* element from the silent mating type *mat2/3*

region (Thon, Bjerling, & Nielsen, 1999) (Figure 7). Indeed, we found that while

REIII alone is incapable of inducing ectopic silencing, it could induce silencing

when placed adjacent to a variety of fragments derived from the Fragment 1-

Fragment 2 overlap region that were themselves incapable of inducing silencing

(Figure 8).

Chapter III of this dissertation describes the RNAi-independent role of

Seb1, a conserved ncRNA-binding protein, in heterochromatin assembly. The

ortholog of Seb1 in *S. cerevisiae* is Nrd1, a protein that binds to and processes

snoRNAs (Kim et al., 2006). Here we demonstrate that like *REIII,* a snoRNA

gene, *snR30+*, is also capable of acting synergistically with small fragments

derived from the *dh* repeat (Figures 9 and 10). Together, these results provide

clear evidence that RNAi-independent sequence elements such as *REIII* and a

snoRNA gene can cooperate with RNAi-dependent sequence elements such as

the *dg* and *dh* repeats.

In addition to being promoter- and orientation-dependent, the synergistic

silencing induced by *REIII* and small *dh* fragments requires Dcr1 and Pcr1, a

transcription factor shown previously to be necessary for the silencing activity of

the *REIII* element (Figure 11) (Jia et al., 2004; Thon et al., 1999) *REIII* does not induce silencing when placed next to similar-sized control sequences derived from the *S. pombe leu1+* gene, *dh* Fragment 4 (Figure 2) or pBluescript plasmid (Figure 12), suggesting the requirement for specific RNA signals. Furthermore, even in this sensitized system, placement of the strong *act1+* promoter in an anti-sense orientation such that pBluescript sequences are bidirectionally transcribed does not induce silencing (Figures 13 and 14). This finding demonstrates that bidirectional transcription of a random DNA sequence is not sufficient to induce heterochromatic silencing further arguing in support of the requirement for specific RNA signals.

Using this system, we performed a deletion analysis on the *dhR5* segment and found that fragments as small as 200 bp are capable of inducing silencing (Figure 15). Interestingly, while the 200-bp *dhR5L4* fragment is capable of inducing silencing, the similar-sized *dhR5R4* fragment does not trigger silencing of the *ura4+* reporter. Additionally, we found that the silencing induced by the *dhR5L4* fragment is dosage dependent. The *ura4+* silencing becomes stronger as more copies of *dhR5L4* are inserted downstream of the *adh1+* promoter (Figure 16). Furthermore, when 4 copies of the *dhR5L4* fragment are inserted in the reporter construct, the *ura4+* gene can be silenced in the absence of the *REIII* element from the construct (Figure 16). This demonstrates that the *dhR5L4* fragment contains signals necessary for heterochromatic silencing.

Identification of the AAYATG motif that is necessary for silencing

Comparing the sequences of *dhR5L4* and *dhR5R4* fragments, we found a unique AAYATG motif that is present 6 times as tandem repeats in the *dhR5L4* fragment but not in the *dhR5R4* fragment (Figure 17). The AAYATG motif is found throughout the *dg* and *dh* repeats. To determine if the number of the AAYATG motif affects whether or not a fragment can induce silencing, we counted the motif in both forward and reverse orientations in Fragments 1-9 (Table 1). Fragment 1 and Fragment 2 have the highest number of the AAYATG motif in the forward orientation (12 and 14 motifs, respectively). On the other hand, Fragment 9 has the most AAYATG motif in the reverse orientation (5 motifs). Interestingly, these are the fragments that can induce silencing when inserted in the reporter construct (Figure 2).

To determine if the AAYATG repeat is necessary to induce silencing of the *ura4+* reporter, we deleted the repeat from the *dhR5L1, dhR5L2* and *dhR5L3* fragments. We found that when the AAYATG repeat is deleted from these fragments, these fragments are no longer able to induce silencing of the *ura4+* reporter gene. Furthermore, we randomly mutated the AAYATG repeat on *dhR5L4* and *dhR5L3* and found that this random mutation causes lost of *ura4+* silencing (Figure 17). Together, these results indicate that the AAYATG repeat is necessary to induce silencing.

Next, we sought to determine if the AAYATG repeat is sufficient to induce silencing of the *ura4+* reporter gene. We inserted 10 AAYATG motifs as tandem repeats downstream of the *adh1+* promoter in the *ura4+* reporter construct with *REIII*. We found that this repeat is incapable of inducing silencing of the *ura4+* gene (Figure 18). It is possible that in order for the AAYATG repeat to induce silencing, it needs to be flanked by larger DNA sequences. To test this, we inserted 6 AAYATG motifs flanked by random sequences from pBluescript plasmid downstream of the *adh1+* promoter in the *ura4+* reporter construct with *REIII*. We found that the AAYATG repeat flanked by random DNA sequences is also incapable of inducing silencing (Figure 18). Finally, we added the AAYATG repeat to the 3' end of the *dhR5R4* fragment to test if the addition of this repeat allows the *dhR5R4* fragment to silence the *ura4+* gene. However, we still did not observe silencing of the *ura4+* gene when this modified *dhR5R4* is inserted in the reporter construct (Figure 18). Therefore, we conclude that the AAYATG repeat is necessary but not sufficient to induce silencing.

Conclusions

The systematic dissection of the *dg* and *dh* repeats reveals that multiple large fragments derived from these repeats are able to trigger heterochromatic silencing at an ectopic locus. We demonstrated that silencing by these fragments is gradually lost as regions are deleted, suggesting the existence of numerous, distributed weak signals necessary for silencing. We found that RNAi-independent sequence elements such as *REIII* and a snoRNA gene are capable

of sensitizing the silencing reporter as demonstrated by the synergy silencing between the *REIII* or *snR30* sequence element and small fragments derived from the *dh* repeat. Furthermore, we identified a unique sequence motif that is necessary but not sufficient to induce heterochromatic silencing. Future studies are required to determine how this motif functions in triggering silencing. It is likely that the AAYATG motif serves as a signal to recruit unknown protein factors to nucleate heterochromatin.

MATERIALS AND METHODS

Strain Construction and Growth Conditions

Strains were constructed by lithium acetate transformation of plasmid DNA
containing 500 bp of targeting homology. Strains were grown in YS medium (5
g/liter Difco yeast extract + 250 mg/liter each of L-histidine, L-leucine, adenine,
uracil, and L-lysine and 3% glucose) at 30°C unless noted otherwise.

Silencing Assays

The strains were grown overnight to saturation and diluted to OD_{600} of 1 at the
highest dilution. Serial dilutions were performed with dilution factor of 5 and cells
were grown on non-selective and 5-FOA (2 grams/liter of 5-fluoroorotic acid)
containing media at 30°C for 2-3 days.

Chromatin Immunoprecipitation

The ChIP assays were performed as described previously (Rougemaille,
Shankar, Braun, Rowley, & Madhani, 2008) except for a few minor changes: 1.
Cells were lysed by bead beating 7 times for 1 min each with 2 min rests on ice.
2. Chromatin fraction was sonicated 20 times for 30 s each with 1-min rest in
between cycles using a Bioruptor®. 3. Ab1220 (Abcam) antibody was used for
H3K9Me2 ChIP. 4. Protein A Dynabeads were used instead of Sepharose beads.

<u>Reverse Transcription quantitative Polymerase Chain Reaction (RT-qPCR)</u>

RNA extraction was performed as described previously (Rougemaille et al.,

2008). Five μg of total RNA was treated with 2 U of Turbo DNase I (Ambion) and

used in each reverse transcription reaction with 2.5 U of AMV RT (Promega) and

strand-specific primers or random 9-mer. The reverse transcription reaction was

performed at 42°C for 2 hours. The cDNA samples were analyzed by quantitative

PCR using SYBR Green (Invitrogen).

<u>Primers used in quantitative PCR following ChIP and RT experiments</u>

For *ura4+* locus: P581 (5'-CAGCAATATCGTACTCCTGAA-3') and P582 (5'-

ATGCTGAGAAAGTCTTTGCTG-3')

For *act1+* locus: P638 (5'- AACCCTCAGCTTTGGGTCTT-3') and P639 (5'-

TTTGCATACGATCGGCAATA-3')

FIGURE LEGENDS

Figure 1: Schematic of the ectopic heterochromatic silencing reporter construct. The construct consists of the *adh1+* promoter driving transcription of inserted fragments derived from pericentromeric *dg* and *dh* repeats, a bidirectional terminator ('term'), B-boxes boundary element ('B') and a resistant drug marker ('natR'). The entire construct was inserted downstream of the endogenous *ura4+* gene.

Figure 2: Fragments derived from the *dg* and *dh* repeats of centromere 1 can induce ectopic silencing. Top: schematic of nine fragments derived from *dh* and *dg* repeats. The previously identified L5 sequence is indicated. Bottom: Silencing assays of indicated strains grown on non-selective (N/S) YS and 5-FOA-containing media. 'F' indicates an arbitrary forward orientation while 'R' indicates the reverse orientation.

Figure 3: Silencing by Fragment 1 is orientation dependent, requires Clr4, RNAi and transcription by the *adh1+* promoter. Silencing assays of strains with different variations or mutations of the ectopic heterochromatic silencing reporter construct with Fragment 1. 'No fragment' indicates that no fragment is inserted downstream of the *adh1+* promoter. 'No promoter' indicates that the *adh1+* promoter is absent from the construct. Cells were plated on non-selective YS media (N/S) and YS media with 5-FOA (5-FOA).

Figure 4: Silencing by Fragment 1 induces H3K9Me at the *ura4+* locus. ChIP analysis of H3K9Me2 levels at *ura4+* locus (normalized to H3K9Me2 levels at *act1+* locus) in strains described in Figure 3. Shown are mean values relative to the 'No fragment' strain ± SD of three parallel IP samples of one representative experiment.

Figure 5: Silencing by Fragment 1 causes reduction of the *ura4+* transcript level. RT-qPCR analysis of *ura4+* transcript levels (normalized to *act1+* transcript levels) in strains described in Figure 3. Shown are mean values relative to the 'No fragment' strain ± SD of three parallel RT reactions of one representative experiment.

Figure 6: Heterochromatic silencing of the *ura4+* gene is gradually lost as larger regions are deleted from *dh*-derived fragments. Top: schematic of the dissection of Fragment 1 and Fragment 2 overlap region. The length of each fragment (in bp) is indicated on the ruler on top. Bottom: silencing assays of strains with indicated fragments inserted in the reporter construct described in Figure 1.

Figure 7: Schematic of the silencing reporter construct with *REIII*. *padh1+*: the *adh1+* promoter; insert: position where *dh* fragments are inserted; term: terminator; B: B-boxes boundary element containing TFIIIC binding sites to prevent spread of heterochromatin; *natR*: *natMX6* marker.

Figure 8: Synergistic silencing induced by *REIII* and *dh* fragments. Top: schematic of the dissection of Fragment 1 and Fragment 2 overlap region. The length of each fragment (in bp) is indicated on the ruler on top. Bottom: silencing assay of strains with indicated fragments inserted in the *REIII* reporter construct. Strains were grown on non-selective YS (N/S) and 5-FOA-containing media.

Figure 9: Schematic of the silencing reporter construct with *snR30+*. *padh1+*: the *adh1+* promoter; insert: position where *dh* fragments are inserted; term: terminator; B: B-boxes boundary element containing TFIIIC binding sites to prevent spread of heterochromatin; *natR*: *natMX6* marker.

Figure 10: Synergistic silencing induced by *snR30+* and the *dh1* fragment. Silencing assay of strains with indicated fragments inserted in the *REIII* reporter construct. Strains were grown on non-selective YS (N/S) and 5-FOA-containing media.

Figure 11: Silencing mediated by *REIII+dhR5* requires Dcr1, Pcr1, the *adh1+* promoter and it is orientation dependent. Silencing assays of indicated strains grown on non-selective (N/S) and 5-FOA-containing media.

Figure 12: Silencing mediated by *REIII* requires specific inserted sequences. Silencing assays of indicated strains grown on non-selective (N/S) and 5-FOA-containing media.

Figure 13: Schematic of a silencing reporter construct. The *act1+* promoter is placed in the opposite direction of the *adh1+* promoter (convergent promoters). *padh1+*: *adh1+* promoter; insert: position where *dh* fragments are inserted; *pact1+*: *act1+* promoter; B: B-boxes boundary element containing TFIIIC binding sites to prevent spread of heterochromatin; *natR*: *natMX6* marker.

Figure 14: Bidirectional transcription of a 978-bp sequence from pBluescript is not sufficient to induce silencing of *ura4+* gene in the *REIII*-sensitized reporter construct. Silencing assays of indicated strains grown on non-selective (N/S) and 5-FOA-containing media.

Figure 15: Small fragments derived from *dhR5* fragment are capable of inducing silencing in the *REIII* reporter construct. Top: schematic of *dhR5* fragment dissection. The length of each fragment (in bp) is indicated on the ruler on top. Bottom: silencing assay of strains with indicated fragments inserted in the *REIII* reporter construct. Strains were grown on non-selective (N/S) and 5-FOA-containing media.

Figure 16: Silencing induced by *REIII* and the *dhR5L4* fragment is dosage dependent. Silencing assay of strains with indicated fragments inserted in the *REIII* reporter construct. Strains were grown on non-selective (N/S) and 5-FOA-containing media.

Figure 17: The AAYATG repeat is necessary for silencing. Top: schematic of

dhR5 fragment dissection. The length of each fragment (in bp) is indicated on the

ruler on top. Red asterisks represent AAYATG motifs. Bottom: silencing assay of

strains with indicated fragments inserted in the *REIII* reporter construct. 'del'

indicates that the AAYATG repeat is deleted from the fragment. 'mut' indicates

that the AAYATG repeat is randomly mutated on the fragment. Strains were

grown on non-selective (N/S) and 5-FOA-containing media.

Figure 18: The AAYATG repeat is not sufficient for silencing. Silencing assay of

strains with indicated fragments inserted in the *REIII* reporter construct.

REFERENCES

Allshire, R. C., Javerzat, J. P., Redhead, N. J., & Cranston, G. (1994). Position effect variegation at fission yeast centromeres. [Research Support, Non-U.S. Gov't

Research Support, U.S. Gov't, P.H.S.]. *Cell, 76*(1), 157-169.

Bannister, A. J., Zegerman, P., Partridge, J. F., Miska, E. A., Thomas, J. O., Allshire, R. C., & Kouzarides, T. (2001). Selective recognition of methylated lysine 9 on histone H3 by the HP1 chromo domain. *Nature, 410*(6824), 120-124.

Bayne, E. H., White, S. A., Kagansky, A., Bijos, D. A., Sanchez-Pulido, L., Hoe, K. L., . . . Allshire, R. C. (2010). Stc1: a critical link between RNAi and chromatin modification required for heterochromatin integrity. [Research Support, Non-U.S. Gov't]. *Cell, 140*(5), 666-677. doi: S0092-8674(10)00073-5 [pii]

10.1016/j.cell.2010.01.038

Cam, H. P., Sugiyama, T., Chen, E. S., Chen, X., FitzGerald, P. C., & Grewal, S. I. (2005). Comprehensive analysis of heterochromatin- and RNAi-mediated epigenetic control of the fission yeast genome. *Nat Genet, 37*(8), 809-819. doi: 10.1038/ng1602

Chen, E. S., Zhang, K., Nicolas, E., Cam, H. P., Zofall, M., & Grewal, S. I. (2008). Cell cycle control of centromeric repeat transcription and heterochromatin assembly. *Nature, 451*(7179), 734-737. doi: nature06561 [pii]

10.1038/nature06561

Fischer, T., Cui, B., Dhakshnamoorthy, J., Zhou, M., Rubin, C., Zofall, M., . . . Grewal, S. I. (2009). Diverse roles of HP1 proteins in heterochromatin assembly and functions in fission yeast. [Research Support, N.I.H., Intramural]. *Proc Natl Acad Sci U S A, 106*(22), 8998-9003. doi: 10.1073/pnas.0813063106

Grewal, S. I. (2010). RNAi-dependent formation of heterochromatin and its diverse functions. [Research Support, N.I.H., Intramural

Review]. *Curr Opin Genet Dev, 20*(2), 134-141. doi: 10.1016/j.gde.2010.02.003

Grewal, S. I., & Jia, S. (2007). Heterochromatin revisited. [Research Support, N.I.H., Intramural

Review]. *Nat Rev Genet, 8*(1), 35-46. doi: 10.1038/nrg2008

Jia, S., Noma, K., & Grewal, S. I. (2004). RNAi-independent heterochromatin nucleation by the stress-activated ATF/CREB family proteins. *Science, 304*(5679), 1971-1976. doi: 10.1126/science.1099035

304/5679/1971 [pii]

Kim, M., Vasiljeva, L., Rando, O. J., Zhelkovsky, A., Moore, C., & Buratowski, S. (2006). Distinct pathways for snoRNA and mRNA termination. *Mol Cell, 24*(5), 723-734. doi: S1097-2765(06)00782-9 [pii]

10.1016/j.molcel.2006.11.011

Kloc, A., Zaratiegui, M., Nora, E., & Martienssen, R. (2008). RNA interference guides histone modification during the S phase of chromosomal replication. *Curr Biol, 18*(7), 490-495. doi: S0960-9822(08)00316-3 [pii]

10.1016/j.cub.2008.03.016

Lejeune, E., & Allshire, R. C. (2011). Common ground: small RNA programming and chromatin modifications. *Curr Opin Cell Biol, 23*(3), 258-265. doi: S0955-0674(11)00022-6 [pii]

10.1016/j.ceb.2011.03.005

Nakayama, J., Rice, J. C., Strahl, B. D., Allis, C. D., & Grewal, S. I. (2001). Role of histone H3 lysine 9 methylation in epigenetic control of heterochromatin assembly. *Science, 292*(5514), 110-113.

Noma, K., Sugiyama, T., Cam, H., Verdel, A., Zofall, M., Jia, S., . . . Grewal, S. I. (2004). RITS acts in cis to promote RNA interference-mediated transcriptional and post-transcriptional silencing. *Nat Genet, 36*(11), 1174-1180. doi: ng1452 [pii]

10.1038/ng1452

Partridge, J. F., Scott, K. S., Bannister, A. J., Kouzarides, T., & Allshire, R. C. (2002). cis-acting DNA from fission yeast centromeres mediates histone H3 methylation and recruitment of silencing factors and cohesin to an ectopic site. [Research Support, Non-U.S. Gov't

Research Support, U.S. Gov't, P.H.S.]. *Curr Biol, 12*(19), 1652-1660.

Rougemaille, M., Shankar, S., Braun, S., Rowley, M., & Madhani, H. D. (2008). Ers1, a rapidly diverging protein essential for RNA interference-dependent heterochromatic silencing in Schizosaccharomyces pombe. *J Biol Chem, 283*(38), 25770-25773.

Sadaie, M., Kawaguchi, R., Ohtani, Y., Arisaka, F., Tanaka, K., Shirahige, K., & Nakayama, J. (2008). Balance between distinct HP1 family proteins controls heterochromatin assembly in fission yeast. *Mol Cell Biol, 28*(23), 6973-6988. doi: MCB.00791-08 [pii]

10.1128/MCB.00791-08

Steiner, N. C., Hahnenberger, K. M., & Clarke, L. (1993). Centromeres of the fission yeast Schizosaccharomyces pombe are highly variable genetic loci. [Research Support, U.S. Gov't, Non-P.H.S.

Research Support, U.S. Gov't, P.H.S.]. *Mol Cell Biol, 13*(8), 4578-4587.

Sugiyama, T., Cam, H. P., Sugiyama, R., Noma, K., Zofall, M., Kobayashi, R., & Grewal, S. I. (2007). SHREC, an effector complex for heterochromatic transcriptional silencing. *Cell, 128*(3), 491-504. doi: S0092-8674(07)00059-1 [pii]

10.1016/j.cell.2006.12.035

Thon, G., Bjerling, K. P., & Nielsen, I. S. (1999). Localization and properties of a silencing element near the mat3-M mating-type cassette of Schizosaccharomyces pombe. [Research Support, Non-U.S. Gov't]. *Genetics, 151*(3), 945-963.

Thon, G., & Verhein-Hansen, J. (2000). Four chromo-domain proteins of Schizosaccharomyces pombe differentially repress transcription at various chromosomal locations. [Research Support, Non-U.S. Gov't]. *Genetics, 155*(2), 551-568.

Verdel, A., Jia, S., Gerber, S., Sugiyama, T., Gygi, S., Grewal, S. I., & Moazed, D. (2004). RNAi-mediated targeting of heterochromatin by the RITS complex. [Research Support, Non-U.S. Gov't

Research Support, U.S. Gov't, P.H.S.]. *Science, 303*(5658), 672-676. doi: 10.1126/science.1093686

Verdel, A., Vavasseur, A., Le Gorrec, M., & Touat-Todeschini, L. (2009). Common themes in siRNA-mediated epigenetic silencing pathways. *Int J Dev Biol, 53*(2-3), 245-257. doi: 082691av [pii]

10.1387/ijdb.082691av

Wood, V., Gwilliam, R., Rajandream, M. A., Lyne, M., Lyne, R., Stewart, A., . . . Nurse, P. (2002). The genome sequence of Schizosaccharomyces pombe. [Research Support, Non-U.S. Gov't]. *Nature, 415*(6874), 871-880. doi: 10.1038/nature724

Zhang, K., Mosch, K., Fischle, W., & Grewal, S. I. (2008). Roles of the Clr4 methyltransferase complex in nucleation, spreading and maintenance of heterochromatin. *Nat Struct Mol Biol, 15*(4), 381-388. doi: nsmb.1406 [pii]

10.1038/nsmb.1406

Figure 1

Figure 2

Figure 3

Figure 4

H3K9Me2 ChIP
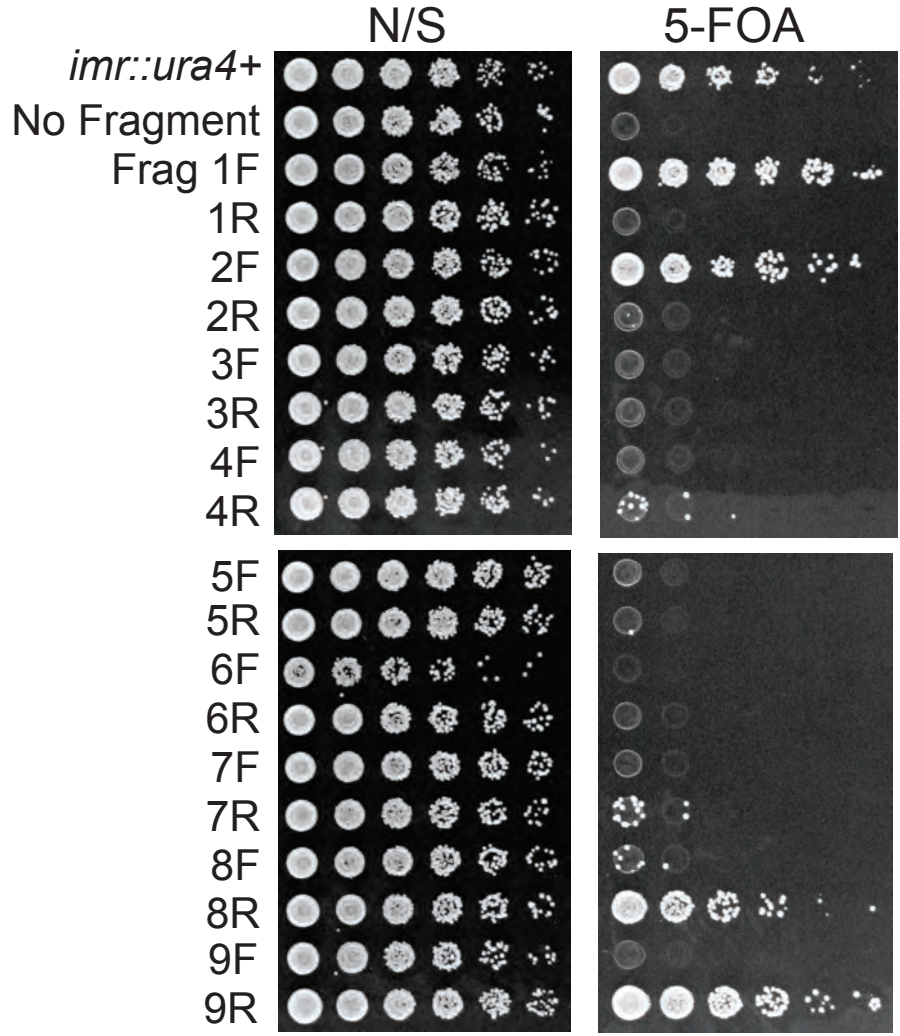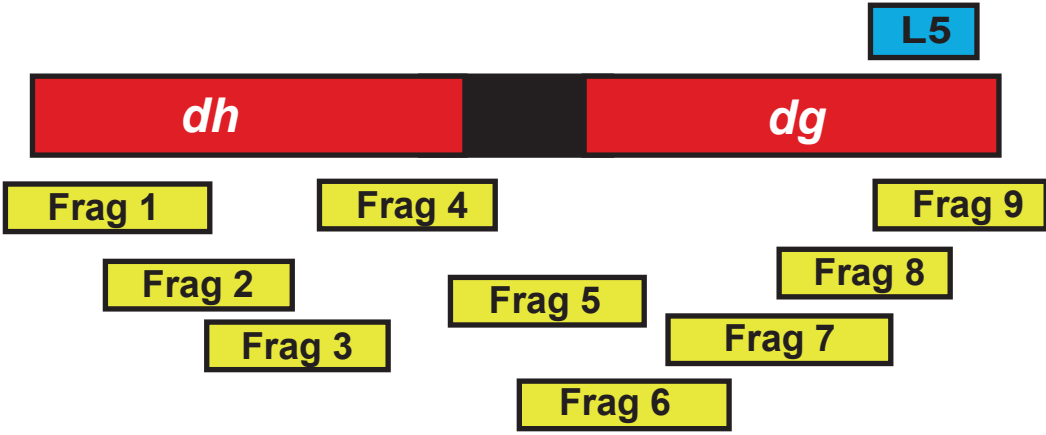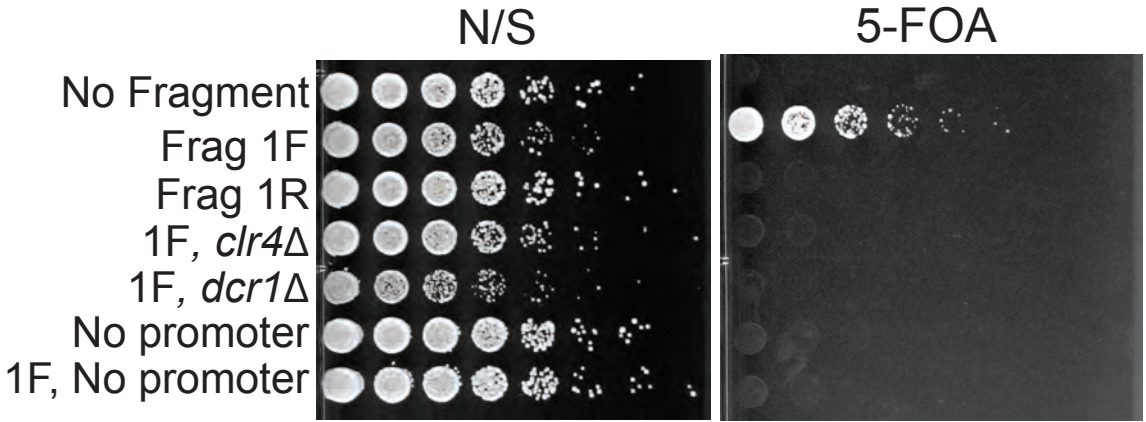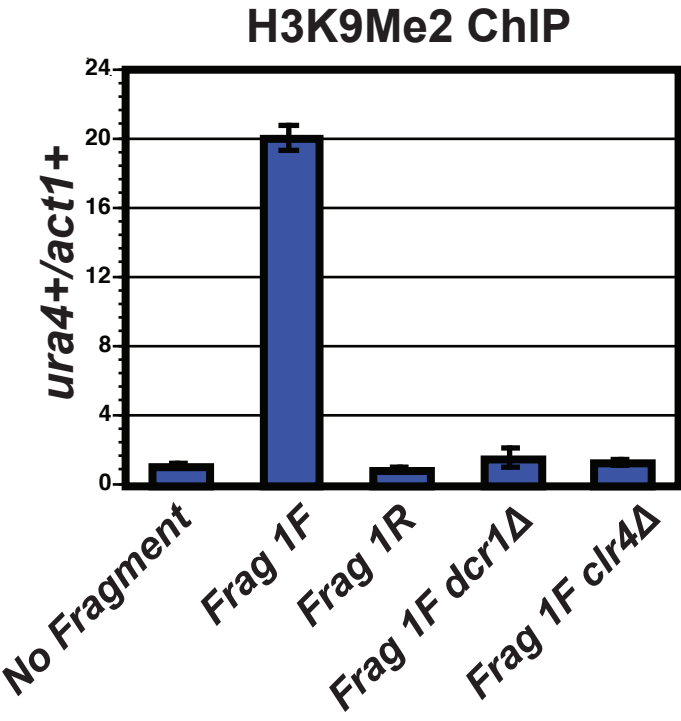
Figure 5

RT-qPCR
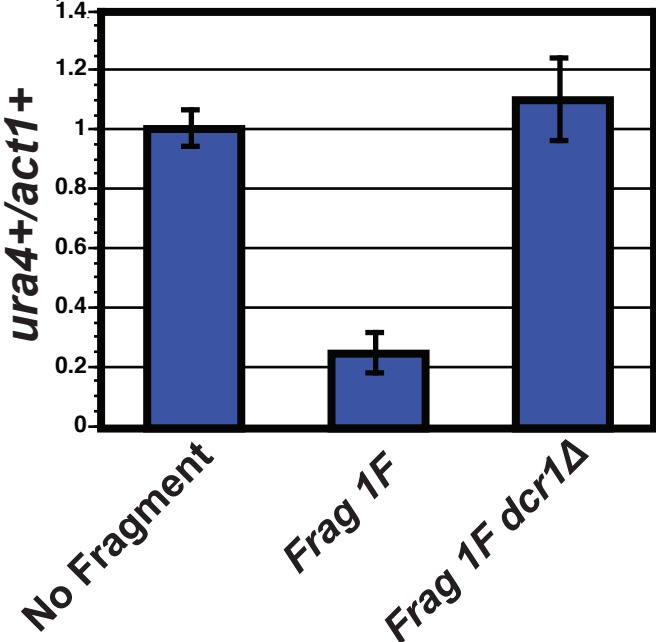
Figure 6
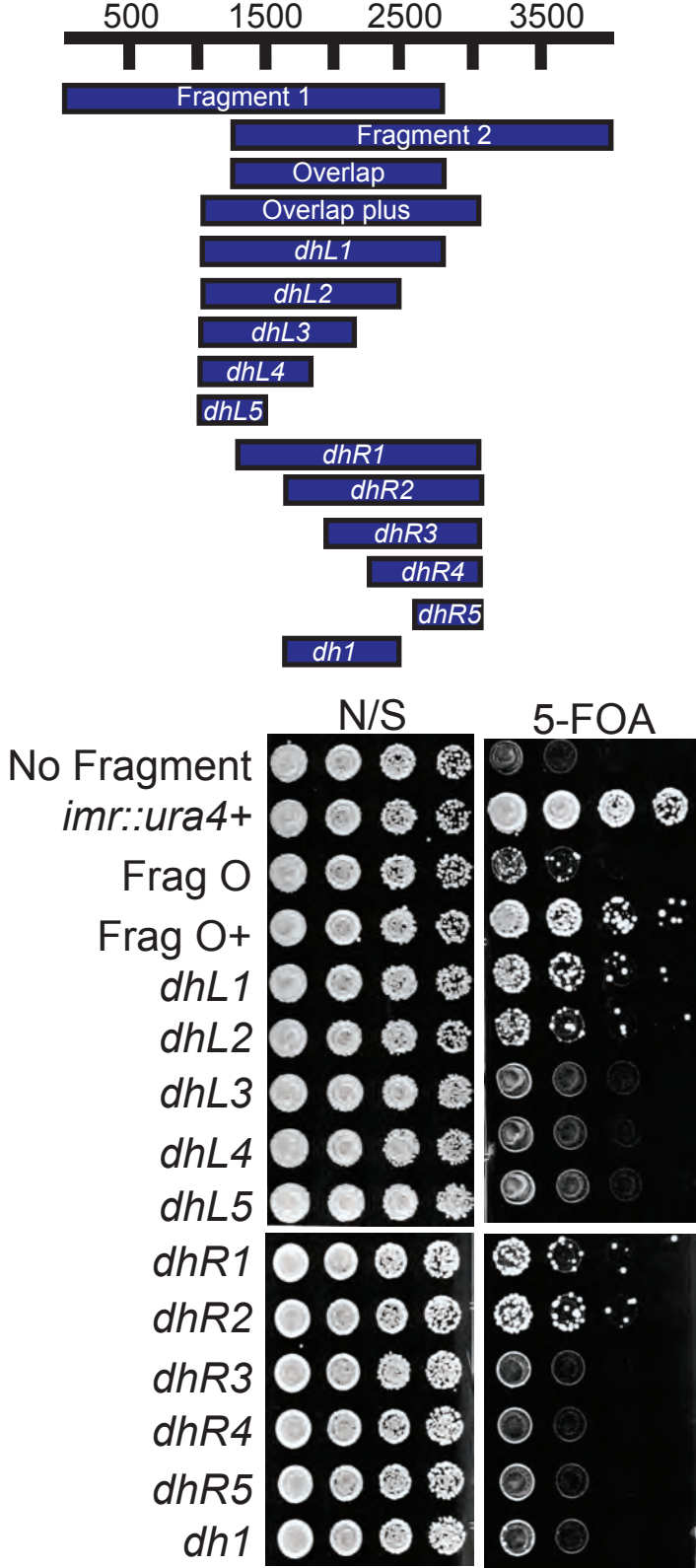
Figure 7
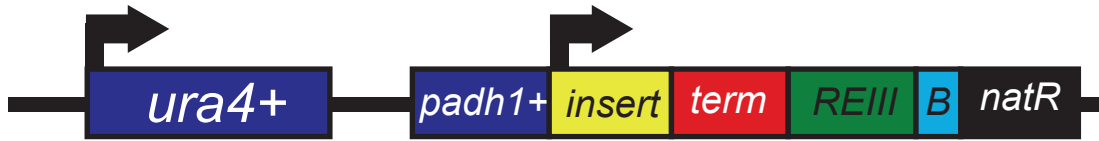
Figure 8

Figure 9

Figure 10

	N/S	5-FOA
snR30+no insert		
dh1		
snR30+dh1		
snR30+dh1		

Figure 11

	N/S	5-FOA
dhR5		
REIII+no insert		
REIII+*dhR5*		
REIII+*dhR5 dcr1Δ*		
REIII+*dhR5 pcr1Δ*		
REIII+*dhR5* Reverse		
REIII+*dhR5*, No promoter		
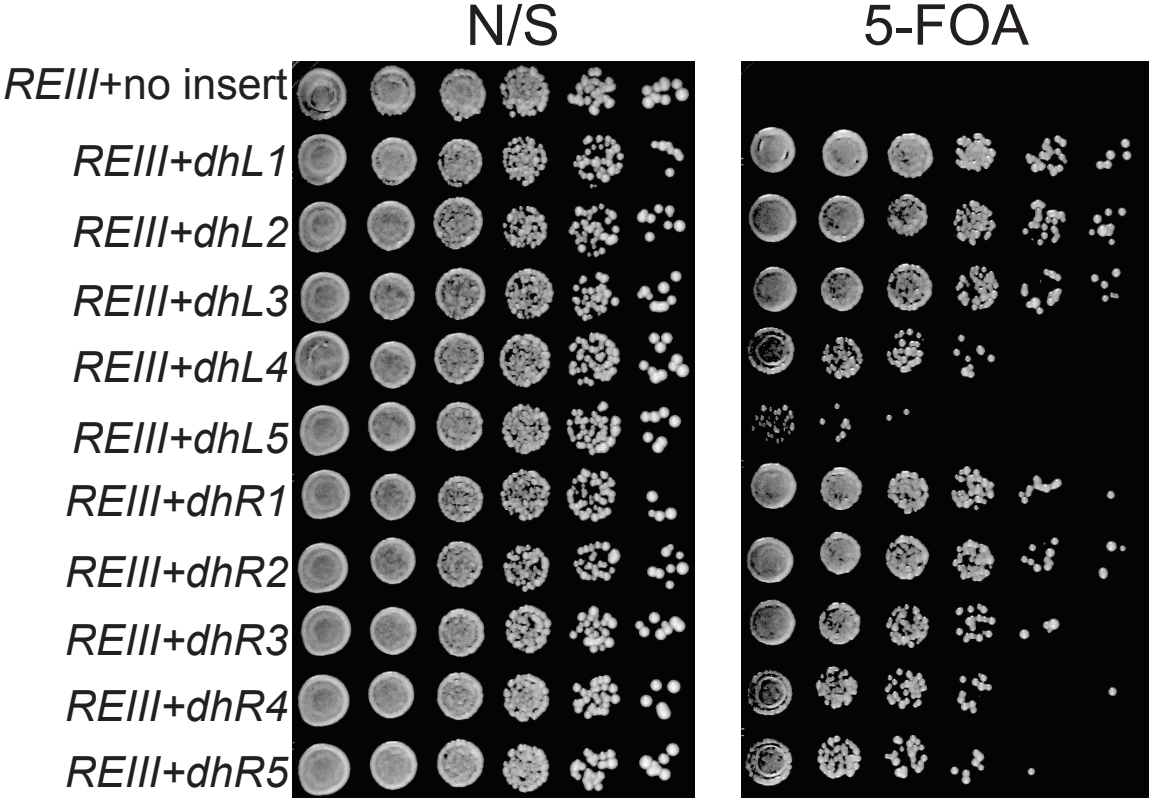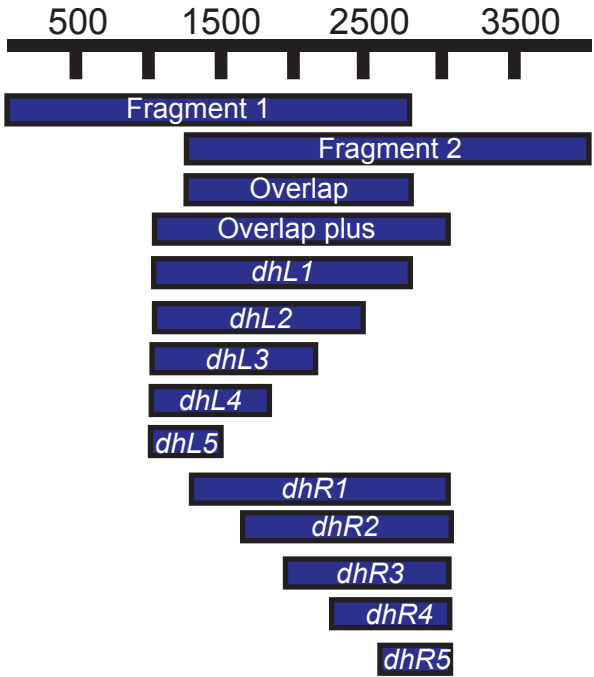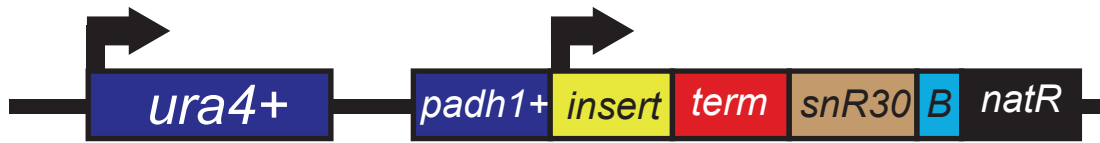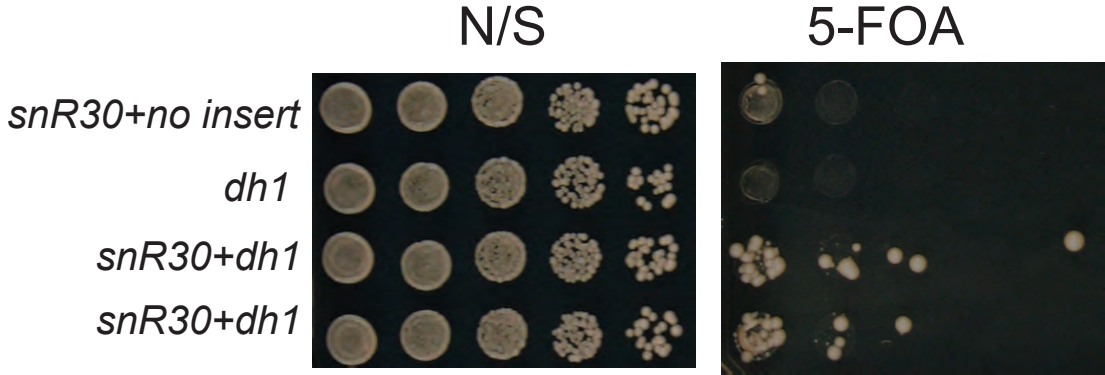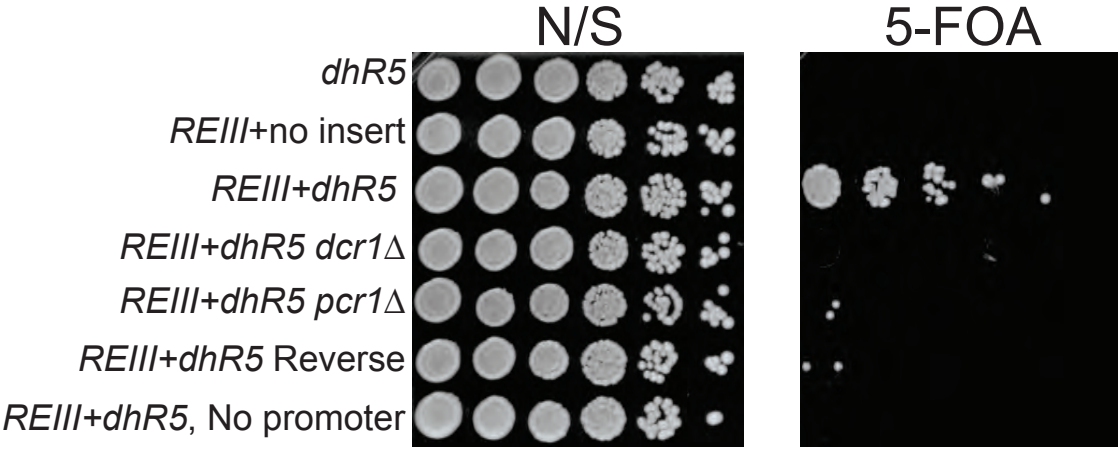
Figure 12

Figure 13

Figure 14

	N/S	5-FOA
conv.promoters+*REIII*+no insert		
conv.promoters+*REIII*+dhR5		
conv.promoters+*REIII*+pbluescript		

Figure 15

Figure 16

N/S 5-FOA

REIII+no insert
REIII+1XdhR5L4
REIII+3XdhR5L4
REIII+3XdhR5L4
REIII+2XdhR5L4
REIII+2XdhR5L4

4XdhR5L4
4XdhR5L4

Figure 17

Figure 18

N/S 5-FOA

REIII+10XAAYATG

REIII+6XAAYATG+pbluescript

REIII+no insert

REIII+dhR5

REIII+dhR5R4+6XAAYATG
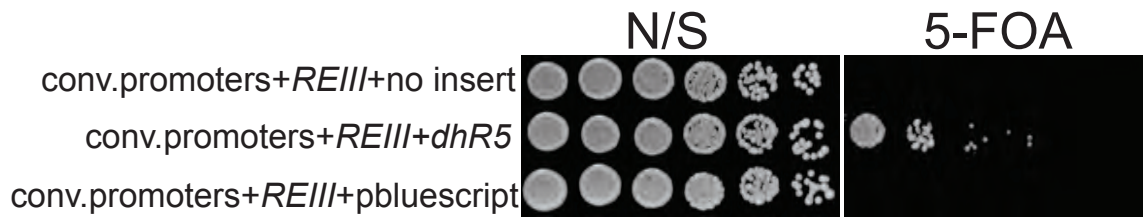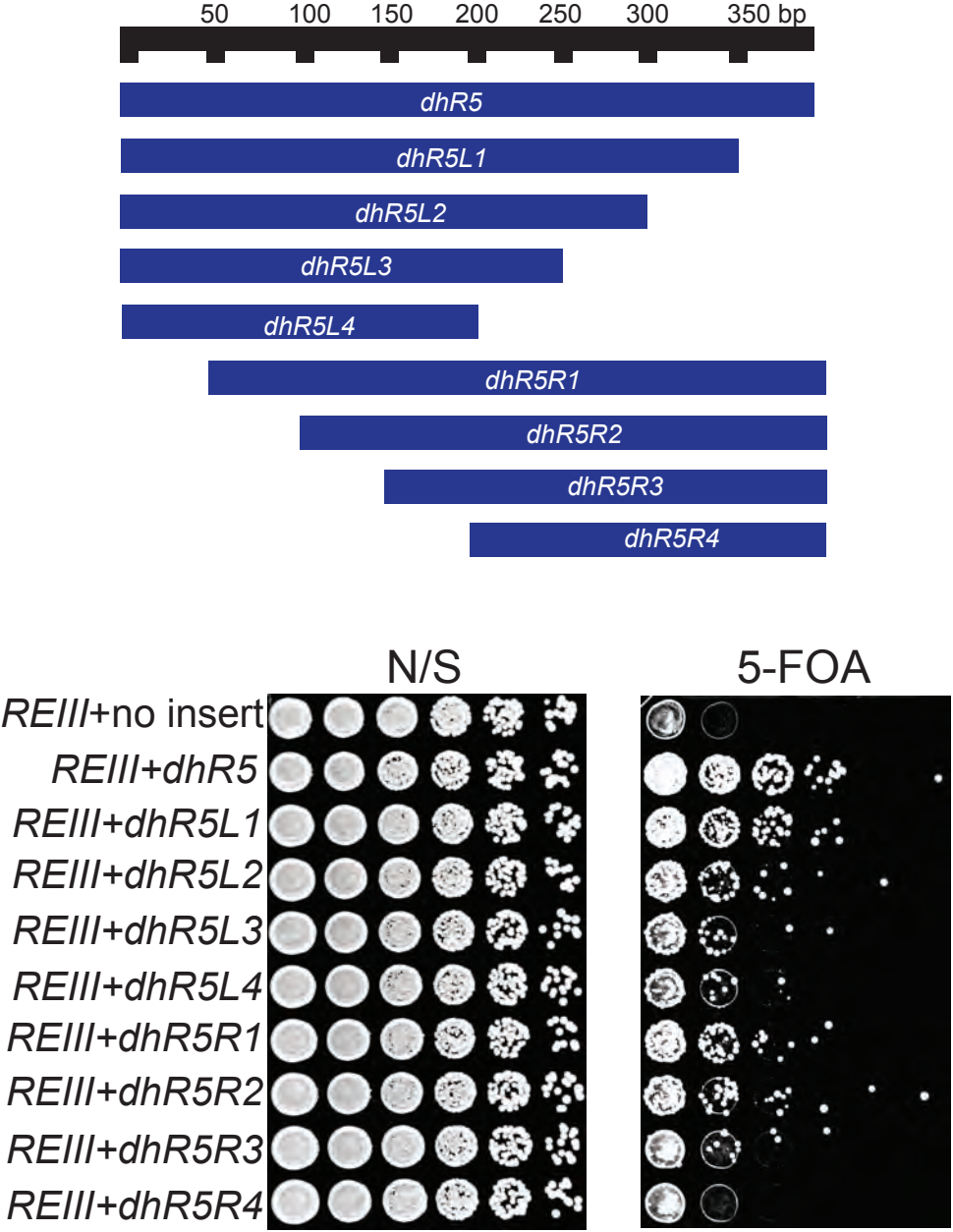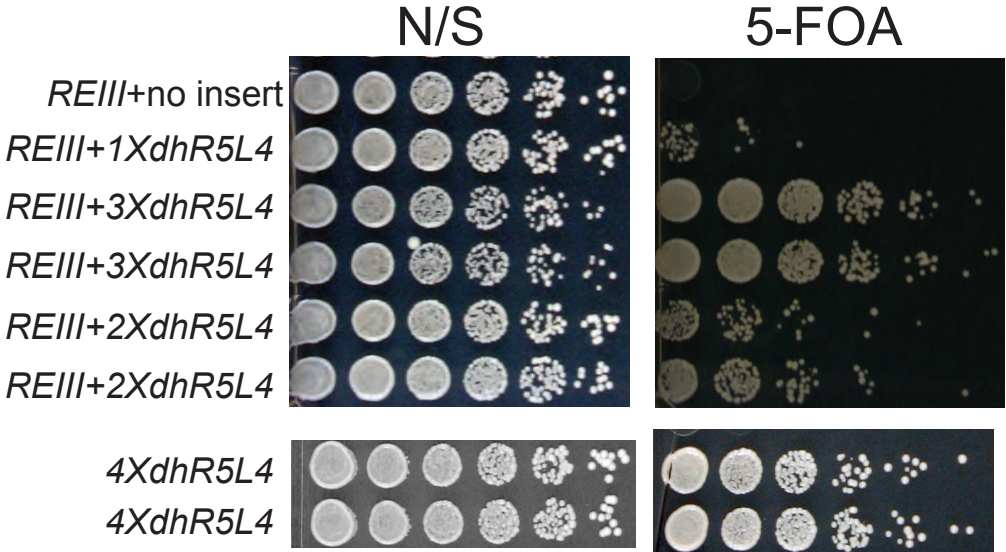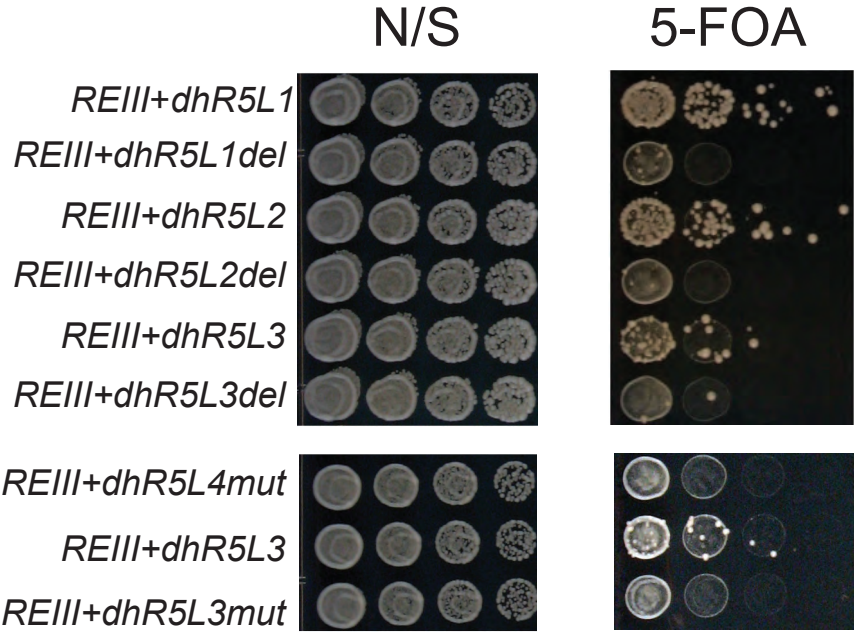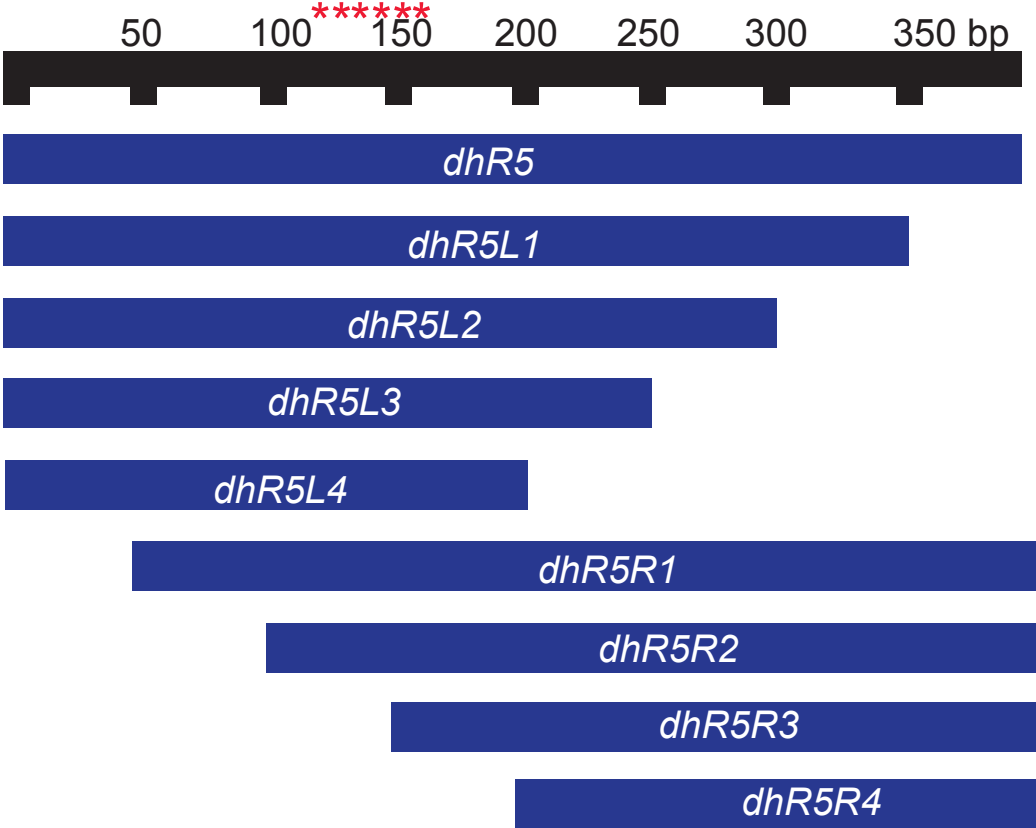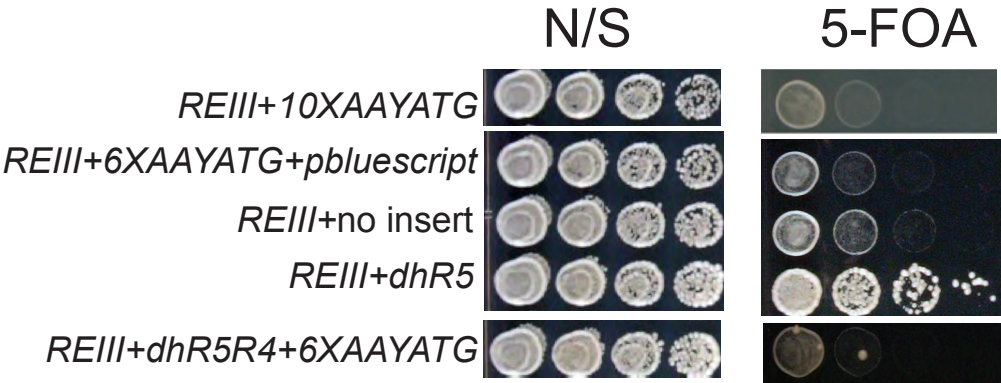
Table 1. Number of the AAYATG motif in Fragments 1-9

Fragment #	# of AAYATG in 'forward' orientation	# of AAYATG in 'reverse' orientation
1	12	2
2	14	2
3	6	0
4	4	3
5	1	3
6	1	0
7	1	2
8	1	3
9	2	5

Table 2. List of chromosome coordinates of different fragments used in this study

Fragment	Chromosome	Chromosome coordinate
padh1+	3	1590559..1591323
terminator	1	2274985..2275583
B-boxes	N/A	Synthetic boundary element*
REIII	2	Mating type locus (13409..15415)
pact1+	2	1477277..1478103
Fragment 1	1	Reverse complement(3787059..3789869)
Fragment 2	1	Reverse complement(3785843..3788836)
Fragment 3	1	Reverse complement(3784847..3787081)
Fragment 4	1	Reverse complement(3783812..3785861)
Fragment 5	1	Reverse complement(3782652..3784867)
Fragment 6	1	Reverse complement(3781725..3783833)
Fragment 7	1	Reverse complement(3780535..3782675)
Fragment 8	1	Reverse complement(3779557..3781747)
Fragment 9	1	Reverse complement(3778457..3780555)
Overlap	1	Reverse complement(3787059..3788836)
Overlap plus	1	Reverse complement(3786849..3789022)
dhL1	1	Reverse complement(3787059..3789022)
dhL2	1	Reverse complement(3787459..3789022)
dhL3	1	Reverse complement(3787859..3789022)
dhL4	1	Reverse complement(3788259..3789022)
dhL5	1	Reverse complement(3788659..3789022)
dhR1	1	Reverse complement(3786849..3788836)
dhR2	1	Reverse complement(3786849..3788436)
dhR3	1	Reverse complement(3786849..3788036)
dhR4	1	Reverse complement(3786849..3787636)
dhR5	1	Reverse complement(3786849..3787236)
dh1	1	Reverse complement(3787459..3788436)
dhR5L1	1	Reverse complement(3786887..3787236)
dhR5L2	1	Reverse complement(3786937..3787236)
dhR5L3	1	Reverse complement(3786987..3787236)
dhR5L4	1	Reverse complement(3787037..3787236)
dhR5R1	1	Reverse complement(3786849..3787198)
dhR5R2	1	Reverse complement(3786849..3787148)
dhR5R3	1	Reverse complement(3786849..3787098)
dhR5R4	1	Reverse complement(3786849..3787048)
snR30+	1	3393950..3395684

*B-boxes sequence:
TGTTCGTAGCAACGTAATAATCGAAAGTAGCAGGACTCGAACCATTCGCAAA
TCGAACCGATCAAAAGTAGAACC

Table 3. List of *S. pombe* strains used in this study.

Strain name	Genotype
PM06	*S. pombe* wild type strain 972 *M(h-)*
PM251[#]	*P(h+), ura4-DS/E, ade6-210, leu1-32, imr1L(NcoI)::ura4+, otr1R(SphI)::ade6+*
PM131	PM06, *ura4::padh1*+-ter-Bboxes-*natMX*
PM26	PM06, *ura4::padh1*+-Fragment 1F-ter-Bboxes-*natMX*
PM27	PM06, *ura4::padh1*+-Fragment 1R-ter-Bboxes-*natMX*
PM28	PM06, *ura4::padh1*+-Fragment 2F-ter-Bboxes-*natMX*
PM31	PM06, *ura4::padh1*+-Fragment 2R-ter-Bboxes-*natMX*
PM68	PM06, *ura4::padh1*+-Fragment 3F-ter-Bboxes-*natMX*
PM34	PM06, *ura4::padh1*+-Fragment 3R-ter-Bboxes-*natMX*
PM37	PM06, *ura4::padh1*+-Fragment 4F-ter-Bboxes-*natMX*
PM39	PM06, *ura4::padh1*+-Fragment 4R-ter-Bboxes-*natMX*
PM42	PM06, *ura4::padh1*+-Fragment 5F-ter-Bboxes-*natMX*
PM45	PM06, *ura4::padh1*+-Fragment 5R-ter-Bboxes-*natMX*
PM48	PM06, *ura4::padh1*+-Fragment 6F-ter-Bboxes-*natMX*
PM51	PM06, *ura4::padh1*+-Fragment 6R-ter-Bboxes-*natMX*
PM54	PM06, *ura4::padh1*+-Fragment 7F-ter-Bboxes-*natMX*
PM57	PM06, *ura4::padh1*+-Fragment 7R-ter-Bboxes-*natMX*
PM60	PM06, *ura4::padh1*+-Fragment 8F-ter-Bboxes-*natMX*
PM63	PM06, *ura4::padh1*+-Fragment 8R-ter-Bboxes-*natMX*
PM70	PM06, *ura4::padh1*+-Fragment 9F-ter-Bboxes-*natMX*
PM65	PM06, *ura4::padh1*+-Fragment 9F-ter-Bboxes-*natMX*
PM428	PM06, *ura4::padh1*+-Fragment 1F (barcode)-ter-Bboxes-*natMX*
PM1033	PM428, *dcr1Δ::kanMX*
PM259	PM06, *ura4:*ter-Bboxes-*natMX*
PM959	PM06, *ura4:*Fragment 1F-ter-Bboxes-*natMX*
PM174	PM06, *ura4::padh1*+-Fragment Overlap-ter-Bboxes-*natMX*
PM176	PM06, *ura4::padh1*+-Fragment Overlap plus-ter-Bboxes-*natMX*
PM243	PM06, *ura4::padh1*+-*dhL1*-ter-Bboxes-*natMX*
PM213	PM06, *ura4::padh1*+-*dhL2*-ter-Bboxes-*natMX*
PM215	PM06, *ura4::padh1*+-*dhL3*-ter-Bboxes-*natMX*
PM217	PM06, *ura4::padh1*+-*dhL4*-ter-Bboxes-*natMX*
PM219	PM06, *ura4::padh1*+-*dhL5*-ter-Bboxes-*natMX*
PM221	PM06, *ura4::padh1*+-*dhR1*-ter-Bboxes-*natMX*
PM223	PM06, *ura4::padh1*+-*dhR2*-ter-Bboxes-*natMX*
PM225	PM06, *ura4::padh1*+-*dhR3*-ter-Bboxes-*natMX*
PM227	PM06, *ura4::padh1*+-*dhR4*-ter-Bboxes-*natMX*
PM245	PM06, *ura4::padh1*+-*dhR5*-ter-Bboxes-*natMX*
PM1251	PM06, *ura4::padh1*+-*dh1*-ter-Bboxes-*natMX*
PM1035	PM428, *clr4Δ::kanMX*

PM1129	PM06, *ura4::padh1+*-ter-*REIII*-Bboxes-*natMX*
PM1137	PM06, *ura4::padh1+-dhL1*-ter-*REIII*-Bboxes-*natMX*
PM1138	PM06, *ura4::padh1+-dhL2*-ter-*REIII*-Bboxes-*natMX*
PM1139	PM06, *ura4::padh1+-dhL3*-ter-*REIII*-Bboxes-*natMX*
PM1140	PM06, *ura4::padh1+-dhL4*-ter-*REIII*-Bboxes-*natMX*
PM1141	PM06, *ura4::padh1+-dhL5*-ter-*REIII*-Bboxes-*natMX*
PM1142	PM06, *ura4::padh1+-dhR1*-ter-*REIII*-Bboxes-*natMX*
PM1143	PM06, *ura4::padh1+-dhR2*-ter-*REIII*-Bboxes-*natMX*
PM1144	PM06, *ura4::padh1+-dhR3*-ter-*REIII*-Bboxes-*natMX*
PM1145	PM06, *ura4::padh1+-dhR4*-ter-*REIII*-Bboxes-*natMX*
PM1146	PM06, *ura4::padh1+-dhR5*-ter-*REIII*-Bboxes-*natMX*
PM1153	PM1146, *dcr1Δ::kanMX*
PM1148	PM1146, *pcr1Δ::kanMX*
PM1149	PM06, *ura4::padh1+-dhR5 reverse*-ter-*REIII*-Bboxes-*natMX*
PM1150	PM06, *ura4::dhR5*-ter-*REIII*-Bboxes-*natMX*
PM1147	PM06, *ura4::padh1+*-Fragment 4-ter-*REIII*-Bboxes-*natMX*
PM1151	PM06, *ura4::padh1+*-pbluescript-ter-*REIII*-Bboxes-*natMX*
PM1152	PM06, *ura4::padh1+-leu1*-ter-*REIII*-Bboxes-*natMX*
PM1134	PM06, *ura4::padh1+-pact1+**-*REIII*-Bboxes-*natMX*
PM1135	PM06, *ura4::padh1+-dhR5-pact1+**-*REIII*-Bboxes-*natMX*
PM1136	PM06, *ura4::padh1+*-pbluescript-*pact1+**-*REIII*-Bboxes-*natMX*
PM1220	PM06, *ura4::padh1+-dhR5L1*-ter-*REIII*-Bboxes-*natMX*
PM1221	PM06, *ura4::padh1+-dhR5L2*-ter-*REIII*-Bboxes-*natMX*
PM1222	PM06, *ura4::padh1+-dhR5L3*-ter-*REIII*-Bboxes-*natMX*
PM1130	PM06, *ura4::padh1+-dhR5L4*-ter-*REIII*-Bboxes-*natMX*
PM1223	PM06, *ura4::padh1+-dhR5R1*-ter-*REIII*-Bboxes-*natMX*
PM1224	PM06, *ura4::padh1+-dhR5R2*-ter-*REIII*-Bboxes-*natMX*
PM1225	PM06, *ura4::padh1+-dhR5R3*-ter-*REIII*-Bboxes-*natMX*
PM1226	PM06, *ura4::padh1+-dhR5R4*-ter-*REIII*-Bboxes-*natMX*
PM2071/1132	PM06, *ura4::padh1+-3XdhR5L4*-ter-*REIII*-Bboxes-*natMX*
PM2072/1131	PM06, *ura4::padh1+-2XdhR5L4*-ter-*REIII*-Bboxes-*natMX*
PM2073/1133	PM06, *ura4::padh1+-4XdhR5L4*-ter-Bboxes-*natMX*
PM2074	PM06,*ura4::padh1+-dhR5L1del***-ter-*REIII*-Bboxes-*natMX*
PM2075	PM06,*ura4::padh1+-dhR5L2del***-ter-*REIII*-Bboxes-*natMX*
PM2076	PM06,*ura4::padh1+-dhR5L3del***-ter-*REIII*-Bboxes-*natMX*
PM2077	PM06,*ura4::padh1+-dhR5L3mut****-ter-*REIII*-Bboxes-*natMX*
PM2078	PM06,*ura4::padh1+-dhR5L4mut****-ter-*REIII*-Bboxes-*natMX*
PM2079	PM06,*ura4::padh1+-10XAAYATG*-ter-*REIII*-Bboxes-*natMX*
PM2080	PM06,*ura4::padh1+-6XAAYATG+pbluescript*-ter-*REIII*-Bboxes-*natMX*
PM2081	PM06, *ura4::padh1+-dhR5R4+6XAAYATG*-ter-*REIII*-Bboxes-*natMX*

PM2082	PM06, *ura4::padh1+*-ter-*snR30*-Bboxes-*natMX*
PM2083	PM06, *ura4::padh1+*-*dh1*-ter-*snR30*-Bboxes-*natMX*
PM2084	PM06, *ura4::snR30*-*padh1+^*-Bboxes-*natMX*
PM2085	PM06, *ura4::snR30*-*pact1+^*-Bboxes-*natMX*
PM2086	PM06, *ura4::padh1+*-*pact1+**-*snR30*-Bboxes-*natMX*
PM2087	PM06, *ura4::padh1+*-*dhR5*-*pact1+**-*snR30*-Bboxes-*natMX*
PM2088	PM06, *ura4::padh1+*-*dhR5*-ter-*snR30*-Bboxes-*natMX*
PM2089	PM06, *ura4::padh1+*-*dh1*-*pact1+**-*snR30*-Bboxes-*natMX*

* *act1+* promoter is in the opposite direction of the *adh1+* promoter (reverse complement orientation).

** 6 tandem copies of AAYATG motif are deleted from the fragment.

*** 6 tandem copies of AAYATG motif are randomly mutated on the fragment.

\# From Karl Ekwall

'ter' = terminator (for sequence information see table 2)

'B-boxes' = synthetic boundary element (for sequence information see table 2)

^ *adh1+* or *act1+* promoter is in the reverse complement orientation.

Table 4. List of plasmids used in this study

BHM#	Former name	Type of reporter	Fragment inserted	Used in PM Strains
2002	pSSKF02	*ura4::padh1*+-ter-Bboxes *natMX*	None	PM131
	pKFPM03	*ura4::padh1*+-ter-Bboxes *natMX*	*Fragment 1F*	PM26
	pKFPM04	*ura4::padh1*+-ter-Bboxes *natMX*	*Fragment 1R*	PM27
	pKFPM05	*ura4::padh1*+-ter-Bboxes *natMX*	*Fragment 2F*	PM28
	pKFPM06	*ura4::padh1*+-ter-Bboxes *natMX*	*Fragment 2R*	PM31
	pKFPM07	*ura4::padh1*+-ter-Bboxes *natMX*	*Fragment 3F*	PM68
	pKFPM08	*ura4::padh1*+-ter-Bboxes *natMX*	*Fragment 3R*	PM34
	pKFPM09	*ura4::padh1*+-ter-Bboxes *natMX*	*Fragment 4F*	PM37
	pKFPM10	*ura4::padh1*+-ter-Bboxes *natMX*	*Fragment 4R*	PM39
	pKFPM11	*ura4::padh1*+-ter-Bboxes *natMX*	*Fragment 5F*	PM42
	pKFPM12	*ura4::padh1*+-ter-Bboxes *natMX*	*Fragment 5R*	PM45
	pKFPM13	*ura4::padh1*+-ter-Bboxes *natMX*	*Fragment 6F*	PM48
	pKFPM14	*ura4::padh1*+-ter-Bboxes *natMX*	*Fragment 6R*	PM51
	pKFPM15	*ura4::padh1*+-ter-Bboxes *natMX*	*Fragment 7F*	PM54
	pKFPM16	*ura4::padh1*+-ter-Bboxes *natMX*	*Fragment 7R*	PM57
	pKFPM17	*ura4::padh1*+-ter-Bboxes *natMX*	*Fragment 8F*	PM60
	pKFPM18	*ura4::padh1*+-ter-Bboxes *natMX*	*Fragment 8R*	PM63
	pKFPM19	*ura4::padh1*+-ter-Bboxes *natMX*	*Fragment 9F*	PM70
	pKFPM20	*ura4::padh1*+-ter-Bboxes *natMX*	*Fragment 9R*	PM65
	pSSPM01	*ura4::padh1*+-ter-Bboxes *natMX*	*Fragment overlap*	PM174
	pSSPM02	*ura4::padh1*+-ter-Bboxes *natMX*	*Fragment overlap plus*	PM176
	pdhL1	*ura4::padh1*+-ter-Bboxes *natMX*	*dhL1*	PM243
	pdhL2	*ura4::padh1*+-ter-Bboxes *natMX*	*dhL2*	PM213
	pdhL3	*ura4::padh1*+-ter-Bboxes *natMX*	*dhL3*	PM215
	pdhL4	*ura4::padh1*+-ter-Bboxes *natMX*	*dhL4*	PM217
	pdhL5	*ura4::padh1*+-ter-Bboxes *natMX*	*dhL5*	PM219
	pdhR1	*ura4::padh1*+-ter-Bboxes *natMX*	*dhR1*	PM221
	pdhR2	*ura4::padh1*+-ter-Bboxes *natMX*	*dhR2*	PM223
	pdhR3	*ura4::padh1*+-ter-Bboxes *natMX*	*dhR3*	PM225
	pdhR4	*ura4::padh1*+-ter-Bboxes *natMX*	*dhR4*	PM227
	pdhR5	*ura4::padh1*+-ter-Bboxes *natMX*	*dhR5*	PM245
	pdh1	*ura4::padh1*+-ter-Bboxes *natMX*	*dh1*	PM1251
	pSSPM05	*ura4*::ter-Bboxes-*natMX*	None	PM259
	pSSPM26	*ura4*::ter-Bboxes-*natMX*	*Fragment 1F*	PM959
1932	pDM06	*ura4::padh1*+-ter-*REIII*-Bboxes-*natMX*	None	PM1129
1933	pDM14	*ura4::padh1*+-ter-*REIII*-Bboxes-*natMX*	*dhL1*	PM1137
1934	pDM15	*ura4::padh1*+-ter-*REIII*-Bboxes-*natMX*	*dhL2*	PM1138
1935	pDM16	*ura4::padh1*+-ter-*REIII*-Bboxes-*natMX*	*dhL3*	PM1139
1936	pDM17	*ura4::padh1*+-ter-*REIII*-Bboxes-*natMX*	*dhL4*	PM1140
1937	pDM18	*ura4::padh1*+-ter-*REIII*-Bboxes-*natMX*	*dhL5*	PM1141
1938	pDM22	*ura4::padh1*+-ter-*REIII*-Bboxes-*natMX*	*dhR1*	PM1142
1939	pDM23	*ura4::padh1*+-ter-*REIII*-Bboxes-*natMX*	*dhR2*	PM1143
1940	pDM24	*ura4::padh1*+-ter-*REIII*-Bboxes-*natMX*	*dhR3*	PM1144

1941	pDM25	*ura4::padh1+-ter-REIII-*Bboxes-*natMX*	*dhR4*	PM1145
1942	pDM26	*ura4::padh1+-ter-REIII-*Bboxes-*natMX*	*dhR5*	PM1146
1943	pDM161	*ura4::padh1+-ter-REIII-*Bboxes-*natMX*	*dhR5 reverse*	PM1149
1944	pDM162	*ura4::*ter-*REIII-*Bboxes-*natMX*	*dhR5*	PM1150
1945	pDM137	*ura4::padh1+-ter-REIII-*Bboxes-*natMX*	*Fragment 4F*	PM1147
1946	pDM37	*ura4::padh1+-ter-REIII-*Bboxes-*natMX*	*pBluescript*	PM1151
1947	pDM36	*ura4::padh1+-ter-REIII-*Bboxes-*natMX*	*leu1+*	PM1152
1948	pDM146	*ura4::padh1+-pact1+*-REIII-*Bboxes-*natMX*	None	PM1134
1949	pDM152	*ura4::padh1+-pact1+*-REIII-*Bboxes-*natMX*	*dhR5*	PM1135
1950	pDM154	*ura4::padh1+-pact1+*-REIII-*Bboxes-*natMX*	*pBluescript*	PM1136
1951	pDM44	*ura4::padh1+-ter-REIII-*Bboxes-*natMX*	*dhR5L1*	PM1220
1952	pDM45	*ura4::padh1+-ter-REIII-*Bboxes-*natMX*	*dhR5L2*	PM1221
1953	pDM46	*ura4::padh1+-ter-REIII-*Bboxes-*natMX*	*dhR5L3*	PM1222
1954	pDM47	*ura4::padh1+-ter-REIII-*Bboxes-*natMX*	*dhR5L4*	PM1130
1955	pDM48	*ura4::padh1+-ter-REIII-*Bboxes-*natMX*	*dhR5R1*	PM1223
1956	pDM49	*ura4::padh1+-ter-REIII-*Bboxes-*natMX*	*dhR5R2*	PM1224
1957	pDM50	*ura4::padh1+-ter-REIII-*Bboxes-*natMX*	*dhR5R3*	PM1225
1958	pDM51	*ura4::padh1+-ter-REIII-*Bboxes-*natMX*	*dhR5R4*	PM1226
1959	pDM138	*ura4::padh1+-ter-REIII-*Bboxes-*natMX*	*3XdhR5L4*	PM2071/ PM1132
1960	pDM139	*ura4::padh1+-ter-REIII-*Bboxes-*natMX*	*2XdhR5L4*	PM2072/ PM1131
1961	pDM156	*ura4::padh1+-ter-*Bboxes *natMX*	*4XdhR5L4*	PM2073/ PM1133
1962	pDM58	*ura4::padh1+-ter-REIII-*Bboxes-*natMX*	*dhR5L1del***	PM2074
1963	pDM59	*ura4::padh1+-ter-REIII-*Bboxes-*natMX*	*dhR5L2del***	PM2075
1964	pDM60	*ura4::padh1+-ter-REIII-*Bboxes-*natMX*	*dhR5L3del***	PM2076
1965	pDM68	*ura4::padh1+-ter-REIII-*Bboxes-*natMX*	*dhR5L3mut****	PM2077
1966	pDM67	*ura4::padh1+-ter-REIII-*Bboxes-*natMX*	*dhR5L4mut****	PM2078
1967	pDM57	*ura4::padh1+-ter-REIII-*Bboxes-*natMX*	*10XAAYATG*	PM2079
1968	pDM69	*ura4::padh1+-ter-REIII-*Bboxes-*natMX*	*6XAAYATG+pbl uescript*	PM2080
1969	pDM61	*ura4::padh1+-ter-REIII-*Bboxes-*natMX*	*dhR5R4+6XAAY ATG*	PM2081
1974	pDM180	*ura4::snR30-padh1+^-*Bboxes-*natMX*	None	PM2084
1975	pDM181	*ura4::snR30-pact1+^-*Bboxes-*natMX*	None	PM2085
1976	pDM182	*ura4::padh1+-pact1+*-snR30-*Bboxes-*natMX*	None	PM2086
1977	pDM183	*ura4::padh1+-ter-snR30-*Bboxes-*natMX*	None	PM2082
1978	pDM185	*ura4::padh1+-pact1+*-snR30-*Bboxes-*natMX*	*dhR5*	PM2087
1979	pDM186	*ura4::padh1+-pact1+*-snR30-*Bboxes-*natMX*	*dh1*	PM2089
1980	pDM187	*ura4::padh1+-ter-snR30-*Bboxes-*natMX*	*dhR5*	PM2088

| 1981 | pDM188 | *ura4::padh1+*-ter-*snR30*-Bboxes-*natMX* | *dh1* | PM2083 |

* *act1+* promoter is in the opposite direction of the *adh1+* promoter.
** 6 tandem copies of AAYATG motif are deleted from the fragment.
*** 6 tandem copies of AAYATG motif are randomly mutated on the fragment.
^ *adh1+* or *act1+* promoter is in the reverse complement orientation

Chapter III: A conserved ncRNA-binding protein recruits heterochromatin silencing factors through an RNAi-independent mechanism

Diana B. Marina, Smita Shankar, Prashanthi Natarajan, Jennifer F. Garcia,

Kenneth J. Finn and Hiten D. Madhani

Author contributions:

D.B.M. performed experiments for Figure 1, Figures 3B-D, Figures 4-7, Supplementary Figures S2, S4, S5B and S6. S.S. performed experiments for Figure 2, Supplementary Figures S1 and S3. P.N. performed experiments for Figure 3A and Supplementary Fig. S5A. J.G. constructed the tethered Clr4 reporter strain. K.F. constructed the ectopic heterochromatic silencing reporter strain. D.B.M. and H.D.M. wrote the manuscript. All authors contributed in editing the manuscript.

ABSTRACT

Long non-coding RNAs (lncRNAs) can trigger repressive chromatin. Proteins that link lncRNAs and heterochromatin silencing factors have not been described. In *Schizosaccharomyces pombe,* the assembly of heterochromatin on transcribed non-coding pericentromeric repeats is promoted by RNAi-related enzymes. However, repressive histone methylation (H3K9Me) is only partially reduced in RNAi mutants, indicating the existence of RNAi-independent triggers. In *Saccharomyces cerevisiae*, which lacks H3K9Me, unstable ncRNAs are recognized by the RNA-binding protein Nrd1. Here, we show that the *S. pombe* ortholog, Seb1, is recruited to pericentromeric long ncRNAs to mediate the RNAi-independent pathway. Individual mutation of *dcr1+* (encoding Dicer) or *seb1+* results in equivalent partial reductions of pericentromeric H3K9Me2 levels, but a double mutation eliminates this mark. To accomplish its function, Seb1 physically associates with and recruits NuRD-related chromatin-modifying complex SHREC, whose HDAC and ATPase activities are required for RNAi-independent silencing.   These studies identify a conserved ncRNA-binding protein that mediates heterochromatin assembly independently of RNAi

INTRODUCTION

A major unsolved question in chromatin biology is how long intergenic ncRNAs (lincRNAs) trigger the formation of repressed chromatin. Notable examples of this phenomenon include the inactivation of the X chromosome in female mammals by the XIST ncRNA and the silencing of the INK4a/ARF tumor suppressor locus by the ANRIL ncRNA(Aguilo, Zhou, & Walsh, 2011; Augui, Nora, & Heard, 2011). More recently, a large number of mammalian lincRNAs have been identified by systematic studies(Guttman et al., 2009). Many of these ncRNAs associate with chromatin-modifying complexes(Khalil et al., 2009). Multiple models have been proposed for how these ncRNAs are recognized and recruit chromatin-modifying factors, but little is understood mechanistically(Guttman & Rinn, 2012).

In the fission yeast *S. pombe*, pericentromeric heterochromatin assembly is promoted by transcription of the *dg* and *dh* repeat sequences by RNA polymerase II (PolII) (Djupedal et al., 2005; Kato et al., 2005). The corresponding long ncRNAs are converted into double-stranded RNAs and processed into siRNAs by the combined action of <u>R</u>NA-<u>d</u>irected <u>R</u>NA Polymerase <u>c</u>omplex (RDRC) and Dicer (Dcr1) (Lejeune & Allshire, 2011; Verdel, Vavasseur, Le Gorrec, & Touat-Todeschini, 2009). The factors that initially target these RNAi-related enzymes to the *dg* and *dh* transcripts remain unknown. Candidates include the primal RNAs (priRNAs), RNA polymerase II and the

spliceosome(Bayne et al., 2008; Djupedal et al., 2005; Halic & Moazed, 2010; Kato et al., 2005). The latter two complexes function at many sites in the genome suggesting that signals within the repeats may influence their ability to recruit the siRNA biosynthesis machinery. siRNAs produced by Dicer are bound by Argonaute (Ago1), a component of the RNA induced transcriptional silencing (RITS) complex, and together they promote both degradation of pericentromeric ncRNAs and transcriptional silencing *via* repressive histone methylation (Verdel et al., 2004). These complexes, in turn, recruit the Clr4 methyltransferase complex (CLRC), which methylates lysine 9 on histone H3 (H3K9Me) (Nakayama, Rice, Strahl, Allis, & Grewal, 2001; Zhang, Mosch, Fischle, & Grewal, 2008). The methyl mark serves as a binding platform for the repressive HP1 proteins Swi6 and Chp2(Bannister et al., 2001; Fischer et al., 2009; Thon & Verhein-Hansen, 2000). Both proteins promote the recruitment of SHREC (Snf2-HDAC repressor complex) to pericentromeric heterochromatin(Sadaie et al., 2008; Sugiyama et al., 2007). Moreover, Chp2 has been found to associate with SHREC to form the so-called SHREC2 complex (SHREC complex associated with Chp2) (Motamedi et al., 2008).   Because HP1 proteins promote its recruitment, SHREC has been termed an "effector" of histone methylation(Sugiyama et al., 2007). The core of SHREC consists of silencing factors Clr1 and Clr2, the histone deacetylase Clr3 and the putative chromatin-remodeling enzyme Mit1(Sugiyama et al., 2007). SHREC and SHREC2 resemble the mammalian Nucleosome Remodeling and Deacetylase (NuRD) complex(Motamedi et al., 2008; Sugiyama et al., 2007).

Although RNAi plays a key role in heterochromatin assembly, several lines of evidence indicate the existence of an RNAi-independent pathway that promotes H3K9Me at pericentromeric repeats. Most significantly, mutation of the RNAi machinery reduces H3K9Me2 only two- to five-fold at the *dg* and *dh* repeats(Sadaie, Iida, Urano, & Nakayama, 2004). Additionally, deletion of *clr3+* reduces the levels of pericentromeric H3K9Me2 in cells lacking RNAi(Reyes-Turcu, Zhang, Zofall, Chen, & Grewal, 2011; Yamada, Fischle, Sugiyama, Allis, & Grewal, 2005). At non-pericentromeric heterochromatin, Clr3/SHREC recruitment requires DNA-binding proteins (Sugiyama et al., 2007; Yamada et al., 2005), and it has been suggested that an unknown DNA-binding protein might also recruit SHREC to pericentromeric heterochromatin(Sugiyama et al., 2007). However, the identification of mutations in RNA processing factors (Mlo3, Cid14) that can suppress the pericentromeric silencing defect of RNAi mutants led to the more recent suggestion that the ncRNA might act in the RNAi-independent pathway of heterochromatin assembly, possibly *via* cotranscriptional mechanisms(Reyes-Turcu et al., 2011). These findings point to the possibility that pericentromeric ncRNAs might play a role in recruiting the chromatin-modifying activities of SHREC independently of small RNAs. Here we identify a conserved ncRNA-binding protein, Seb1/Nrd1 that binds pericentromeric ncRNAs and is required for H3K9Me in cells deficient for RNAi. We demonstrate that this ncRNA-binding protein functions by recruiting the activities of SHREC.

RESULTS

Seb1 physically associates with *dg* and *dh* ncRNAs

To investigate how ncRNAs lead to the formation of repressed chromatin, we identified a candidate ncRNA recognition factor in *S. pombe* based on prior studies of ncRNAs in the budding yeast *S. cerevisiae*. There, a class of unstable ncRNAs called cryptic unstable transcripts (CUTs) is recognized by the sequence-specific RNA-binding protein called Nrd1 (Arigo, Eyler, Carroll, & Corden, 2006; Houseley, Kotovic, El Hage, & Tollervey, 2007; Thiebaut, Kisseleva-Romanova, Rougemaille, Boulay, & Libri, 2006). Nrd1 globally associates with PolII *via* a C-terminal domain-interacting domain (CID) and recognizes a specific RNA oligonucleotide through its RNA-recognition motif (RRM) domain(Carroll, Pradhan, Granek, Clarke, & Corden, 2004; Chinchilla et al., 2012; Conrad et al., 2000; Creamer et al., 2011; Jamonnak et al., 2011; H. Kim et al., 2010; Meinhart & Cramer, 2004; Steinmetz & Brow, 1996, 1998; Vasiljeva, Kim, Mutschler, Buratowski, & Meinhart, 2008). Nrd1 also plays a role in recognizing precursors to stable ncRNAs such as snoRNAs and snRNAs to promote their 3' end formation(Dheur et al., 2003; M. Kim et al., 2006; Steinmetz, Conrad, Brow, & Corden, 2001). Although the *S. cerevisiae* lineage lost both H3K9Me and RNAi during its evolution, we hypothesized that the role of Nrd1 in ncRNA recognition might be conserved. To test this, we tagged the *S. pombe* Nrd1 ortholog, Seb1(Mitsuzawa, Kanda, & Ishihama, 2003), and used crosslinking and RNA immunoprecipitation (RIP) to assess its association with *dg*

and *dh* ncRNAs as well as the snoRNA, *snR30*. Seb1 displays a strong association with these ncRNAs but not with the *act1+* RNA (Fig. 1a). As expected, Hrr1, an RNAi factor, physically associates with *dg* and *dh* ncRNAs but not with *snR30* or *act1+* RNA (Fig. 1b). The association of Seb1 with *dg* and *dh* transcripts is maintained in a *clr4Δ* mutant that lacks H3K9Me indicating that this conserved heterochromatic methyl mark is not required for the recruitment of Seb1 to pericentromeric transcripts (Fig. 1c). This is in contrast to RNAi factors which require H3K9Me to display a RIP signal on the *dg* and *dh* transcripts(Rougemaille et al., 2012).

seb1-1 mutant is defective in heterochromatic silencing

We next isolated a mutation in *seb1+* that was defective in heterochromatic silencing. Because *seb1+*, like *NRD1*, is an essential gene(Mitsuzawa et al., 2003), we mutagenized a gene-targeting construct for the endogenous *seb1+* locus (Fig. 2a) and transformed this library into a strain harboring an ectopic heterochromatic silencing reporter system that we had developed for other studies. This system involves the insertion of a 2811-bp fragment of *dh* repeat downstream of the endogenous *ura4+* gene, such that the transcription of this fragment is driven by the *adh1+* promoter (Supplementary Fig. S1a). This fragment ("Fragment 1") was identified as a highly potent inducer of *ura4+* silencing in a systematic study of the activities of *dg* and *dh* fragments (data not shown). Silencing by Fragment 1 requires functional Clr4 and RNAi as well as the *adh1+* promoter; the latter observation indicates that transcription is

72

required for silencing (Supplementary Fig. S1b). Silencing by Fragment 1 also

causes a decrease of *ura4+* transcript level (Supplementary Fig. S1c) and an

increase of H3K9Me2 at the *ura4+* locus (Supplementary Fig. S1d). Screening of

~10,000 colonies produced by transformation of the *seb1+* mutant library yielded

a single mutant that displays a defect in growth on 5-fluoroorotic acid (5-FOA)

media, which selects for strains with a silenced *ura4+* gene (Fig. 2a). This allele,

seb1-1, has 7 nucleotide substitutions in the *seb1+* coding sequence, three of

which change the amino acid sequence. Replacement of *seb1+* with the *seb1-1*

allele in the parental strain recapitulates the 5-FOA phenotype (Fig. 2b). This

mutation also causes a silencing defect at endogenous heterochromatin: a strain

harboring a *ura4+* reporter gene inserted into the inner most repeat (*imr*) region

of centromere 1 displays reduced growth on 5-FOA when harboring the *seb1-1*

allele (Fig. 2c). The *seb1-1* mutation causes an accumulation of the *ura4+*

transcript (Fig. 2d) and a strong defect in H3K9Me2 at the *ura4+* gene (Fig. 2e),

supporting the growth defect observed using the 5-FOA assay.

We constructed all combinations of the three amino acid changes present

in the *seb1-1* allele (G76S, R442G, I524V) and used them to replace the wild-

type *seb1+* sequence in the reporter strain. We found that all three mutations are

required to produce a silencing defect on 5-FOA media (Fig. 2b). However, the

mutant with the three-amino-acid changes (triple mutant) has a milder silencing

defect on 5-FOA when compared to the original *seb1-1* mutant. The silencing

defect of the triple mutant is only obvious at 2 days of growth on 5-FOA,

indicating that the silent mutations also contribute to the phenotype (Fig. 2b).

Moreover, the triple mutant displays an intermediate defect in H3K9Me2 at the

ura4+ locus when compared to the *seb1-1* allele (20X defect for *seb1-1*, 6.5X for

seb1-G76S, R442G, I524V) (Fig. 2e). The triple mutant displays nearly

comparable accumulation of *ura4+* transcript to that of the *seb1-1* mutant (Fig.

2d), likely reflecting distinct sensitivities and thresholds to gene function of the 5-

FOA, RNA and H3K9Me2 assays. As each of the four silent mutations (A45G,

T132A, T1194C, T1260A) changes the wild-type codon to a more rare

synonymous codon(Forsburg, 1994), they could impact protein expression.

Indeed, the level of Seb1 protein is lower in the *seb1-1* mutant when compared to

its level in the wild-type *seb1+* strain (Supplementary Fig. S2). Since the *seb1-1*

allele has a more robust silencing defect compared to the triple mutant, we used

the *seb1-1* allele in our further analyses.

seb1-1 mutant has normal levels of pericentromeric siRNAs

We examined the effect of *seb1-1* mutation on pericentromeric siRNA

production using Northern hybridization and discovered that, unlike *clr4 Δ*

mutant*, seb1-1* displays normal levels of pericentromeric siRNA accumulation

(Fig. 3a). Consistent with the lack of a defect in siRNA production, the *seb1-1*

mutation does not cause an accumulation of *dg* transcripts and only causes a

slight increase in the level of *dh* transcripts (Fig. 3b). In contrast, a catalytically

dead Dcr1 mutant (*dcr1-R1R2;* (Colmenares, Buker, Buhler, Dlakic, & Moazed,

2007)) displays a dramatic increase in *dg* and *dh* transcript levels, presumably

due to a block in their processing into siRNAs (Fig. 3b). We serendipitously

discovered that *seb1-1* confers a temperature-sensitive phenotype at 37°C

(Supplementary Fig. S3a). As with the silencing phenotype, all 7 mutations of

seb1+ are required to produce the temperature sensitivity (Supplementary Fig.

S3a). Northern hybridization demonstrated no defect in siRNA levels in *seb1-1*

mutant, even at the non-permissive temperature (Supplementary Fig. S3b).

Taken together, these data argue that the silencing defect of the *seb1-1* allele

cannot simply be explained by a defect in RNAi.

seb1-1 mutation reduces H3K9Me levels independently of RNAi

To test whether Seb1 functions in the RNAi-independent pathway of

heterochromatin formation, we performed chromatin immunoprecipitation (ChIP)

experiments to measure H3K9Me2 levels at the *dg* and *dh* repeats in the single

and double combinations of *seb1-1* and *dcr1-R1R2* alleles. Strikingly, while the

levels of H3K9Me2 are reduced by only three- to five-fold in the single mutants,

H3K9Me2 is virtually abolished in the *dcr1-R1R2 seb1-1* double mutant

(1.72±0.35 residual fold-enrichment value at *dg* and 3.08±0.49 at *dh*; Fig. 3c).

We observed similar results across the entire pericentromeric region in ChIP-

qPCR experiments using tiled pairs of primers (Braun et al., 2011) (Fig. 3d).

These data demonstrate that Seb1 is an essential mediator of the RNAi-

independent pathway that triggers H3K9Me2 at pericentromeric repeats. To rule

out the trivial possibility that the *dcr1-R1R2 seb1-1* double mutation reduces the

transcription of components of the Clr4 methyltransferase complex (CLRC)

thereby affecting H3K9Me2 indirectly, we performed RT-qPCR analyses and found no reduction in them in the mutant (Supplementary Fig. S4).

seb1-1 mutation does not affect the overall pattern of pericentromeric transcripts

Although classical heterochromatin mediated by H3K9 methylation was ancestrally lost during the evolution of *S. cerevisiae*, Nrd1 has been reported to play a role in promoting a different type of silencing that occurs in the rDNA repeats of budding yeast (Vasiljeva, Kim, Terzi, Soares, & Buratowski, 2008). In this organism, cryptic unstable PolII transcripts of unknown function are produced from rDNA, which is predominantly transcribed by RNA Polymerase I. These PolII transcripts are terminated and targeted for degradation by Nrd1 (Vasiljeva, Kim, Terzi, et al., 2008). In Nrd1 mutants, the defect in termination and turnover leads to dramatic increases in the level of rDNA-derived PolII transcripts and the accumulation of longer transcripts (Vasiljeva, Kim, Terzi, et al., 2008). This transcriptional read-through is associated with increased histone acetylation, reduced nucleosome occupancy, activation of inserted PolII reporter genes and increased recombination between rDNA repeats(Vasiljeva, Kim, Terzi, et al., 2008). We tested whether Seb1 might act by such a mechanism in *S. pombe* pericentromeric regions by determining whether the *seb1-1* mutation causes an increase in pericentromeric transcript size and levels in cells mutated for Dcr1. Northern hybridization using a riboprobe complementary to the region of the *dh* repeats encoded by Fragment 1 revealed heterogeneously-sized transcripts

76

produced from this region that accumulate in the *dcr1-R1R2* mutant (Supplementary Fig. S5a). This pattern is consistent with previous reports(Zaratiegui et al., 2011). No obvious increase in transcript size was apparent nor was there a significant increase in transcript level in the *seb1-1 dcr1-R1R2* double mutant relative to the *dcr1-R1R2* single mutant (Supplementary Fig. S5a). Careful quantification using RT-qPCR also yielded no increase in the abundance of *dh* transcript produced by the *seb1-1* mutation in a *dcr1-R1R2* genetic background (Supplementary Fig. S5b). These data indicate that mechanisms observed previously in *S. cerevisiae* cannot easily explain our observations in *S. pombe*.

Seb1 functions in the same pathway as SHREC in promoting H3K9Me

To further investigate the RNAi-independent mechanism of Seb1 action, we took advantage of the observation that artificially tethering Clr4 without its chromodomain to a euchromatic locus can nucleate heterochromatin and that this maneuver bypasses the requirement for RNAi (Kagansky et al., 2009). We fused the Gal4-DNA-binding domain to Clr4 lacking its chromodomain in a strain that contains four Gal4 binding sites (UAS) upstream of an *ade6+* reporter gene. We inserted this construct by homologous recombination into the middle of the endogenous *can1+* gene. As expected, the tethered Clr4 nucleates heterochromatin at the *ade6+* locus as evidenced by silencing of the *ade6+* gene (Fig. 4a) and an increase of H3K9Me2 at the *ade6+* locus (Fig. 4b). Consistent with published data, the silencing of *ade6+* gene is still observed in the *dcr1Δ*

mutant indicating that heterochromatin formation at this locus occurs independently of RNAi(Kagansky et al., 2009). Also consistent with published data, silencing of the *ade6+* gene requires SHREC as indicated by the loss of silencing in the *clr3Δ* mutant(Kagansky et al., 2009). Importantly, heterochromatin assembly at this reporter gene requires functional Seb1 (Figs. 4a and 4b) as demonstrated by the loss of silencing and H3K9Me2 at the *ade6+* locus in *seb1-1* mutant.   This result clearly indicates a mechanism of action for Seb1 that is distinct from those of known RNAi factors.

Given the similarity in the phenotypes of *seb1-1* and loss of SHREC in the tethered Clr4 assay, we tested whether Seb1 and SHREC function in the same pathway. We were additionally motivated by the observation that the *clr3Δ* mutant, like the *seb1-1* mutant, has been reported to reduce H3K9Me2 in the *dcr1Δ* mutant, which demonstrates a role for SHREC that is independent of RNAi but upstream of histone methylation(Reyes-Turcu et al., 2011; Yamada et al., 2005). We quantitatively measured the levels of H3K9Me2 at *dg* and *dh* repeats in the *dcr1-R1R2 seb1-1* and *dcr1-R1R2 clr3Δ* double mutants. Consistent with published results(Reyes-Turcu et al., 2011; Yamada et al., 2005), we observed that while H3K9Me2 levels at the *dg* and *dh* repeats are modestly reduced in the *dcr1-R1R2* single mutant, these levels are virtually eliminated in the *dcr1-R1R2 clr3Δ* double mutant, a phenotype strikingly similar to that of the *dcr1-R1R2 seb1-1* double mutant (Fig. 5a). Furthermore, the elimination of H3K9Me2 at *dg* and *dh* repeats was also observed in strains that have the *dcr1-R1R2* mutation

combined with a deletion mutation that eliminates the Clr1, Chp2, or Mit1 subunits of SHREC (Fig. 5a). Finally, a catalytically-dead point mutation in the Clr3 HDAC or the Mit1 ATPase domain also eliminates H3K9Me in *dcr1-R1R2* cells (Fig. 5a). These data demonstrate that all known activities of SHREC are required for the RNAi-independent pathway that promotes H3K9Me at pericentromeric repeats.

To further test if Seb1 functions in the same pathway as SHREC in promoting H3K9Me, we compared H3K9Me2 levels at *dg* and *dh* repeats of the *seb1-1 clr3Δ* double mutant to those of the corresponding single mutants. Significantly, the double and single mutants display very similar levels of H3K9Me2, approximately 20-30% of wild-type levels (Fig. 5b). Similar results were obtained when comparing H3K9Me2 levels at *dg* and *dh* repeats of the *seb1-1 clr1Δ* double mutant to the levels of the corresponding single mutants (Fig. 5c). These data provide strong genetic support that Seb1 and SHREC proteins function in the same pathway in promoting H3K9Me at pericentromeric repeats. Moreover, we performed Pol II ChIP experiments and found that the *seb1-1* mutation increases Pol II occupancy at *dg* and *dh* repeats by approximately five- and two-fold (Fig. 5d), respectively, similar to that reported previously for the *clr3Δ* mutation(Motamedi et al., 2008; Sugiyama et al., 2007). To rule out the possibility that *seb1-1* mutation indirectly affects heterochromatin assembly by decreasing the levels of mRNAs that encode the subunits of SHREC, we measured their levels in the wild-type and *seb1-1* strains. We found

that the *seb1-1* mutation does not reduce the levels of the mRNAs encoding any of the subunits of SHREC (Supplementary Fig. S6) further arguing for a direct role of Seb1 in heterochromatin formation.

Seb1 physically interacts with SHREC

Because Seb1 and SHREC function genetically in the same pathway, we hypothesized that Seb1 physically interacts with SHREC to recruit it to pericentromeric repeats. An observation that supports this hypothesis is that the purification of the Clr2 subunit of SHREC was reported to have yielded two peptides from Seb1 – see Supplementary Table S1 in Motamedi et al. (Motamedi et al., 2008). However, Seb1 peptide coverage was low and it was not obtained in other purifications reported.   To test for a physical interaction between Seb1 and SHREC using a more sensitive assay, we epitope-tagged proteins at their endogenous loci, and performed coimmunoprecipitation-immunoblotting experiments(Sugiyama et al., 2007). We found that FLAG-tagged Seb1 coimmunoprecipitated with Clr3-myc (Fig. 6a) but not with a control protein (Cdc2 detected by anti-PSTAIRE), indicating that these 2 proteins physically interact *in vivo*. This interaction is not bridged by RNA since we could still detect the interaction in the presence of RNAse A (Fig. 6b). Seb1 also coimmunoprecipitated with other components of SHREC including Clr1 and Mit1 (Figs. 6c and 6d).   These data provide strong evidence that not only do Seb1 and SHREC function in the same pathway, they also physically interact *in vivo*.

Seb1 recruits SHREC to pericentromeric *dg* and *dh* repeats

To gain further insight of how Seb1 functions to promote H3K9Me, we tested if Seb1 acts upstream of SHREC as might be expected for a recruitment factor. We performed ChIP experiments to measure the enrichment of SHREC in strains harboring epitope-tagged version of the proteins. Although chromatin-remodeling enzymes are notoriously difficult to localize by ChIP (Yen, Vinayachandran, Batta, Koerber, & Pugh, 2012), we reproducibly obtained signals at both the *dg* and *dh* repeats for every subunit of SHREC tested (Clr3, Clr1, Mit1 and Chp2). Strikingly, in the *seb1-1* mutant, this enrichment is abolished or strongly reduced (Figs. 7a-d). In contrast, RIP experiments demonstrate that Seb1 still associates with *dg* and *dh* transcripts in cells lacking SHREC, indicating that Seb1 recruitment to these ncRNAs is not downstream of SHREC (Fig. 7e). Interestingly, we observed a reproducible increase in Seb1 association with *dg* and *dh* ncRNAs in the *clr3Δ* mutant but not the *clr4Δ* mutant suggesting potential feedback regulation of Seb1 recruitment (Figs. 7e and 1c). Together, these data support our hypothesis that Seb1 acts by recruiting SHREC to pericentromeres.

DISCUSSION

Our studies demonstrate a role for the ncRNA-binding protein Seb1 in triggering the RNAi-independent pathway that mediates repressive histone methylation at fission yeast pericentromeric repeat sequences (Fig. 7f). Seb1 is physically recruited to pericentromeric *dh* and *dg* transcripts. Mutation of *seb1+*

yields a silencing defect without impacting the processing of ncRNAs into siRNAs. Most strikingly, in the absence of RNAi, *seb1-1* produces a virtual elimination of pericentromeric repressive histone methylation. Our studies also provide mechanistic insight into how Seb1 functions. Specifically, our data provide strong evidence that Seb1 functions by recruiting the SHREC chromatin-modifying complex (Fig. 7f). SHREC may function to promote H3K9Me by deacetylating the H3 tail, which is presumably necessary for its methylation by the CLRC. Alternatively, SHREC may have non-histone substrates whose deacetylation promotes H3K9Me. As HP1 proteins also promote the recruitment of SHREC, heterochromatin spread may be promoted by a positive feedback loop involving alternating cycles of histone deacetylation and methylation (Fig. 7f). Consequently, SHREC may be considered both an effector and a trigger of histone methylation.

Candidate recruiters of RNAi to heterochromatic regions in *S. pombe* include RNA polymerase II and the spliceosome, (Bayne et al., 2008; Djupedal et al., 2005; Kato et al., 2005) which are essential for viability and operate at a very large number of genomic sites. Presumably additional factors and signals determine where RNAi-related enzymes are recruited by these multi-protein complexes. Likewise, the mediator of RNAi-independent silencing identified here, Seb1, also plays roles outside of heterochromatin specification and is therefore likely to be subject to additional levels of regulation. In *S. cerevisiae*, Nrd1 directly recognizes variably spaced clusters of short degenerate sequences

in CUTs, snoRNAs and snRNAs(Arigo et al., 2006; Carroll et al., 2004; Steinmetz & Brow, 1996; Thiebaut et al., 2006). Given its strong association with a snoRNA (Fig. 1a), Seb1, like Nrd1, is likely to function in the expression of stable ncRNAs such as snoRNAs and snRNAs. We therefore anticipate the existence of anti-silencing mechanisms operative in euchromatin that prevent the triggering of H3K9Me at these sites. Such inhibitory mechanisms that function in euchromatin are plausible since they have recently been identified for the RNAi pathway(Yamanaka et al., 2012). Additionally, there may be additional positive signals encoded in heterochromatic sequences. Nrd1 functions in *S. cerevisiae* with another RNA-binding protein called Nab3; thus Seb1 may also have partners that impact the outcome of its recruitment(Conrad et al., 2000). The nuclear exosome activator Rrp6 has been reported to promote H3K9Me2 in RNAi mutants(Reyes-Turcu et al., 2011). Rrp6 has also been shown to be required for the association of nascent unprocessed RNAs with the DNA template (Libri et al., 2002), which could play a permissive role in keeping Seb1/SHREC near its chromatin substrates.

Our studies demonstrate an essential role for a ncRNA-binding protein in RNAi-independent pericentromeric heterochromatin formation, through recruitment of a chromatin-modifying complex. Because CID-RRM proteins are highly conserved across evolution, it is tempting to speculate that orthologs of Seb1/Nrd1 have a similar function in other contexts in which long ncRNAs trigger the formation of repressive chromatin. Several mammalian noncoding RNAs

involved in chromatin silencing such as *XIST* and *HOTAIR* have been shown to associate with chromatin-modifying activities (Plath et al., 2003; Tsai et al., 2010). However, to our knowledge, no ncRNA-binding proteins have been reported that link long ncRNA to chromatin-modifying activities. In this regard, it is interesting to note that the closest human ortholog of Seb1/Nrd1, a CID-RRM protein called SCAF8 (Becker, Loll, & Meinhart, 2008; Lunde et al., 2010; Patturajan, Wei, Berezney, & Corden, 1998) has yet to be assigned a function.

MATERIALS AND METHODS

Strain Construction and Growth Conditions

Strains were constructed by lithium acetate transformation of plasmid DNA containing 500 bp of targeting homology. Strains were grown in YS medium (5 g/liter Difco yeast extract + 250 mg/liter each of L-histidine, L-leucine, adenine, uracil, and L-lysine and 3% glucose) at 30°C unless noted otherwise.

Silencing Assays

The strains were grown overnight to saturation and diluted to OD_{600} of 1 at the highest dilution. Serial dilutions were performed with dilution factor of 5 and cells were grown on non-selective and 5-FOA (2 grams/liter of 5-fluoroorotic acid) containing media for *ura4+* reporter or SC media (low adenine concentration) for *ade6+* reporter at 30°C for 2-3 days.

Chromatin Immunoprecipitation

The ChIP assays were performed as described previously (Rougemaille, Shankar, Braun, Rowley, & Madhani, 2008) except for a few minor changes: 1. Cells were lysed by bead beating 7 times for 1 min each with 2 min rests on ice. 2. Chromatin fraction was sonicated 20 times for 30 s each with 1-min rest in between cycles using a Bioruptor®. 3. The following antibodies were used: Ab1220 (Abcam) for H3K9Me2 ChIP, Ab817 (Abcam) for Pol II ChIP and Ab32 (Abcam) for Clr3-myc, Clr1-myc, Mit1-myc and Chp2-myc ChIPs. 4. Protein A or G Dynabeads were used instead of Sepharose beads.

Reverse Transcription quantitative Polymerase Chain Reaction (RT-qPCR)

RNA extraction was performed as described previously (Rougemaille et al., 2008). Five μg of total RNA was treated with 2 U of Turbo DNase I (Ambion) and used in each reverse transcription reaction with 2.5 U of AMV RT (Promega) and strand-specific primers or random 9-mer. The reverse transcription reaction was performed at 42°C for 2 hours. The cDNA samples were analyzed by quantitative PCR using SYBR Green (Invitrogen).

RNA Immunoprecipitation

250 ml cultures were grown to OD_{600} of 3-4. Cells were crosslinked by adding 0.25% of formaldehyde. Cell pellets were resuspended in RIPA buffer (1% NP-40, 0.5% sodium deoxycholate, 0.1% SDS, 150 mM NaCl, 50 mM Tris-HCl pH 8.0, 2 mM EDTA) supplemented with 1 mM PMSF and 40 U/ml of RNase

inhibitor (New England Biolabs). Cell lysis was accomplished mechanically using a ball mill (Retsch). Frozen pellets were lysed for 5 cycles (3 minutes per cycle) at 15 Hz. 60 μl of 50% resuspension of Anti-Flag M2 agarose beads (Sigma) were added into each immunoprecipitation (IP) sample. All IP samples were incubated for 2 hours at 4°C with constant nutation. The IP beads were washed 2 times with low salt buffer (150 mM NaCl, 10 mM Tris-HCl pH 7.5, 0.5% Triton X-100) and 3 times with high salt buffer (1 M NaCl, 10 mM Tris-HCl pH 7.5, 0.5% Triton X-100). Each wash was for 10 minutes. After washing, crosslinks were reversed by incubation at 70°C for 45 minutes in reverse buffer (10 mM Tris-HCl pH 6.8, 5 mM EDTA, 10 mM DTT, 1% SDS) and subjected to treatment with 40 μg of proteinase K. RNA extraction was performed by adding sodium acetate (final concentration 0.3 M) and 1X volume of phenol-chloroform followed by ethanol precipitation. DNase treatment and RT-qPCR were performed as described above.

Coimmunoprecipitation

250 ml cultures were grown to OD_{600} of 2.5-3. Cell pellets were resuspended in lysis buffer (25 mM HEPES KOH pH 7.9, 0.1 mM EDTA pH 8.0, 0.5 mM EGTA pH 8.0, 2 mM $MgCl_2$, 20% glycerol, 0.1% Tween and 250 mM KCl) supplemented with 1 mM PMSF, 1.3 mM Benzamidine, Roche complete protease inhibitor cocktail (1 tablet in 50 ml), 0.1 mM $NaVO_4$ and 1 mM of NaN_3. 60 μl of a 50% suspension of Anti-Flag M2 agarose beads (Sigma) were added into each immunoprecipitation (IP) sample. All IP samples were incubated for 3

hours at 4°C with constant nutation. For RNase A treatment, RNase A
(Fermentas) was added to the IP samples at a concentration of 10µg/mL of
extract at the beginning of incubation with FLAG beads. The IP beads were
washed 3 times with cold lysis buffer (10 minutes per wash) followed by heating
at 70°C for 15 minutes to elute the immunoprecipitated proteins. The IP samples
and whole cell extracts were analyzed by immunoblotting using nitrocellulose
membrane. The membrane was blocked using 5% non-fat dry milk in 1X TBST
(0.1% Triton X). The proteins were detected by anti-myc (1:3000 dilution, Abcam
Ab9106), anti-FLAG (1:3000 dilution, Sigma F3165) and anti-PSTAIRE (1:3000
dilution, Santa Cruz SC-53) as primary antibodies and by goat anti-rabbit or goat
anti-mouse IgG-HRP conjugate (1:8000 dilution, Bio-Rad) as the secondary
antibodies.

Northern Analysis

RNA extraction was performed as described previously (Rougemaille et al.,
2008). For the detection of pericentromeric siRNAs, the small RNA fraction was
isolated by precipitating the flow-through from applying the total RNA on a
Qiagen RNeasy Midi column. Thirty micrograms of small RNA was used for
Northern analysis performed as described (Buhler, Haas, Gygi, & Moazed,
2007). Membrane was blocked for 30 minutes and hybridized overnight at 35°C
in Ambion ULTRAhyb Ultrasensitive hybridization buffer. Membrane was washed
twice at 35°C with 2X SSC, 0.1% SDS and another two times with 0.1X SSC,
0.1% SDS. Centromeric *dh* siRNAs were detected by a complementary

radioactively labeled riboprobe (Supplementary Table 2) generated by *in vitro* transcription from a linearized plasmid using the Ambion T7 MAXIscript kit. Loading control transcript, *snoRNA69* and the two oligonucleotides sized 20 and 30 used as markers were detected by complementary labeled oligos listed in Supplementary Table 2. For the detection of full length *dh* transcripts, 10 μ g of total RNA was separated on a 1% agarose gel containing 2.2 M formaldehyde and transferred onto a Hybond N membrane. The membrane was blocked at 65°C for 1 hr and hybridized overnight with a radioactively labeled riboprobe complementary to the *dh* fragment sense transcript. Washes were done at 65°C as described above and the membrane was exposed to a storage phosphor screen for 45 minutes. Ethidium-bromide-stained rRNA was used as a loading control. Fermentas Riboruler was used to determine the size.

Allele Screen

To accomplish the *seb1+* allele screen described in the text, a gene-targeting plasmid containing the gene with 500 bp of upstream and downstream sequences and a selectable marker was constructed. The entire construct was mutagenized by PCR amplification using *Taq* polymerase. The PCR products were used to transform a strain harboring the Fragment 1 reporter construct. Approximately 10,000 colonies were screened on 5-FOA containing media for silencing defective mutants at 30°C. Positives were retested by recloning of the *seb1+* allele, introduction into the parental strain by homologous replacement and re-assessment of the phenotype. A single allele, *seb1-1* passed this test.

ACKNOWLEDGMENTS

FIGURE LEGENDS

Figure 1: Seb1 physically associates with pericentromeric repeat ncRNAs.

(a), (b) and (c) RIP experiments measuring the enrichment of Seb1-FLAG or Hrr1-FLAG at *dg, dh, act1+* transcripts and *snR30* snoRNA in the wild-type and/or *clr4Δ* strains. Shown are mean values relative to the untagged strain ± SD of three parallel IP samples of one representative experiment.

Figure 2: *seb1-1* mutant is defective in heterochromatic silencing at pericentromeric repeats.

(a) Schematic of the *seb1+* allele screen.

(b) Top: Schematic of the ectopic heterochromatic silencing reporter construct used in the allele screen. Bottom: Silencing assays of *seb1+* mutations in the ectopic heterochromatic silencing reporter strain background. Cells were plated on non-selective rich YS media (N/S) and YS media with 5-FOA (5-FOA).

(c) Top: Schematic of centromere 1 with the *ura4+* reporter gene inserted in the *inner most repeat (imr)* region. Bottom: Silencing assay of *seb1-1* mutation in the pericentromeric *ura4+* reporter strain background. Cells were plated on non-selective YS media (N/S) and YS media with 5-FOA (5-FOA).

(d) RT-qPCR analysis of *ura4+* transcript levels (normalized to *act1+* transcript levels) in the wild-type strain, the *seb1-1* mutant and the strain with three amino-acid mutations in *seb1+*. Shown are mean values relative to wild-type ± SD of three parallel RT reactions of one representative experiment.

(e) ChIP analysis of H3K9Me2 levels at *ura4+* locus (normalized to H3K9Me2 levels at *act1+* locus) in the wild-type strain, the *seb1-1* mutant and the strain with three amino-acid mutations in *seb1+*. Shown are mean values relative to wild-type ± SD of three parallel IP samples of one representative experiment.

Figure 3: *seb1-1* mutation does not affect RNAi.

(a) Riboprobe siRNA Northern blots detecting *dh* siRNAs in the wild-type, *clr4Δ* and *seb1-1* strains. *snoRNA69* was used as a loading control.

(b) RT-qPCR analysis of *dg* and *dh* transcript levels (normalized to *act1+* transcript levels) in wild-type, *seb1-1* and *dcr1-R1R2* strains. Shown are mean values relative to wild-type ± SD of three parallel RT reactions of one representative experiment.

(c) ChIP analysis of H3K9Me2 levels at *dg* and *dh* repeats (normalized to H3K9Me2 levels at *act1+* locus) in a wild-type strain, *seb1-1* and *dcr1-R1R2*

single mutants and the *dcr1-R1R2 seb1-1* double mutant. Shown are mean values ± SD of three parallel IP samples of one representative experiment.

(d) ChIP analysis of H3K9Me2 levels at centromere 1 (normalized to H3K9Me2 levels at *act1+* locus) in wild-type strain, *seb1-1* and *dcr1-R1R2* single mutants and the *dcr1-R1R2 seb1-1* double mutant.

Figure 4: Silencing produced by tethering Clr4 to DNA requires Seb1 and Clr3 but not RNAi.

(a) Top: Schematic of the tethered Clr4 strategy. Gal4 DNA-binding domain (GBD) is used to replace the chromodomain (CD) of Clr4. Four Gal4 binding sites (UAS) were placed near the *ade6+* reporter gene. The entire construct was inserted in the *can1+* locus. Bottom: Silencing assays of wild-type, *seb1-1, clr3Δ* and *dcr1Δ* mutations in the tethered Clr4 reporter strain background. Cells were plated on rich (YS) or low adenine (SC) media.

(b) ChIP analysis of H3K9Me2 levels at the *ade6+* locus (normalized to H3K9Me2 levels at *act1+* locus) in strains described in part (a). Shown are mean values relative to wild-type ± SD of three parallel IP samples of one representative experiment.

Figure 5: Seb1 functions in the same pathway as SHREC to promote H3K9Me.

(a) ChIP analysis of H3K9Me2 levels at *dg* and *dh* repeats (normalized to H3K9Me2 levels at *act1+* locus) in wild-type, *dcr1-R1R2, dcr1-R1R2 seb1-1,*

dcr1-R1R2 clr3Δ, dcr1-R1R2 clr3D232N, dcr1-R1R2 mit1Δ, dcr1-R1R2 mit1K587A, dcr1-R1R2 clr1Δ and dcr1-R1R2 chp2Δ strains. Shown are mean values ± SD of three parallel IP samples of one representative experiment.

(b) ChIP analysis of H3K9Me2 levels at *dg* and *dh* repeats (normalized to H3K9Me2 levels at *act1+* locus) in the wild-type strain, the *seb1-1* and *clr3Δ* single mutants and the *seb1-1 clr3Δ* double mutant. Shown are mean values ± SD of three parallel IP samples of one representative experiment.

(c) ChIP analysis of H3K9Me2 levels at *dg* and *dh* repeats (normalized to H3K9Me2 levels at *act1+* locus) in the wild-type strain, the *seb1-1* and *clr1Δ* single mutants and the *seb1-1 clr1Δ* double mutant. Shown are mean values ± SD of three parallel IP samples of one representative experiment.

(d) ChIP analysis of PolII levels at *dg* and *dh* repeats (normalized to PolII levels at *act1+* locus) in the wild-type strain, the *seb1-1* and *clr3Δ* single mutants. Shown are mean values ± SD of three parallel IP samples of one representative experiment.

Figure 6: Seb1 physically associates with SHREC *in vivo*.

(a) Coimmunoprecipitation of Seb1 with Clr3. Strains expressing endogenously tagged Seb1-CBP-2XFLAG, Clr3-4myc or both were subjected to anti-FLAG immunoprecipitation. The whole cell extract (WCE) and immunoprecipitated (IP) samples were detected by anti-myc (top), anti-FLAG (middle) and anti-PSTAIRE (bottom) immunoblots, the latter serves as a loading and specificity control.

(b) Coimmunoprecipitation of Seb1 with Clr3 in the presence of RNAse A. The 2 bottom panels are images of agarose gels of RT-qPCR experiments to detect *dh* transcripts in the presence (+RT) or absence (-RT) of Reverse Transcriptase.

(c) and (d) Coimmunoprecipitation of Seb1 with Clr1 and Mit1. Strains expressing endogenous levels of Seb1-CBP-2XFLAG, Clr1-13myc or both (panel c) and Seb1-CBP-2XFLAG, Mit1-13myc or both (panel d) were subjected to anti-FLAG immunoprecipitation. The whole cell extract (WCE) and immunoprecipitated (IP) samples were detected by anti-myc (top) and anti-FLAG (bottom) immunoblots.

Figure 7: Seb1 recruits SHREC to pericentromeric heterochromatin.

(a) – (d) ChIP analyses of Clr3-myc, Clr1-myc, Mit1-myc and Chp2-myc levels at *dg* and *dh* repeats (normalized to their levels at *act1+* locus) in the wild-type and *seb1-1* strains. Shown are mean values relative to the untagged strain ± SD of three parallel IP samples of one representative experiment.

(e) RIP experiments measuring the enrichment of Seb1-FLAG at *dg, dh* and *act1+* transcripts in the wild-type and *clr3Δ* strains. Shown are mean values relative to the untagged strain ± SD of three parallel IP samples of one representative experiment.

(f) Model for the RNAi-independent role of Seb1 in recruiting SHREC to pericentromeric heterochromatin.

Supplementary Figure S1: Development of an ectopic heterochromatic silencing reporter.

(A) Schematic of the ectopic heterochromatic silencing reporter construct used in the allele screen. The construct consists of a 2.8-kb fragment derived from pericentromeric *dh* repeats (named 'Fragment 1') driven by the *adh1+* promoter, a bidirectional terminator ('term'), B-boxes boundary element ('B') and a resistant drug marker ('natR'). The entire construct was inserted downstream of the endogenous *ura4+* gene.

(B) Silencing assays of strains with different variations or mutations of the ectopic heterochromatic silencing reporter construct described in Supplementary Fig. S1A. 'No fragment' indicates that no fragment is inserted downstream of the *adh1+* promoter. The control fragment is Fragment 1 inserted in the 'reverse' orientation. 'No promoter' indicates that the *adh1+* promoter is absent from the construct. Cells were plated on non-selective YS media (N/S) and YS media with 5-FOA (5-FOA).

(C) RT-qPCR analysis of *ura4+* transcript levels (normalized to *act1+* transcript levels) in strains described in Supplementary Fig. S1B. Shown are mean values relative to the 'No fragment' strain ± SD of three parallel RT reactions of one representative experiment.

(D) ChIP analysis of H3K9Me2 levels at *ura4+* locus (normalized to H3K9Me2 levels at *act1+* locus) in strains described in Supplementary Fig. S1B. Shown are mean values relative to the 'No fragment' strain ± SD of three parallel IP samples of one representative experiment.

Supplementary Figure S2: *seb1-1* mutation lowers the protein level of Seb1.

Western blot analysis comparing levels of Seb1 protein in the wild-type and *seb1-1* strains. In both strains, Seb1 is endogenously tagged with FLAG epitope tag. The cell extracts from both strains were subjected to anti-FLAG and anti-PSTAIRE immunoblots. The latter immunoblot was to detect Cdc2 protein used as a loading control.

Supplementary Figure S3: *seb1-1* mutant is temperature sensitive at 37°C.

(A) Growth assays of *seb1+* mutations at 30°C and 37°C. Cells were plated on non-selective (N/S) YS media.

(B) Riboprobe siRNA Northern blots detecting *dh* siRNAs in the wild-type, *clr4Δ* and *seb1-1* strains grown at 30°C and 37°C.

Supplementary Figure S4: *seb1-1* mutation does not affect CLRC subunit transcript levels.

RT-qPCR analysis of CLRC transcript levels (normalized to *act1+* transcript levels) in wild-type strain, *seb1-1* and *dcr1-R1R2* single and double mutants. Shown are mean values relative to wild-type ± SD of three parallel RT reactions of one representative experiment.

Supplementary Figure S5: *seb1-1* mutation does not affect overall pattern of *dh*-derived transcripts.

(A) Northern blot analysis to detect Fragment 1-homologous *dh* transcripts in wild-type strain, *seb1-1* and *dcr1-R1R2* single and double mutants. The size marker is indicated. 28s rRNA was used as a loading control.

(B) RT-qPCR analysis of *dh* transcript levels (normalized to *act1+* transcript levels) in wild-type, *dcr1-R1R2* and *dcr1-R1R2 seb1-1* strains. Shown are mean values relative to wild-type ± SD of three parallel RT reactions of one representative experiment.

Supplementary Figure S6: *seb1-1* mutation does not affect SHREC subunit transcript levels.

RT-qPCR analysis of SHREC transcript levels (normalized to *act1+* transcript levels) in wild-type and *seb1-1* strains. Shown are mean values relative to wild-type ± SD of three parallel RT reactions of one representative experiment.

REFERENCES

Aguilo, F., Zhou, M. M., & Walsh, M. J. (2011). Long noncoding RNA, polycomb, and the ghosts haunting INK4b-ARF-INK4a expression. [Research Support, N.I.H., Extramural

Research Support, Non-U.S. Gov't

Review]. *Cancer Res, 71*(16), 5365-5369. doi: 10.1158/0008-5472.CAN-10-4379

Arigo, J. T., Eyler, D. E., Carroll, K. L., & Corden, J. L. (2006). Termination of cryptic unstable transcripts is directed by yeast RNA-binding proteins Nrd1 and Nab3. [Research Support, N.I.H., Extramural]. *Mol Cell, 23*(6), 841-851. doi: 10.1016/j.molcel.2006.07.024

Augui, S., Nora, E. P., & Heard, E. (2011). Regulation of X-chromosome inactivation by the X-inactivation centre. [Research Support, N.I.H., Extramural

Review]. *Nat Rev Genet, 12*(6), 429-442. doi: 10.1038/nrg2987

Bannister, A. J., Zegerman, P., Partridge, J. F., Miska, E. A., Thomas, J. O., Allshire, R. C., & Kouzarides, T. (2001). Selective recognition of methylated lysine 9 on histone H3 by the HP1 chromo domain. *Nature, 410*(6824), 120-124.

Bayne, E. H., Portoso, M., Kagansky, A., Kos-Braun, I. C., Urano, T., Ekwall, K., . . . Allshire, R. C. (2008). Splicing factors facilitate RNAi-directed silencing in fission yeast. *Science, 322*(5901), 602-606. doi: 322/5901/602 [pii]

10.1126/science.1164029

Becker, R., Loll, B., & Meinhart, A. (2008). Snapshots of the RNA processing factor SCAF8 bound to different phosphorylated forms of the carboxyl-terminal domain of RNA polymerase II. [Research Support, Non-U.S. Gov't]. *J Biol Chem, 283*(33), 22659-22669. doi: 10.1074/jbc.M803540200

Braun, S., Garcia, J. F., Rowley, M., Rougemaille, M., Shankar, S., & Madhani, H. D. (2011). The Cul4-Ddb1(Cdt)(2) ubiquitin ligase inhibits invasion of a boundary-associated antisilencing factor into heterochromatin. *Cell, 144*(1), 41-54. doi: S0092-8674(10)01373-5 [pii]

10.1016/j.cell.2010.11.051

Buhler, M., Haas, W., Gygi, S. P., & Moazed, D. (2007). RNAi-dependent and -independent RNA turnover mechanisms contribute to heterochromatic gene silencing. *Cell, 129*(4), 707-721. doi: S0092-8674(07)00454-0 [pii]

10.1016/j.cell.2007.03.038

Carroll, K. L., Pradhan, D. A., Granek, J. A., Clarke, N. D., & Corden, J. L. (2004). Identification of cis elements directing termination of yeast nonpolyadenylated snoRNA transcripts. [Research Support, U.S. Gov't, P.H.S.]. *Mol Cell Biol, 24*(14), 6241-6252. doi: 10.1128/MCB.24.14.6241-6252.2004

Chinchilla, K., Rodriguez-Molina, J. B., Ursic, D., Finkel, J. S., Ansari, A. Z., & Culbertson, M. R. (2012). Interactions of Sen1, Nrd1, and Nab3 with multiple phosphorylated forms of the Rpb1 C-terminal domain in Saccharomyces cerevisiae. [Research Support, N.I.H., Extramural

Research Support, Non-U.S. Gov't

Research Support, U.S. Gov't, Non-P.H.S.]. *Eukaryot Cell, 11*(4), 417-429. doi: 10.1128/EC.05320-11

Colmenares, S. U., Buker, S. M., Buhler, M., Dlakic, M., & Moazed, D. (2007). Coupling of double-stranded RNA synthesis and siRNA generation in fission yeast RNAi. *Mol Cell, 27*(3), 449-461.

Conrad, N. K., Wilson, S. M., Steinmetz, E. J., Patturajan, M., Brow, D. A., Swanson, M. S., & Corden, J. L. (2000). A yeast heterogeneous nuclear ribonucleoprotein complex associated with RNA polymerase II. [Research Support, U.S. Gov't, Non-P.H.S.

Research Support, U.S. Gov't, P.H.S.]. *Genetics, 154*(2), 557-571.

Creamer, T. J., Darby, M. M., Jamonnak, N., Schaughency, P., Hao, H., Wheelan, S. J., & Corden, J. L. (2011). Transcriptome-wide binding sites for components of the Saccharomyces cerevisiae non-poly(A) termination pathway: Nrd1, Nab3, and Sen1. [Research Support, N.I.H., Extramural]. *PLoS Genet, 7*(10), e1002329. doi: 10.1371/journal.pgen.1002329

Dheur, S., Vo le, T. A., Voisinet-Hakil, F., Minet, M., Schmitter, J. M., Lacroute, F., . . . Minvielle-Sebastia, L. (2003). Pti1p and Ref2p found in association with the mRNA 3' end formation complex direct snoRNA maturation. [Research Support, U.S. Gov't, P.H.S.]. *EMBO J, 22*(11), 2831-2840. doi: 10.1093/emboj/cdg253

Djupedal, I., Portoso, M., Spahr, H., Bonilla, C., Gustafsson, C. M., Allshire, R. C., & Ekwall, K. (2005). RNA Pol II subunit Rpb7 promotes centromeric transcription and RNAi-directed chromatin silencing. *Genes Dev, 19*(19), 2301-2306. doi: 19/19/2301 [pii]

10.1101/gad.344205

Fischer, T., Cui, B., Dhakshnamoorthy, J., Zhou, M., Rubin, C., Zofall, M., . . . Grewal, S. I. (2009). Diverse roles of HP1 proteins in heterochromatin assembly and functions in fission yeast. [Research Support, N.I.H., Intramural]. *Proc Natl Acad Sci U S A, 106*(22), 8998-9003. doi: 10.1073/pnas.0813063106

Forsburg, S. L. (1994). Codon usage table for Schizosaccharomyces pombe. [Comparative Study

Research Support, U.S. Gov't, P.H.S.]. *Yeast, 10*(8), 1045-1047. doi: 10.1002/yea.320100806

Guttman, M., Amit, I., Garber, M., French, C., Lin, M. F., Feldser, D., . . . Lander, E. S. (2009). Chromatin signature reveals over a thousand highly conserved large non-coding RNAs in mammals. [Research Support, N.I.H., Extramural

Research Support, Non-U.S. Gov't]. *Nature, 458*(7235), 223-227. doi: 10.1038/nature07672

Guttman, M., & Rinn, J. L. (2012). Modular regulatory principles of large non-coding RNAs. [Review]. *Nature, 482*(7385), 339-346. doi: 10.1038/nature10887

Halic, M., & Moazed, D. (2010). Dicer-independent primal RNAs trigger RNAi and heterochromatin formation. [Research Support, N.I.H., Extramural

Research Support, Non-U.S. Gov't]. *Cell, 140*(4), 504-516. doi: 10.1016/j.cell.2010.01.019

Houseley, J., Kotovic, K., El Hage, A., & Tollervey, D. (2007). Trf4 targets ncRNAs from telomeric and rDNA spacer regions and functions in rDNA copy number control. [Research Support, Non-U.S. Gov't]. *EMBO J, 26*(24), 4996-5006. doi: 10.1038/sj.emboj.7601921

Jamonnak, N., Creamer, T. J., Darby, M. M., Schaughency, P., Wheelan, S. J., & Corden, J. L. (2011). Yeast Nrd1, Nab3, and Sen1 transcriptome-wide binding maps suggest multiple roles in post-transcriptional RNA processing. [Research Support, American Recovery and Reinvestment Act

Research Support, N.I.H., Extramural]. *RNA, 17*(11), 2011-2025. doi: 10.1261/rna.2840711

Kagansky, A., Folco, H. D., Almeida, R., Pidoux, A. L., Boukaba, A., Simmer, F., . . . Allshire, R. C. (2009). Synthetic heterochromatin bypasses RNAi and centromeric repeats to establish functional centromeres. *Science, 324*(5935), 1716-1719. doi: 324/5935/1716 [pii]

10.1126/science.1172026

Kato, H., Goto, D. B., Martienssen, R. A., Urano, T., Furukawa, K., & Murakami, Y. (2005). RNA polymerase II is required for RNAi-dependent heterochromatin assembly. *Science, 309*(5733), 467-469. doi: 1114955 [pii]

10.1126/science.1114955

Khalil, A. M., Guttman, M., Huarte, M., Garber, M., Raj, A., Rivea Morales, D., . . . Rinn, J. L. (2009). Many human large intergenic noncoding RNAs associate with chromatin-modifying complexes and affect gene expression. [Research Support, N.I.H., Extramural

Research Support, Non-U.S. Gov't]. *Proc Natl Acad Sci U S A, 106*(28), 11667-11672. doi: 10.1073/pnas.0904715106

Kim, H., Erickson, B., Luo, W., Seward, D., Graber, J. H., Pollock, D. D., . . . Bentley, D. L. (2010). Gene-specific RNA polymerase II phosphorylation and the CTD code. [Comparative Study

Research Support, American Recovery and Reinvestment Act

Research Support, N.I.H., Extramural

Research Support, Non-U.S. Gov't]. *Nat Struct Mol Biol, 17*(10), 1279-1286. doi: 10.1038/nsmb.1913

Kim, M., Vasiljeva, L., Rando, O. J., Zhelkovsky, A., Moore, C., & Buratowski, S. (2006). Distinct pathways for snoRNA and mRNA termination. *Mol Cell, 24*(5), 723-734. doi: S1097-2765(06)00782-9 [pii]

10.1016/j.molcel.2006.11.011

Lejeune, E., & Allshire, R. C. (2011). Common ground: small RNA programming and chromatin modifications. *Curr Opin Cell Biol, 23*(3), 258-265. doi: S0955-0674(11)00022-6 [pii]

10.1016/j.ceb.2011.03.005

Libri, D., Dower, K., Boulay, J., Thomsen, R., Rosbash, M., & Jensen, T. H. (2002). Interactions between mRNA export commitment, 3'-end quality control, and nuclear degradation. [Research Support, Non-U.S. Gov't
Research Support, U.S. Gov't, P.H.S.]. *Mol Cell Biol, 22*(23), 8254-8266.

Lunde, B. M., Reichow, S. L., Kim, M., Suh, H., Leeper, T. C., Yang, F., . . . Varani, G. (2010). Cooperative interaction of transcription termination factors with the RNA polymerase II C-terminal domain. [Comparative Study
Research Support, N.I.H., Extramural
Research Support, Non-U.S. Gov't]. *Nat Struct Mol Biol, 17*(10), 1195-1201. doi: 10.1038/nsmb.1893

Meinhart, A., & Cramer, P. (2004). Recognition of RNA polymerase II carboxy-terminal domain by 3'-RNA-processing factors. [Research Support, Non-U.S. Gov't]. *Nature, 430*(6996), 223-226. doi: 10.1038/nature02679

Mitsuzawa, H., Kanda, E., & Ishihama, A. (2003). Rpb7 subunit of RNA polymerase II interacts with an RNA-binding protein involved in processing of transcripts. [Research Support, Non-U.S. Gov't]. *Nucleic Acids Res, 31*(16), 4696-4701.

Motamedi, M. R., Hong, E. J., Li, X., Gerber, S., Denison, C., Gygi, S., & Moazed, D. (2008). HP1 proteins form distinct complexes and mediate heterochromatic gene silencing by nonoverlapping mechanisms. *Mol Cell, 32*(6), 778-790. doi: S1097-2765(08)00806-X [pii]
10.1016/j.molcel.2008.10.026

Nakayama, J., Rice, J. C., Strahl, B. D., Allis, C. D., & Grewal, S. I. (2001). Role of histone H3 lysine 9 methylation in epigenetic control of heterochromatin assembly. *Science, 292*(5514), 110-113.

Patturajan, M., Wei, X., Berezney, R., & Corden, J. L. (1998). A nuclear matrix protein interacts with the phosphorylated C-terminal domain of RNA polymerase II. [Research Support, U.S. Gov't, P.H.S.]. *Mol Cell Biol, 18*(4), 2406-2415.

Plath, K., Fang, J., Mlynarczyk-Evans, S. K., Cao, R., Worringer, K. A., Wang, H., . . . Zhang, Y. (2003). Role of histone H3 lysine 27 methylation in X inactivation. [Research Support, Non-U.S. Gov't
Research Support, U.S. Gov't, P.H.S.]. *Science, 300*(5616), 131-135. doi: 10.1126/science.1084274

Reyes-Turcu, F. E., Zhang, K., Zofall, M., Chen, E., & Grewal, S. I. (2011). Defects in RNA quality control factors reveal RNAi-independent nucleation of heterochromatin. *Nat Struct Mol Biol, 18*(10), 1132-1138. doi: nsmb.2122 [pii]
10.1038/nsmb.2122

Rougemaille, M., Braun, S., Coyle, S., Dumesic, P. A., Garcia, J. F., Isaac, R. S., . . . Madhani, H. D. (2012). Ers1 links HP1 to RNAi. [Research Support, N.I.H., Extramural
Research Support, Non-U.S. Gov't
Research Support, U.S. Gov't, Non-P.H.S.]. *Proc Natl Acad Sci U S A, 109*(28), 11258-11263. doi: 10.1073/pnas.1204947109

Rougemaille, M., Shankar, S., Braun, S., Rowley, M., & Madhani, H. D. (2008). Ers1, a rapidly diverging protein essential for RNA interference-dependent heterochromatic silencing in Schizosaccharomyces pombe. *J Biol Chem, 283*(38), 25770-25773.

Sadaie, M., Iida, T., Urano, T., & Nakayama, J. (2004). A chromodomain protein, Chp1, is required for the establishment of heterochromatin in fission yeast. *Embo J, 23*(19), 3825-3835.

Sadaie, M., Kawaguchi, R., Ohtani, Y., Arisaka, F., Tanaka, K., Shirahige, K., & Nakayama, J. (2008). Balance between distinct HP1 family proteins controls heterochromatin assembly in fission yeast. [Research Support, Non-U.S. Gov't]. *Mol Cell Biol, 28*(23), 6973-6988. doi: 10.1128/MCB.00791-08

Steinmetz, E. J., & Brow, D. A. (1996). Repression of gene expression by an exogenous sequence element acting in concert with a heterogeneous nuclear ribonucleoprotein-like protein, Nrd1, and the putative helicase Sen1. [Research Support, Non-U.S. Gov't]. *Mol Cell Biol, 16*(12), 6993-7003.

Steinmetz, E. J., & Brow, D. A. (1998). Control of pre-mRNA accumulation by the essential yeast protein Nrd1 requires high-affinity transcript binding and a domain implicated in RNA polymerase II association. [Research Support, Non-U.S. Gov't

Research Support, U.S. Gov't, P.H.S.]. *Proc Natl Acad Sci U S A, 95*(12), 6699-6704.

Steinmetz, E. J., Conrad, N. K., Brow, D. A., & Corden, J. L. (2001). RNA-binding protein Nrd1 directs poly(A)-independent 3'-end formation of RNA polymerase II transcripts. [Research Support, U.S. Gov't, Non-P.H.S.

Research Support, U.S. Gov't, P.H.S.]. *Nature, 413*(6853), 327-331. doi: 10.1038/35095090

Sugiyama, T., Cam, H. P., Sugiyama, R., Noma, K., Zofall, M., Kobayashi, R., & Grewal, S. I. (2007). SHREC, an effector complex for heterochromatic transcriptional silencing. *Cell, 128*(3), 491-504. doi: S0092-8674(07)00059-1 [pii]

10.1016/j.cell.2006.12.035

Thiebaut, M., Kisseleva-Romanova, E., Rougemaille, M., Boulay, J., & Libri, D. (2006). Transcription termination and nuclear degradation of cryptic unstable transcripts: a role for the nrd1-nab3 pathway in genome surveillance. [Research Support, Non-U.S. Gov't]. *Mol Cell, 23*(6), 853-864. doi: 10.1016/j.molcel.2006.07.029

Thon, G., & Verhein-Hansen, J. (2000). Four chromo-domain proteins of Schizosaccharomyces pombe differentially repress transcription at various chromosomal locations. [Research Support, Non-U.S. Gov't]. *Genetics, 155*(2), 551-568.

Tsai, M. C., Manor, O., Wan, Y., Mosammaparast, N., Wang, J. K., Lan, F., . . . Chang, H. Y. (2010). Long noncoding RNA as modular scaffold of histone modification complexes. [Research Support, N.I.H., Extramural

Research Support, Non-U.S. Gov't

Research Support, U.S. Gov't, Non-P.H.S.]. *Science, 329*(5992), 689-693. doi: 10.1126/science.1192002

Vasiljeva, L., Kim, M., Mutschler, H., Buratowski, S., & Meinhart, A. (2008). The Nrd1-Nab3-Sen1 termination complex interacts with the Ser5-phosphorylated RNA polymerase II C-terminal domain. [Research Support, N.I.H., Extramural

Research Support, Non-U.S. Gov't]. *Nat Struct Mol Biol, 15*(8), 795-804. doi: 10.1038/nsmb.1468

Vasiljeva, L., Kim, M., Terzi, N., Soares, L. M., & Buratowski, S. (2008). Transcription termination and RNA degradation contribute to silencing of RNA polymerase II transcription within heterochromatin. [Research Support, N.I.H., Extramural]. *Mol Cell, 29*(3), 313-323. doi: 10.1016/j.molcel.2008.01.011

Verdel, A., Jia, S., Gerber, S., Sugiyama, T., Gygi, S., Grewal, S. I., & Moazed, D. (2004). RNAi-mediated targeting of heterochromatin by the RITS complex. *Science, 303*(5658), 672-676.

Verdel, A., Vavasseur, A., Le Gorrec, M., & Touat-Todeschini, L. (2009). Common themes in siRNA-mediated epigenetic silencing pathways. *Int J Dev Biol, 53*(2-3), 245-257. doi: 082691av [pii]

10.1387/ijdb.082691av

Yamada, T., Fischle, W., Sugiyama, T., Allis, C. D., & Grewal, S. I. (2005). The nucleation and maintenance of heterochromatin by a histone deacetylase in fission yeast. *Mol Cell, 20*(2), 173-185. doi: S1097-2765(05)01672-2 [pii]

10.1016/j.molcel.2005.10.002

Yamanaka, S., Mehta, S., Reyes-Turcu, F. E., Zhuang, F., Fuchs, R. T., Rong, Y., . . . Grewal, S. I. (2012). RNAi triggered by specialized machinery silences developmental genes and retrotransposons. *Nature*. doi: 10.1038/nature11716

Yen, K., Vinayachandran, V., Batta, K., Koerber, R. T., & Pugh, B. F. (2012). Genome-wide nucleosome specificity and directionality of chromatin remodelers. [Research Support, N.I.H., Extramural

Research Support, U.S. Gov't, Non-P.H.S.]. *Cell, 149*(7), 1461-1473. doi: 10.1016/j.cell.2012.04.036

Zaratiegui, M., Castel, S. E., Irvine, D. V., Kloc, A., Ren, J., Li, F., . . . Martienssen, R. A. (2011). RNAi promotes heterochromatic silencing through replication-coupled release of RNA Pol II. *Nature, 479*(7371), 135-138. doi: nature10501 [pii]

10.1038/nature10501

Zhang, K., Mosch, K., Fischle, W., & Grewal, S. I. (2008). Roles of the Clr4 methyltransferase complex in nucleation, spreading and maintenance of heterochromatin. *Nat Struct Mol Biol, 15*(4), 381-388. doi: nsmb.1406 [pii]

10.1038/nsmb.1406

Figure 1

103

Figure 2

A

Library of PCR-mutagenized *seb1+* targeting constructs

*seb1** | *hygB*

Knock into
seb1+ locus

*seb1** *hygB*

seb1+

ura4+ *padh1+* *Frag1* *term* B *natR*

~10,000 colonies

Screen for silencing-defective mutants (5-FOA)

**Test candidates by reintroduction
into reporter gene strain**

***seb1-1* silencing-defective mutant**

B Ectopic heterochromatic
silencing reporter

ura4+ *padh1+* *Frag1* *term* B *natR*

	N/S	5-FOA (2 days)	5-FOA (3 days)
WT			
seb1-1 (orig. isolate)			
seb1-1 (Retest)			
seb1-G76S			
seb1-R442G			
seb1-I524V			
seb1-G76S,R442G			
seb1-G76S,I524V			
seb1-R442G,I524V			
seb1-G76S,R442G,I524V			

Figure 2

C

ura4+

cen1

otr *dh* *dg* imr cnt imr *dg* otr *dh*

N/S   5-FOA

WT

seb1-1

D RT-qPCR

E H3K9Me2 ChIP

Figure 3

A

B
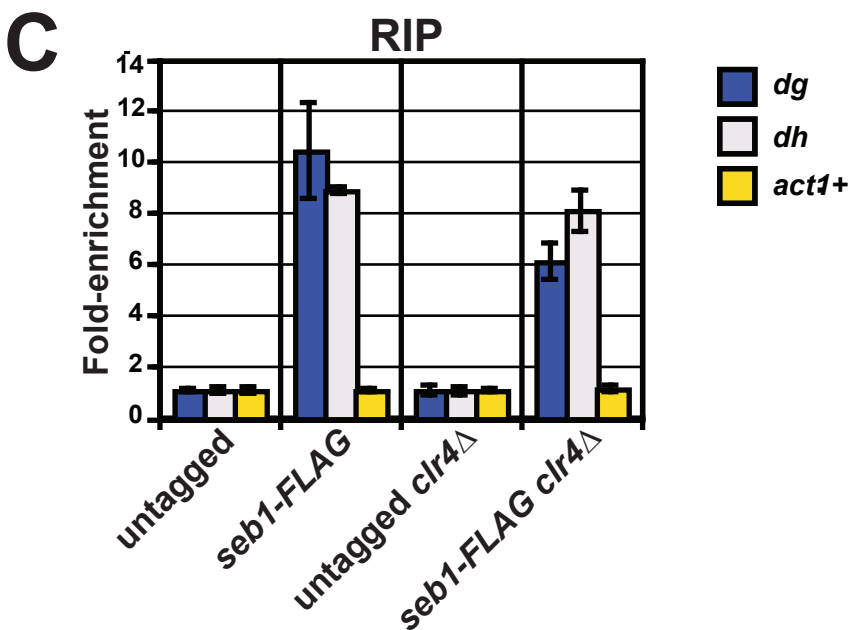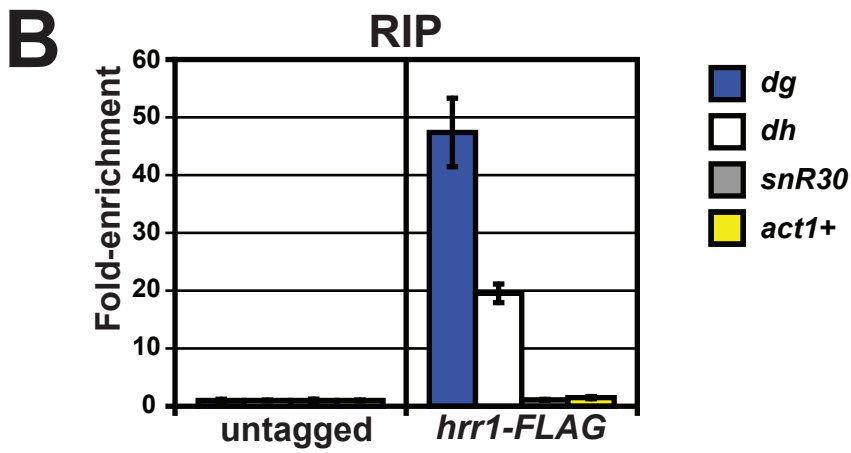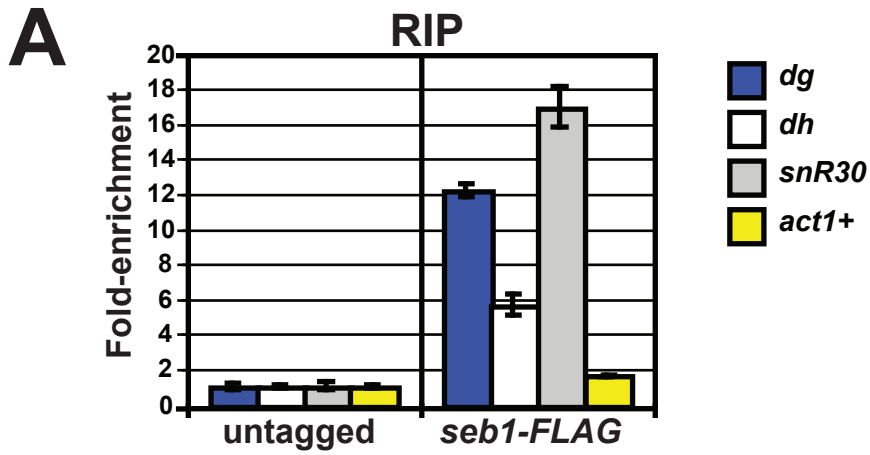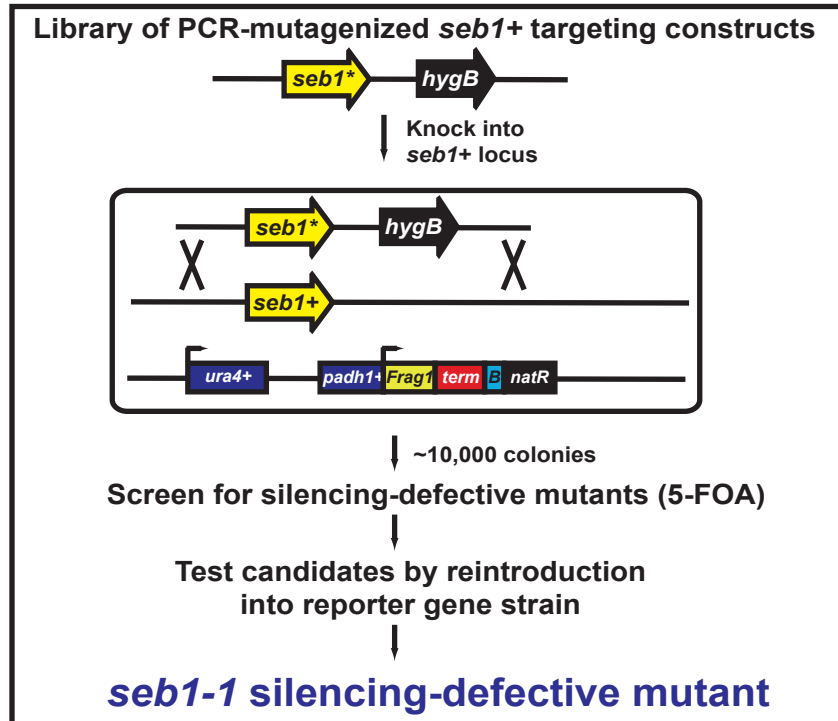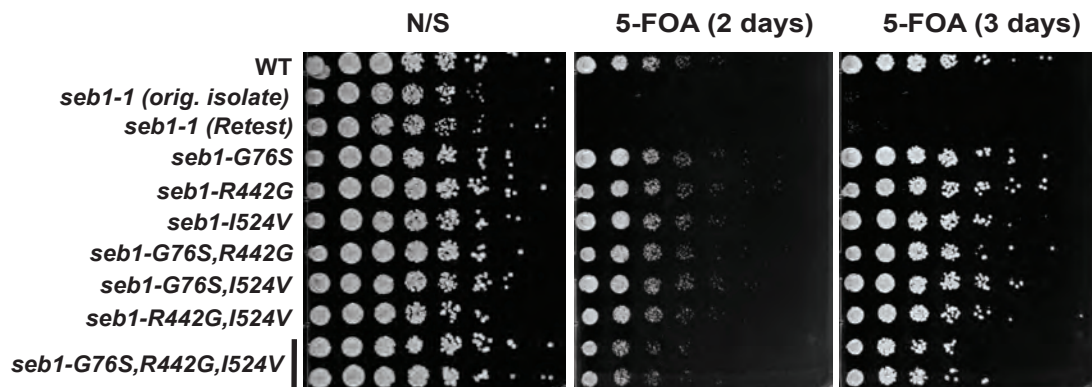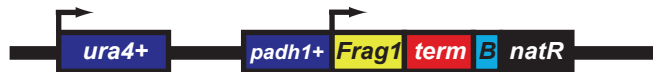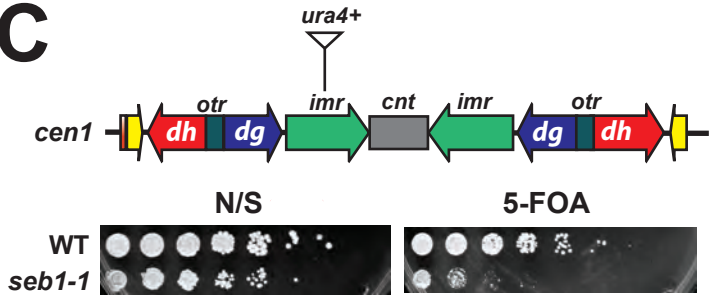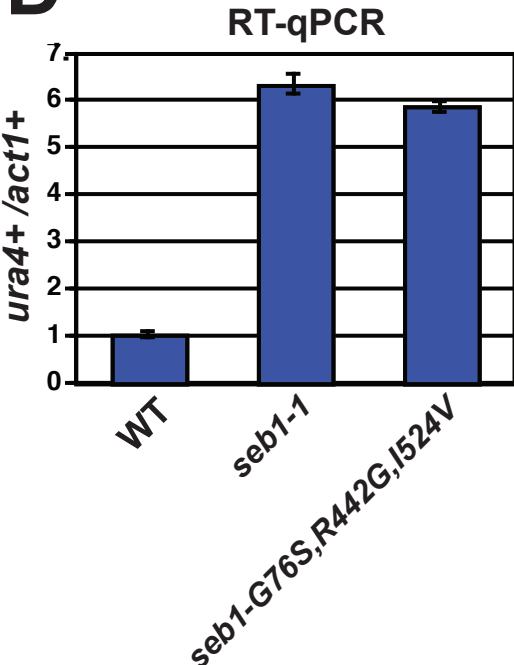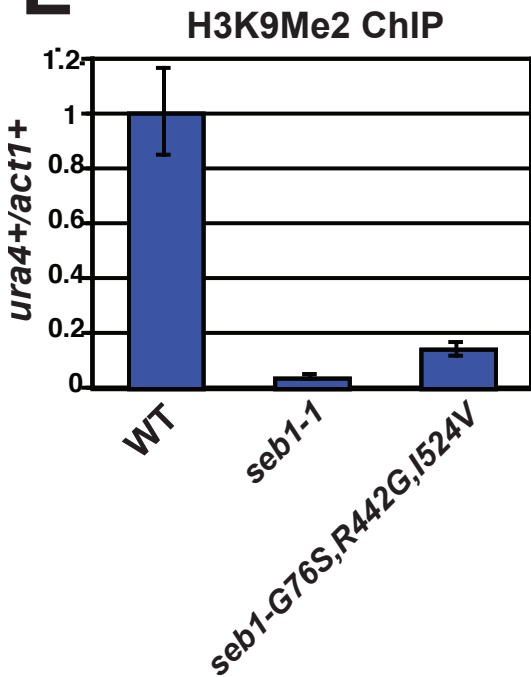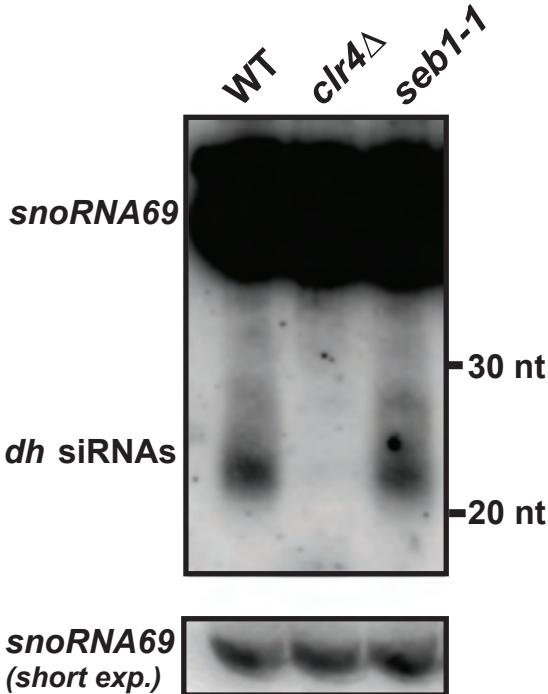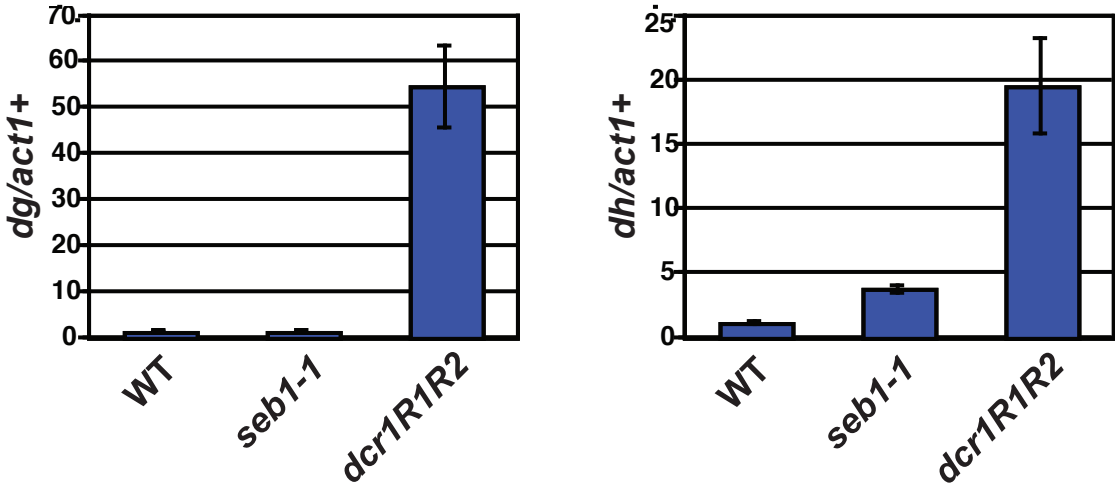
Figure 3

C

H3K9Me2 ChIP

D

H3K9Me2 ChIP

Figure 4

A

Gal4-Clr4ΔCD

can1+ *4xUAS* *ade6+*

	YS	SC
WT		
GAL4-clr4ΔCD		
GAL4-clr4ΔCD seb1-1		
GAL4-clr4ΔCD clr3Δ		
GAL4-clr4ΔCD dcr1Δ		

B

H3K9Me2 ChIP

GAL4-clr4ΔCD: −   +   +   +   +

WT   WT   *seb1-1*   *clr3Δ*   *dcr1Δ*

Figure 5

A

B
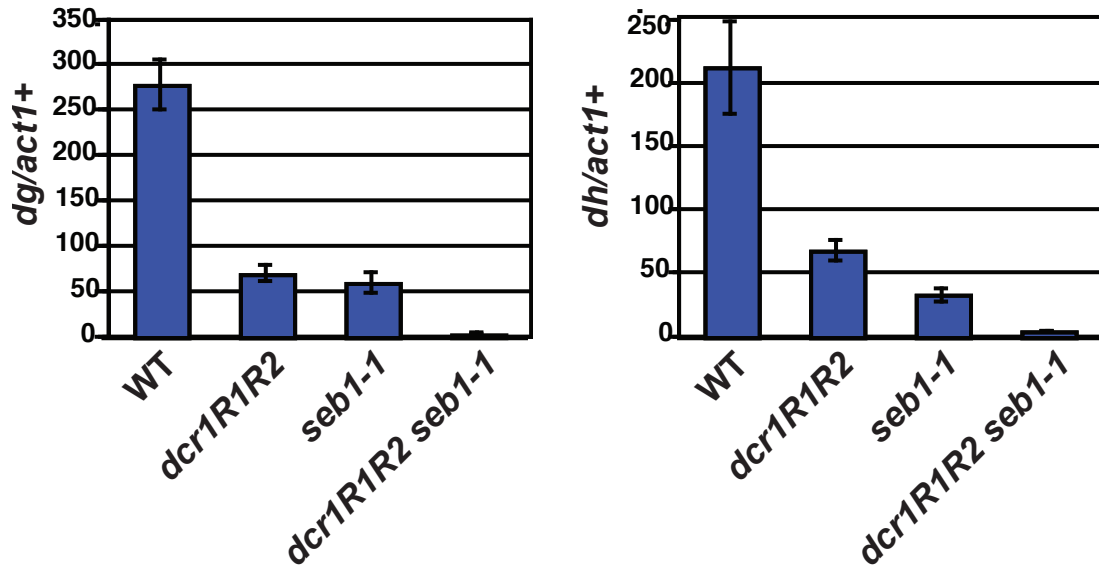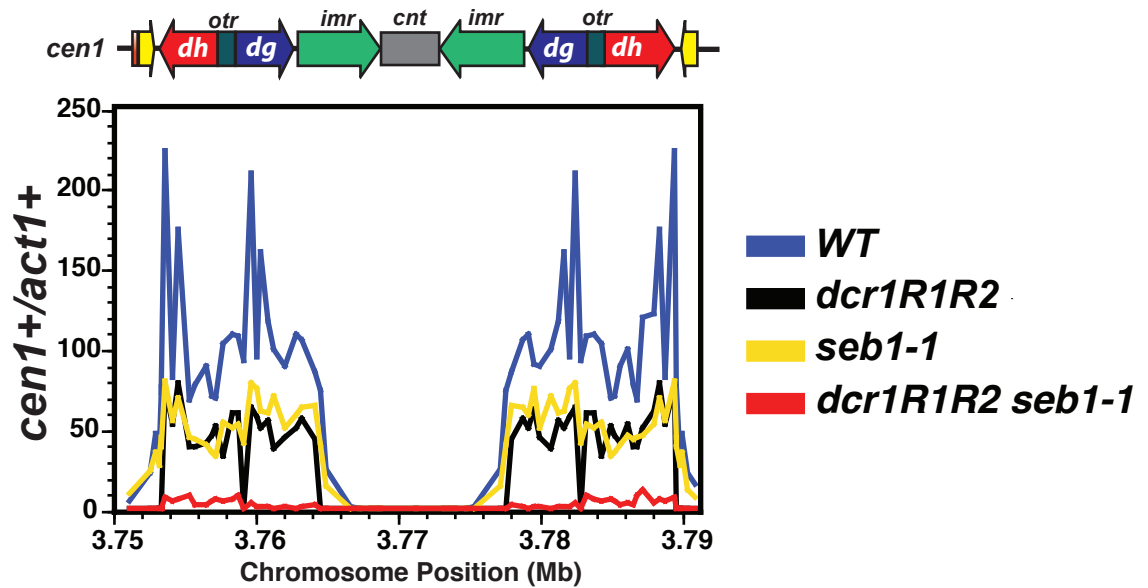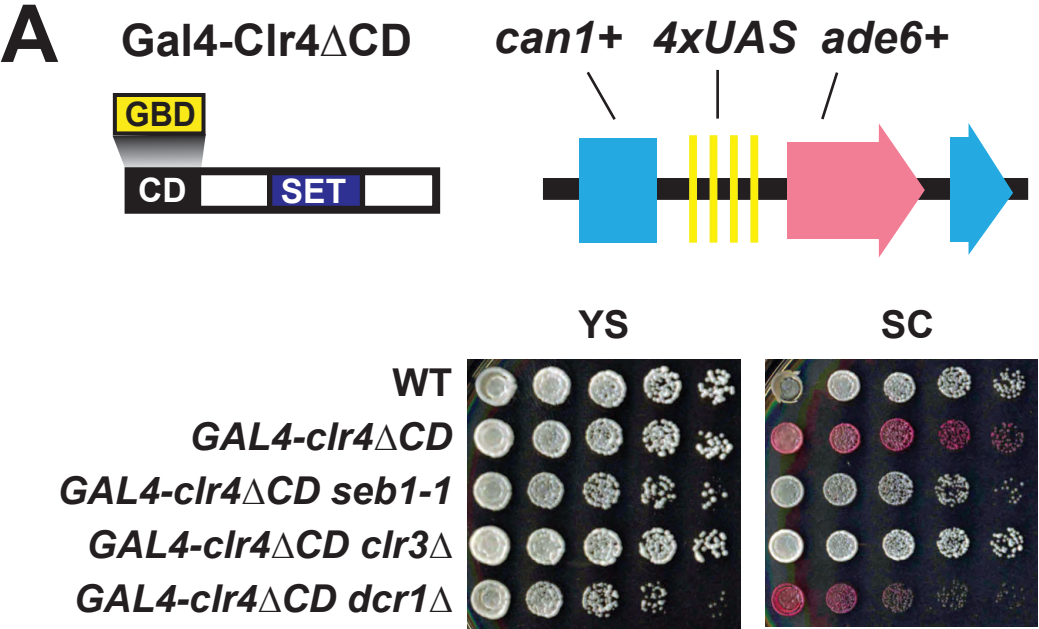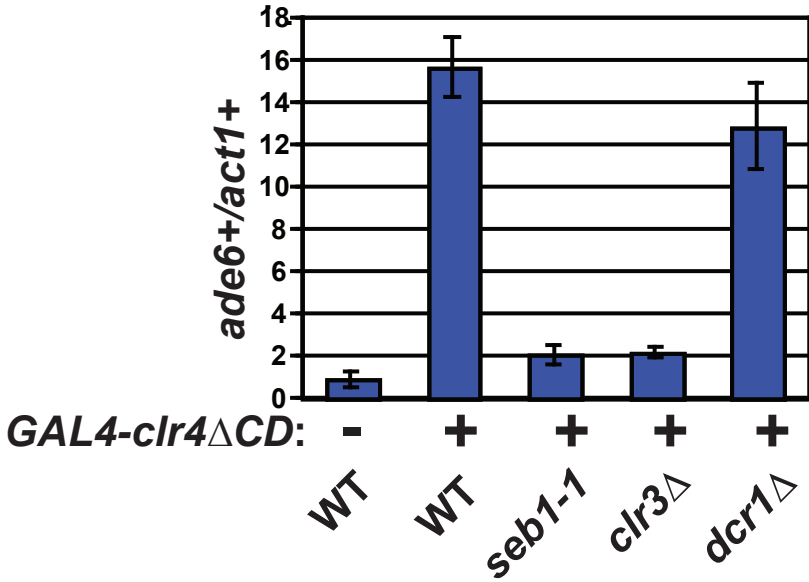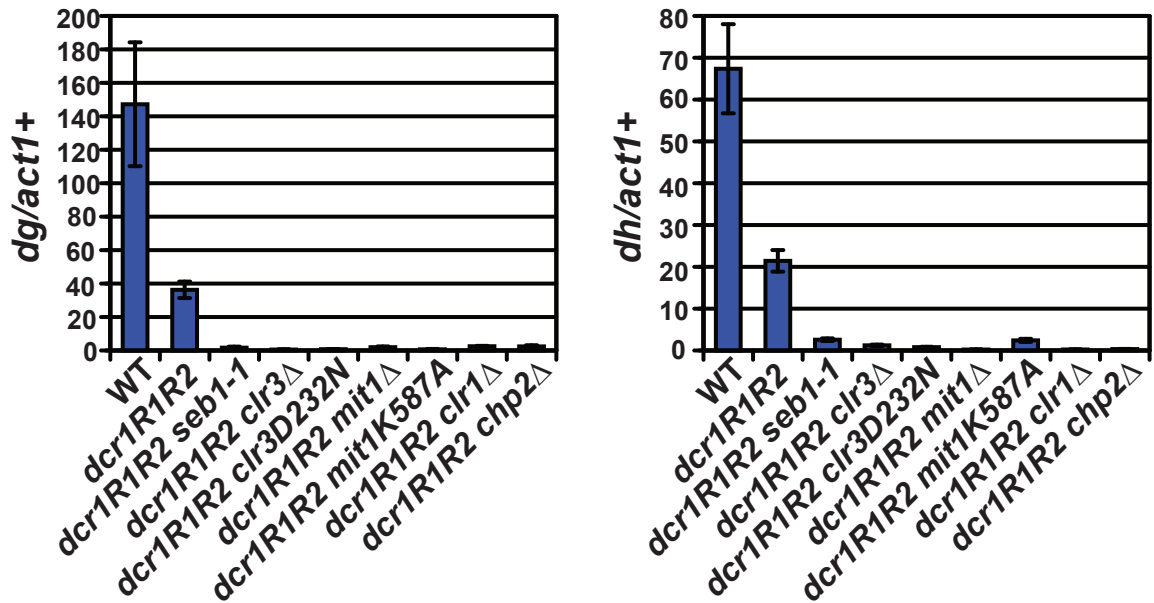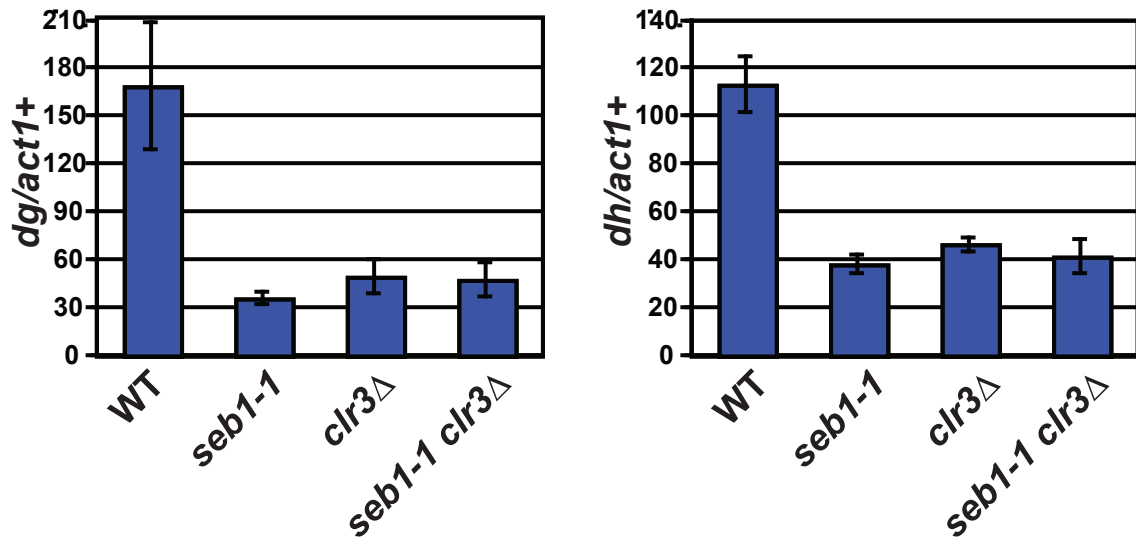
Figure 5

C
               H3K9Me2 ChIP

D
               PolII ChIP

Figure 6

A

B

C

D
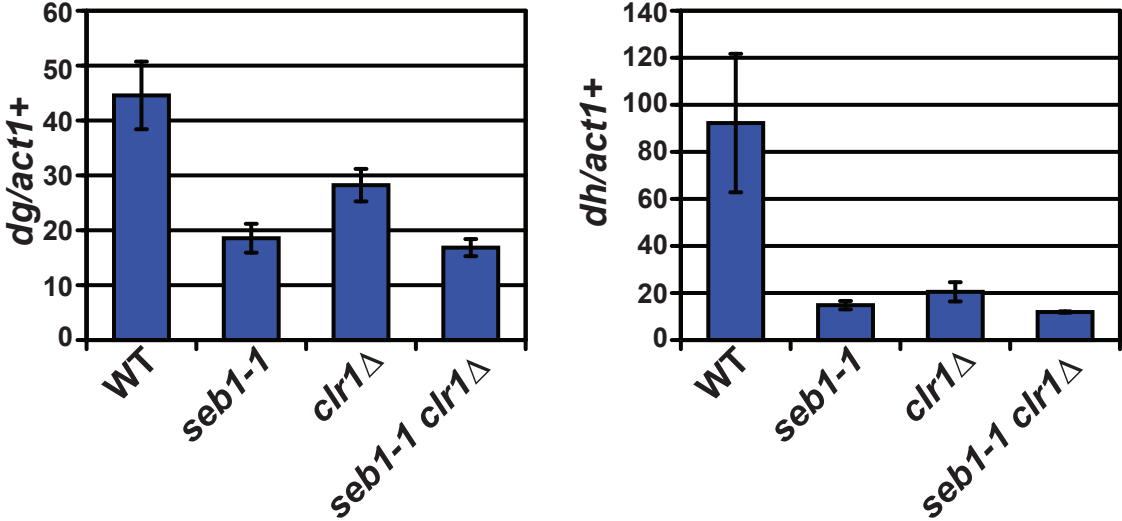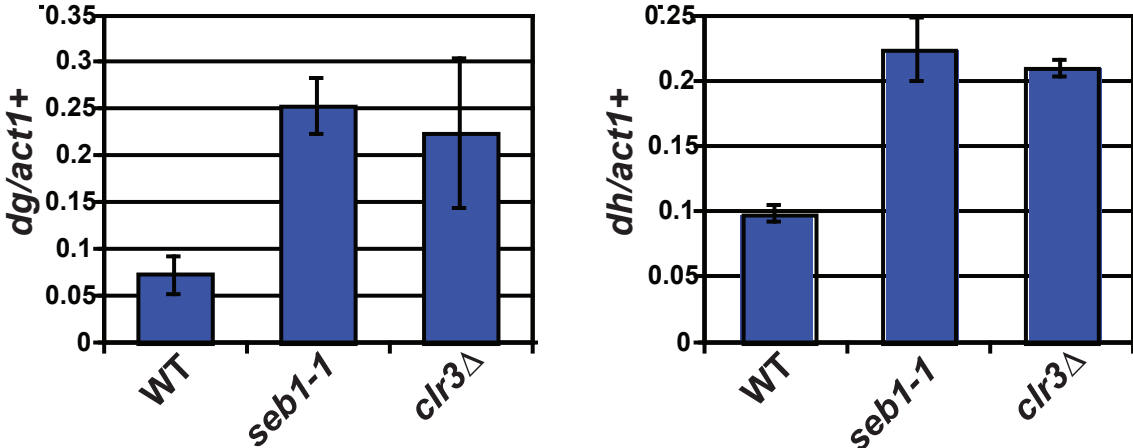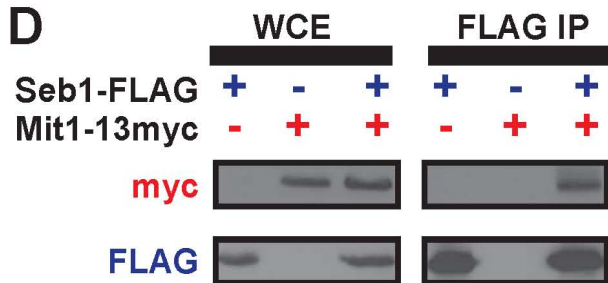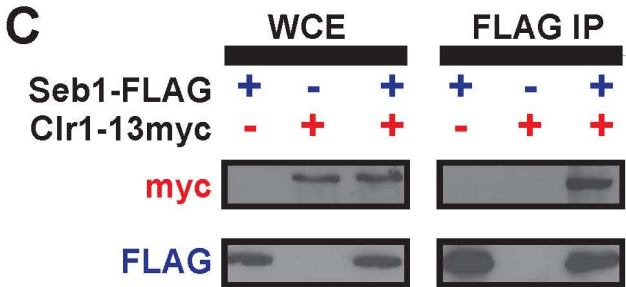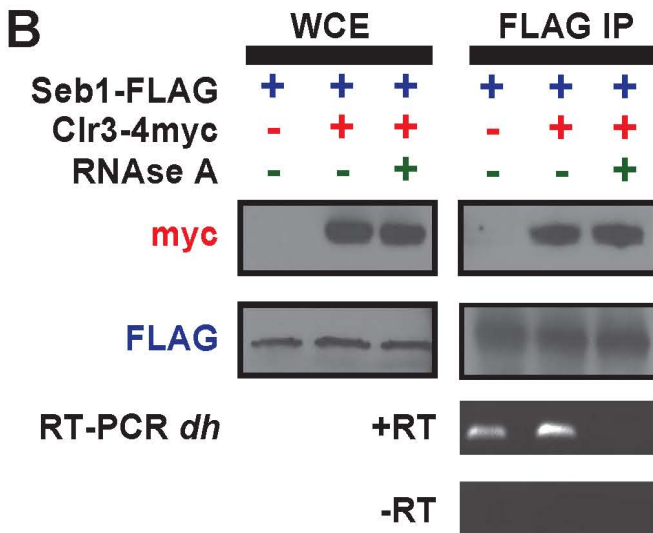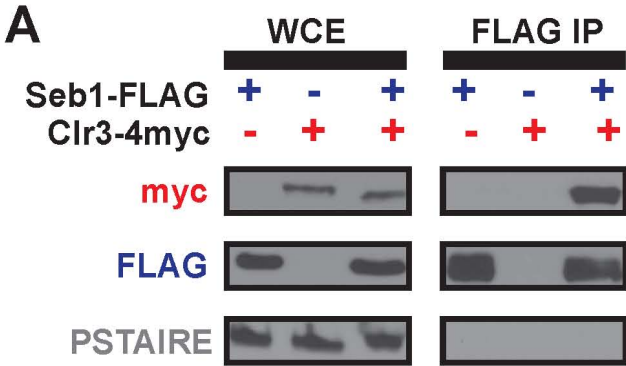
Figure 7

A   Clr3-myc ChIP
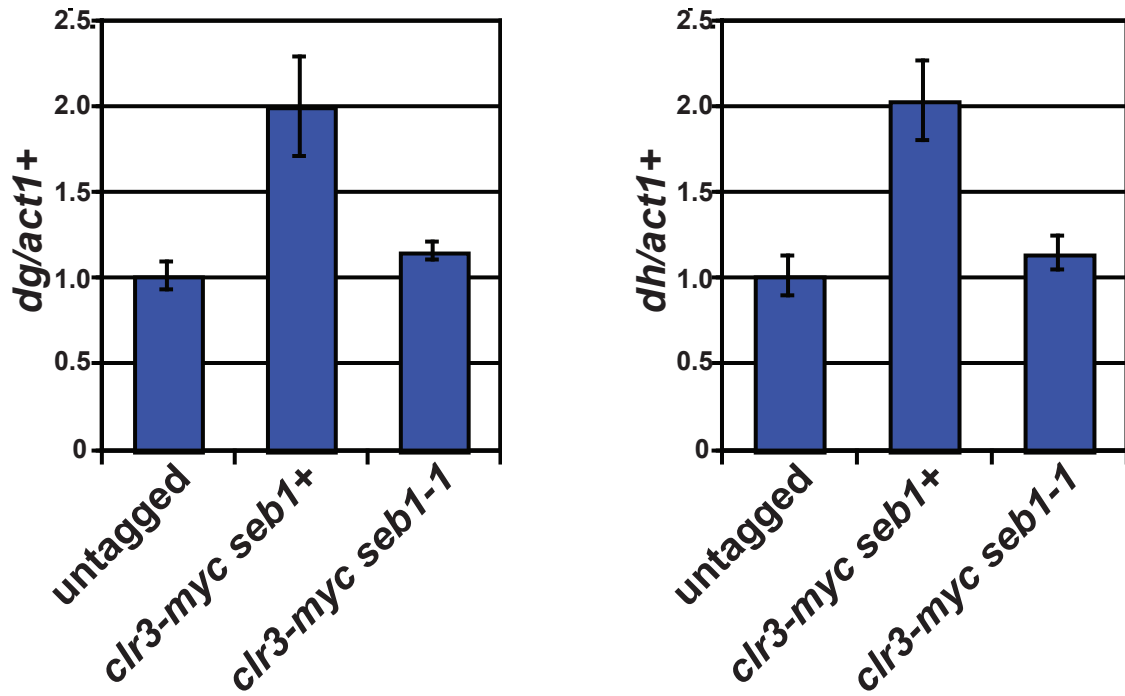
B   Clr1-myc ChIP
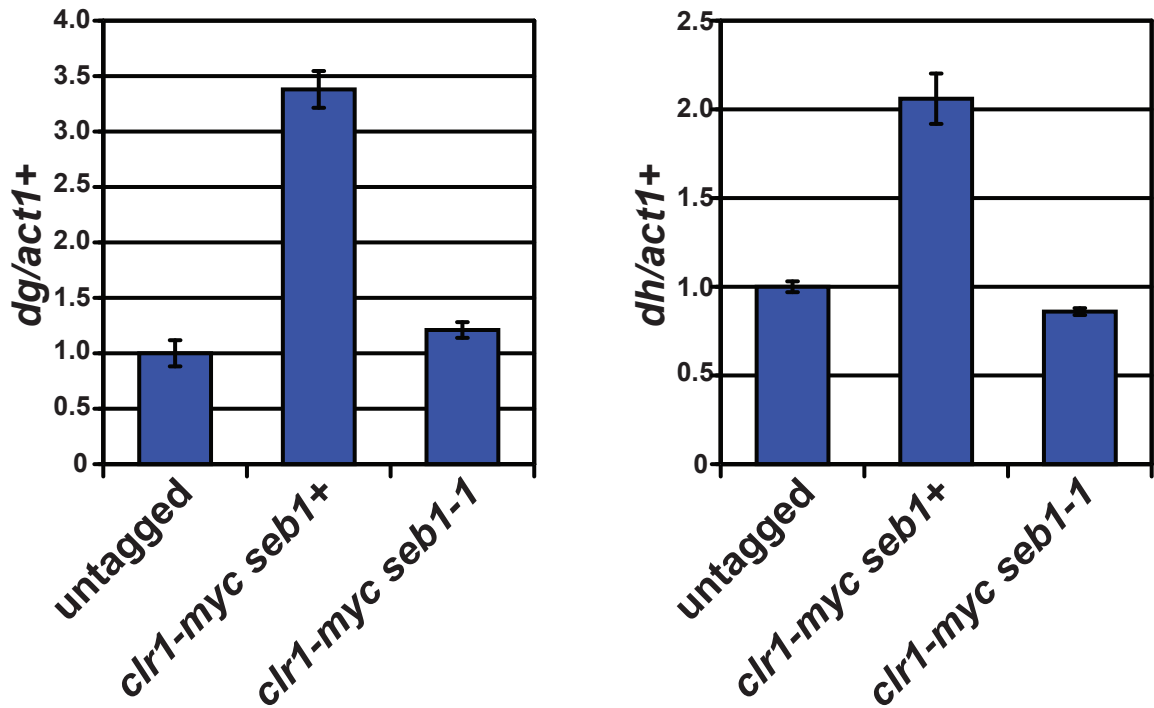
Figure 7

C **Mit1-myc ChIP**
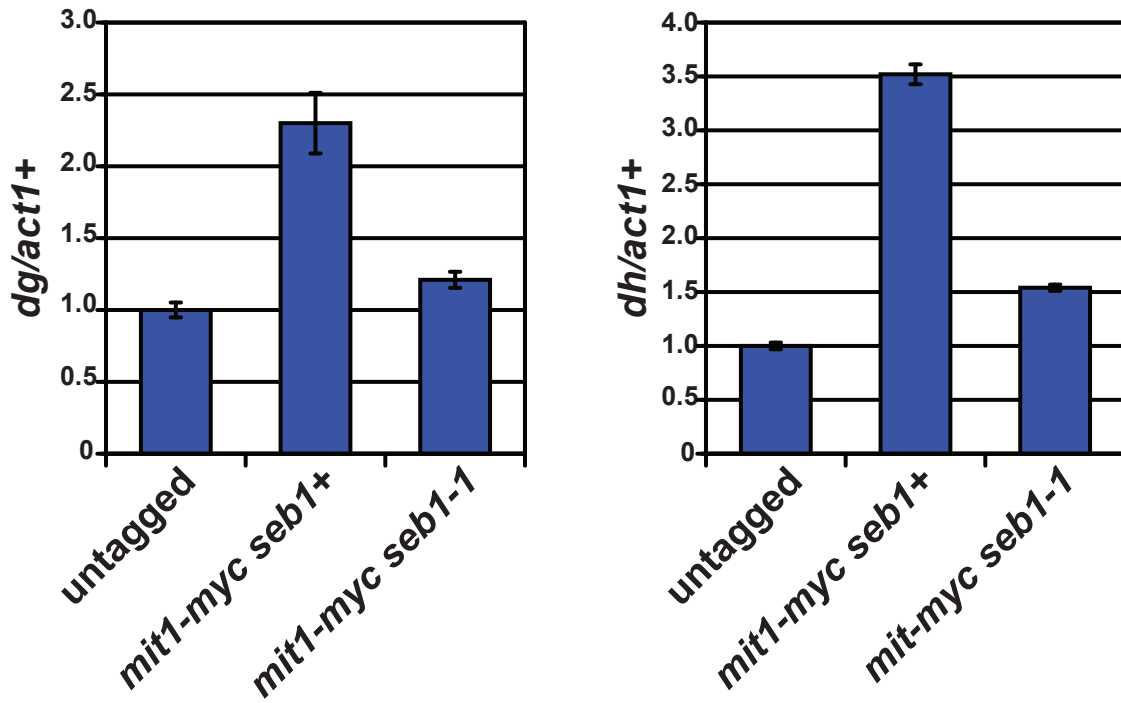
D **Chp2-myc ChIP**

Figure 7

E

RIP

Legend:
- *dg* (blue)
- *dh* (gray)
- *act1+* (yellow)

Y-axis: Fold-enrichment (0–60)

X-axis categories: untagged, seb1-FLAG, untagged clr3Δ, seb1-FLAG clr3Δ
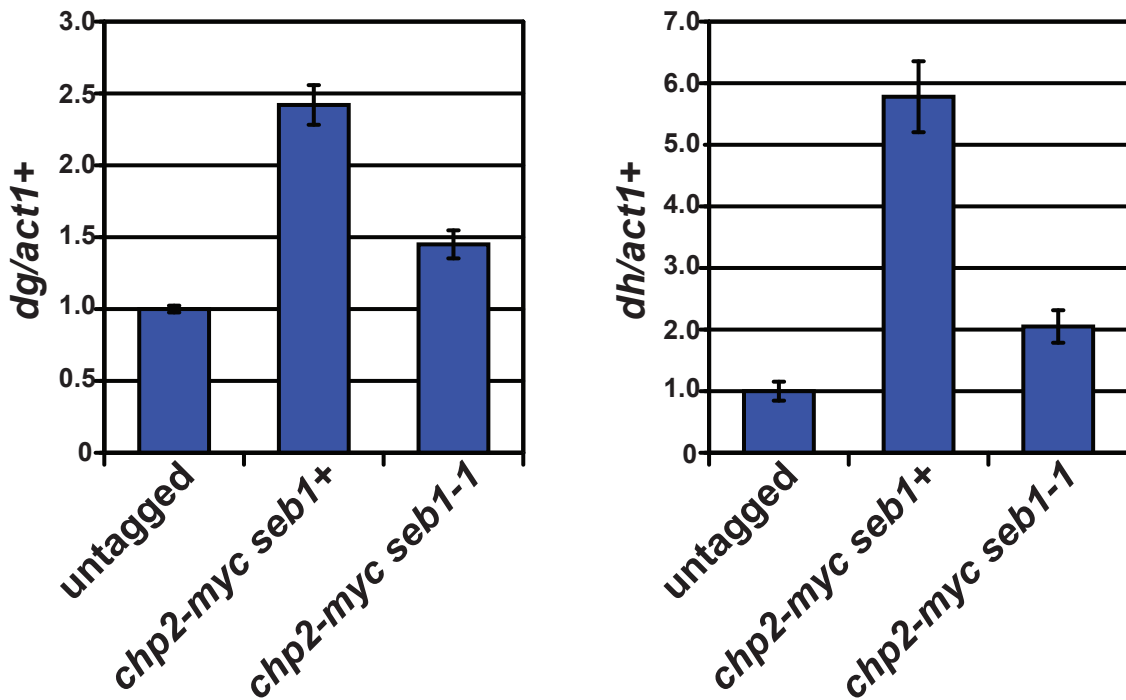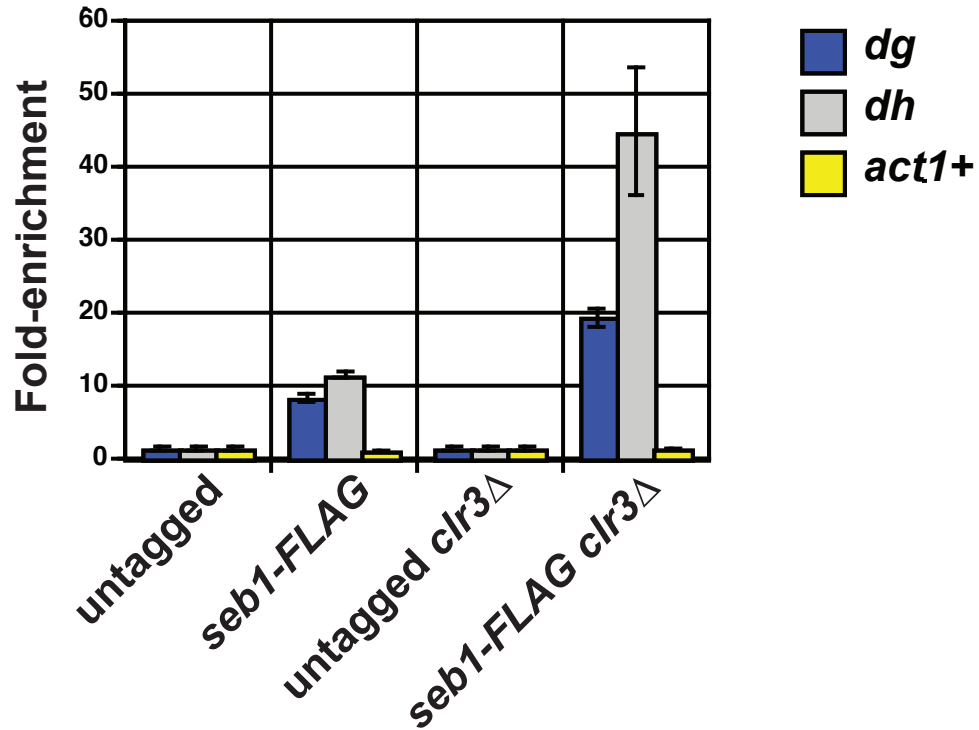
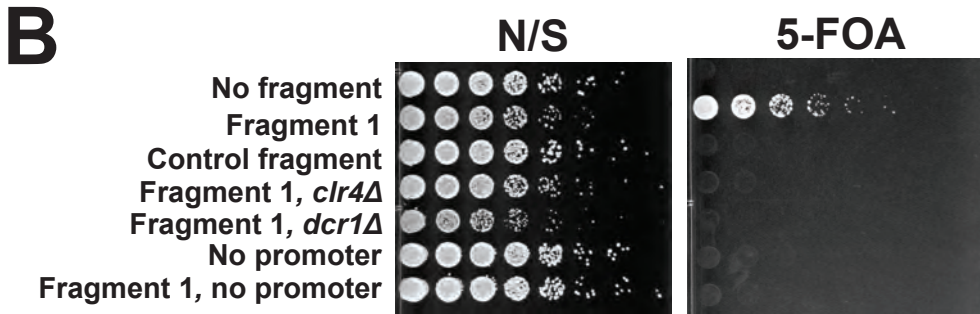**F**
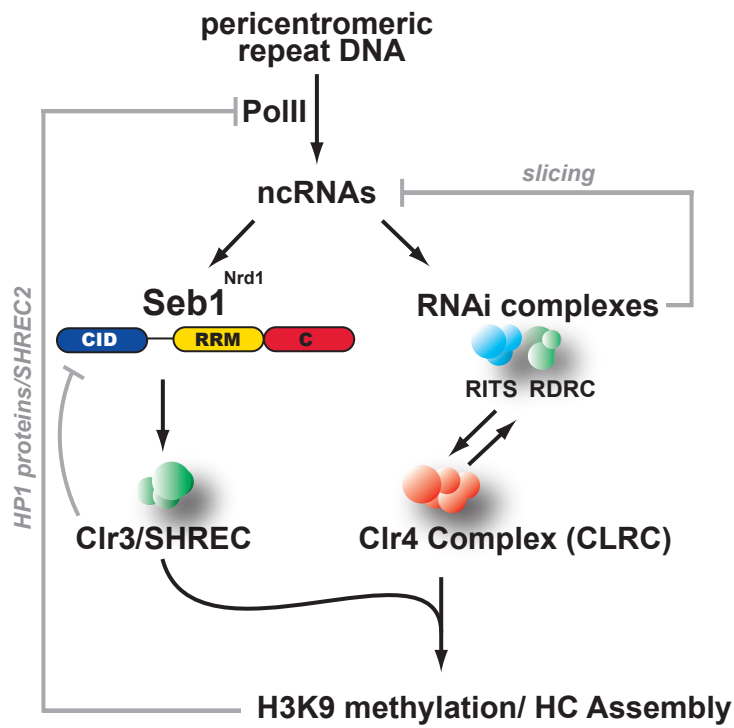
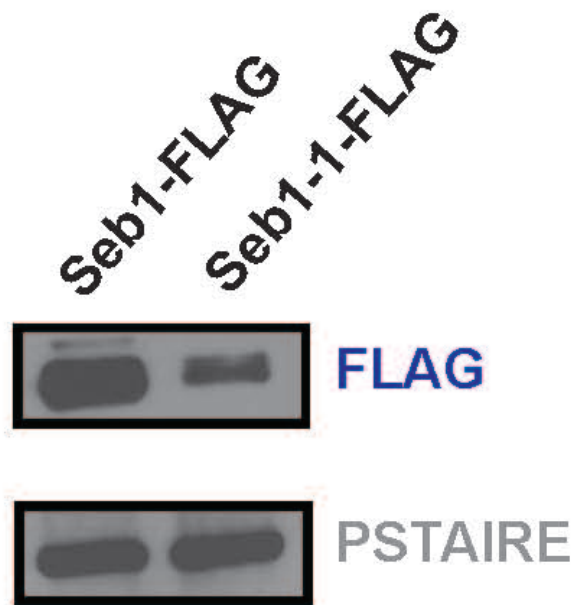# Figure S1

A   Ectopic heterochromatic
        silencing reporter
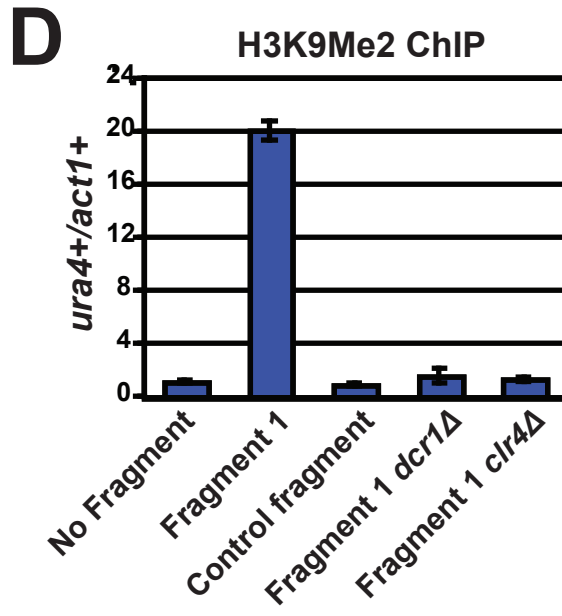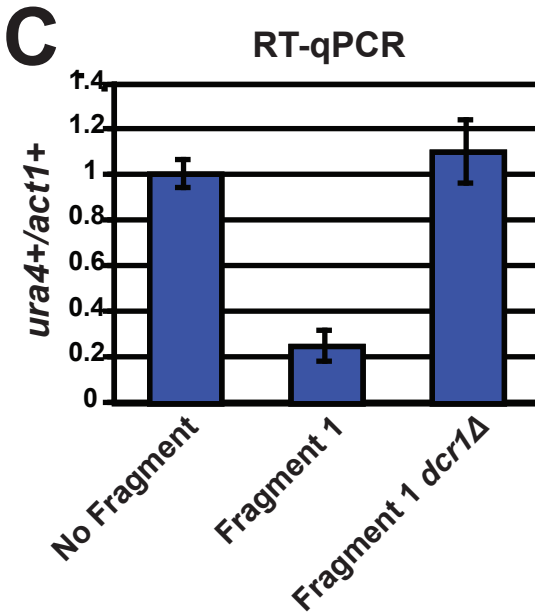
B

C

D

Figure S2

Figure S3
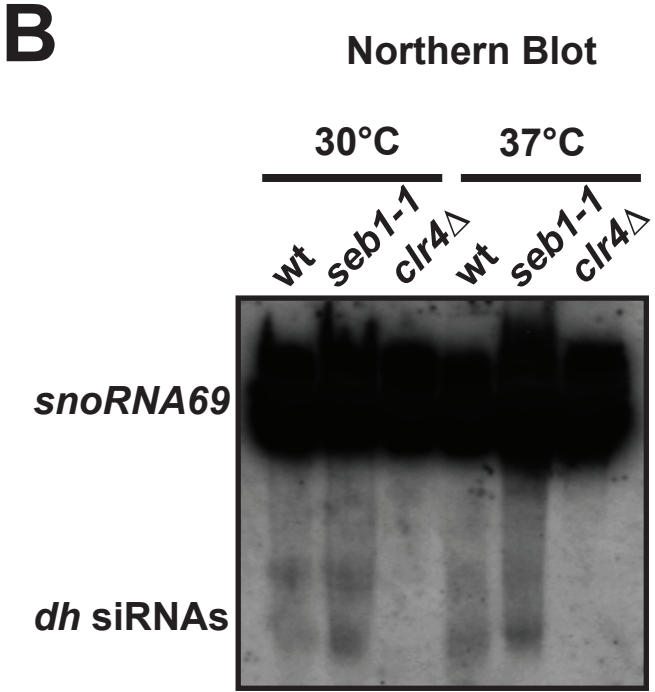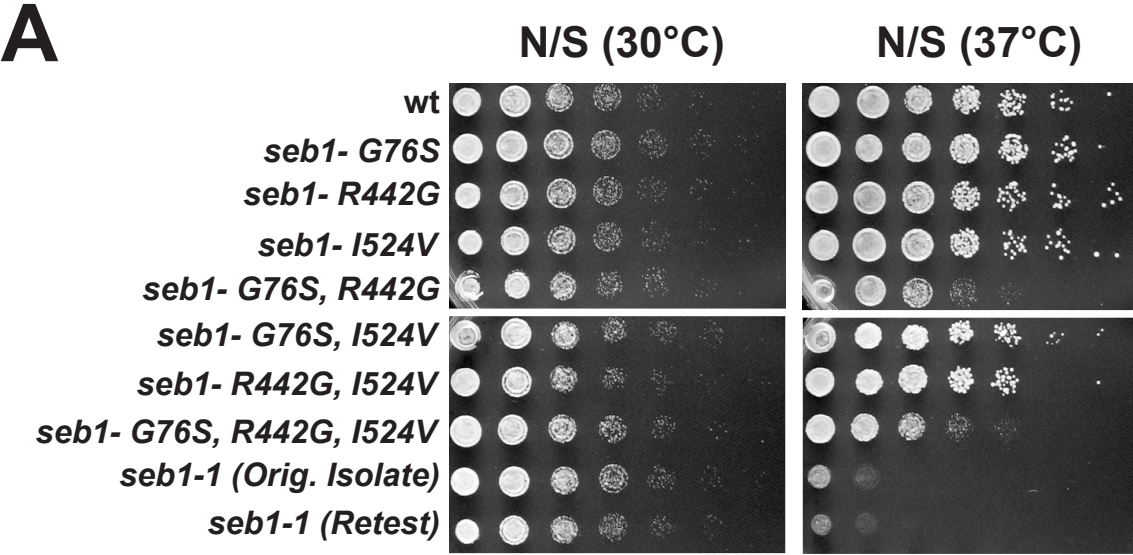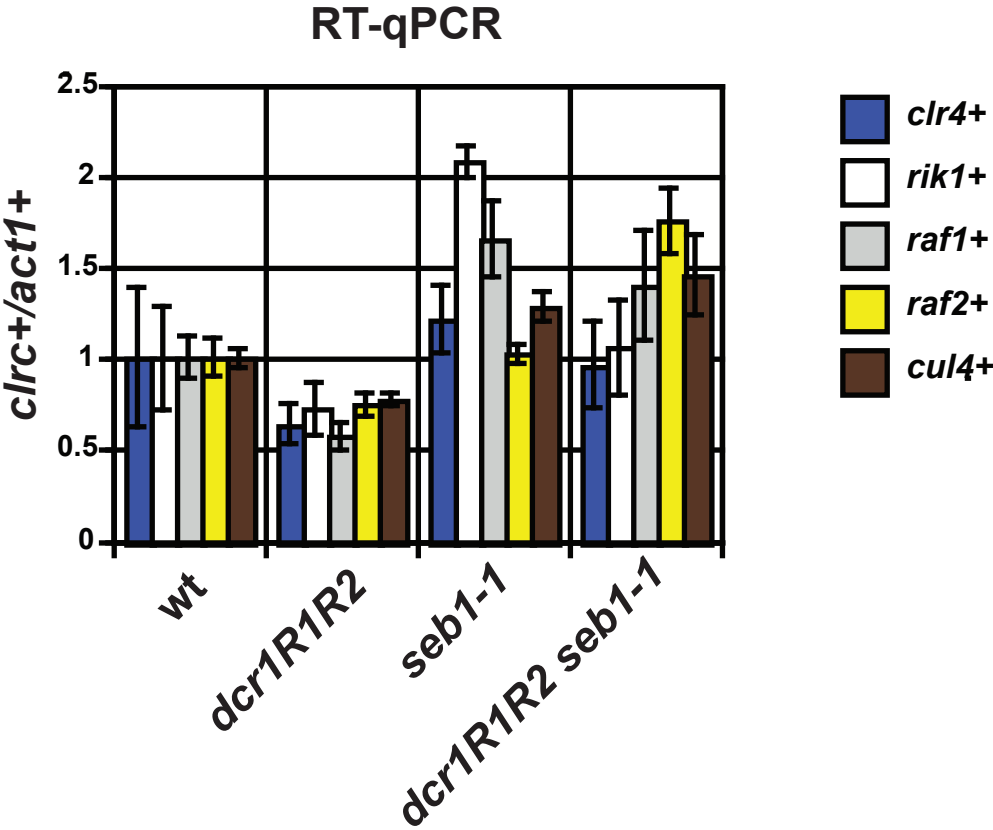
A

B

Figure S4

Figure S5

A

_dh_ transcripts

Ethidium staining of 28S rRNA

B

RT-qPCR

Figure S6

RT-qPCR

Legend:
- clr1+ (blue)
- clr2+ (red)
- clr3+ (green)
- mit1+ (purple)
- chp2+ (orange)

y-axis: *shrec2+/act1+*

x-axis: wt, seb1-1
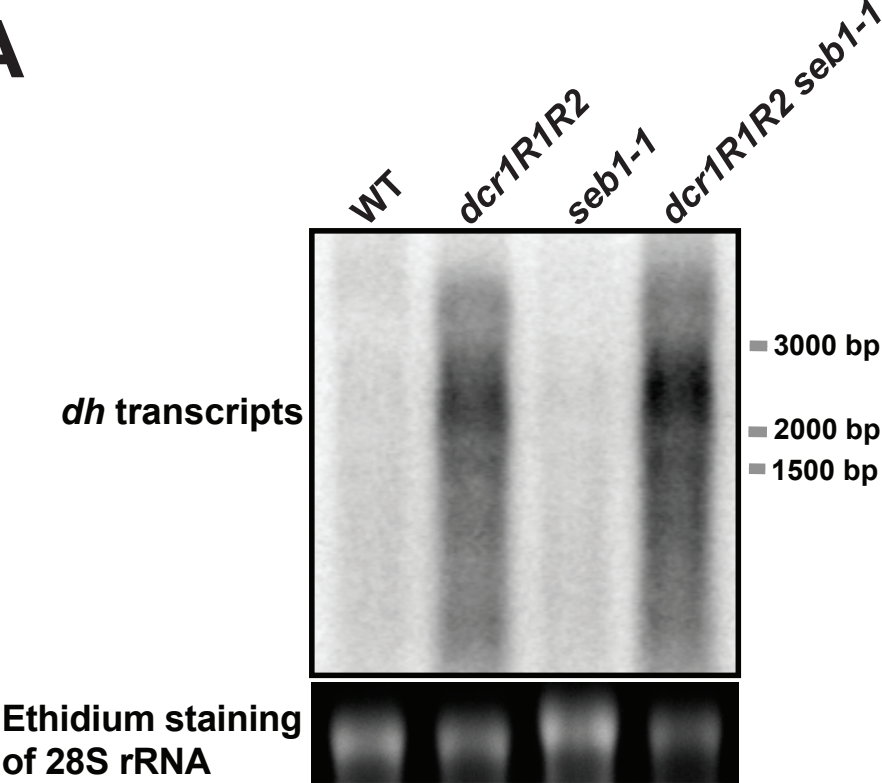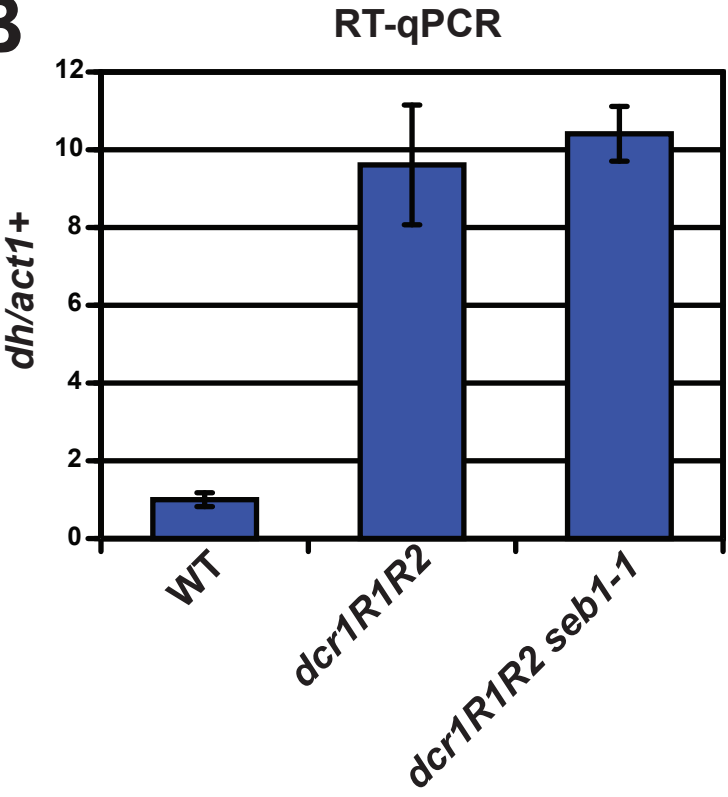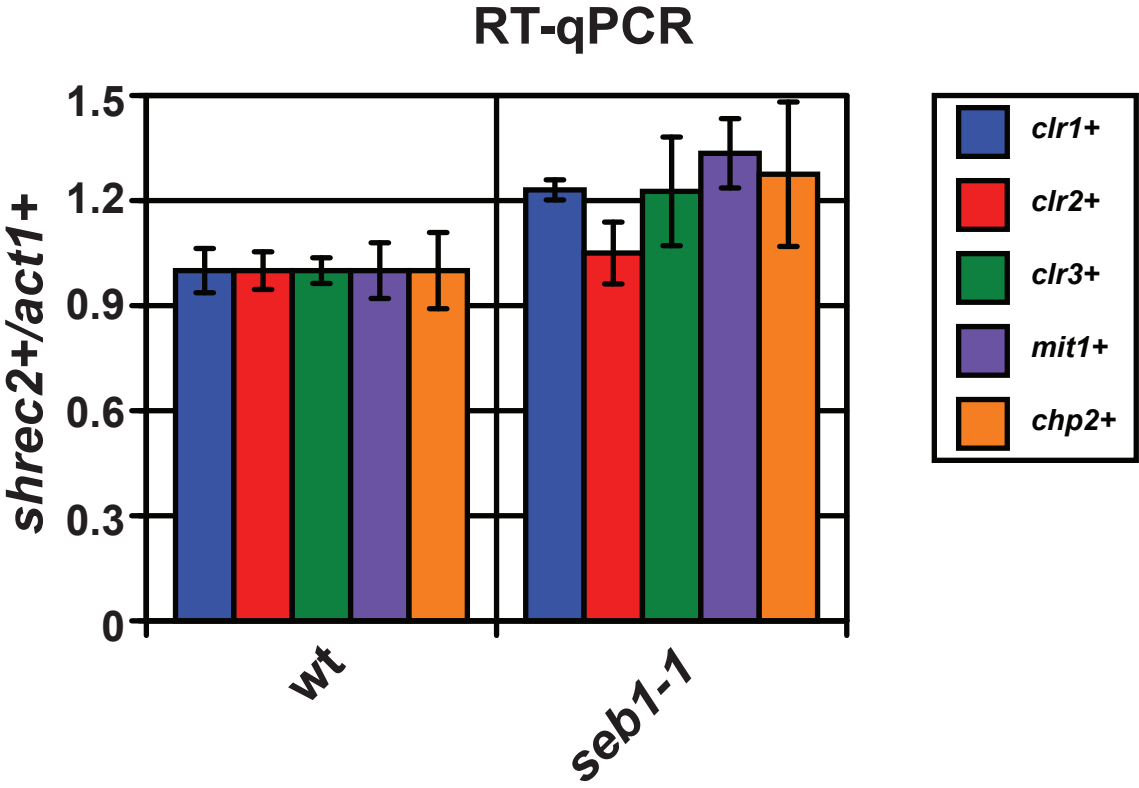
Table 1. List of *S. pombe* strains used in this study

Strain name	Genotype
PM0006	*S. pombe* wild type strain 972 *M(h-)*
PM0026	PM06, *ura4::padh1+-Fragment 1-ter-Bboxes-natMX*
PM0027	PM06, *ura4::padh1+-Control Fragment-ter-Bboxes-natMX*
PM0078	*P(h+), ura4-DS/E, ade6-M210, leu1-32, imr1L(NcoI)::ura4, otr1R(SphI)::ade6, clr1Δ::kanMX*
PM0106	PM26, *clr4Δ::kanMX*
PM0131	PM06, *ura4::padh1+-ter-Bboxes-natMX*
PM0251[#]	*P(h+), ura4-DS/E, ade6-M210, leu1-32, imr1L(NcoI)::ura4, otr1R(SphI)::ade6*
PM0253	PM06, *clr4Δ::kanMX*
PM0259	PM06, *ura4:*ter-Bboxes-*natMX*
PM0428	PM06, *ura4::padh1+-Fragment 1(barcode)-ter-Bboxes-natMX*
PM0959	PM06, *ura4::*Fragment 1-ter-Bboxes-*natMX*
PM1025	PM06, *seb1::CBP-2XFLAG kanMX*
PM0677	PM251, *hrr1::CBP-2XFLAG kanMX*
PM1033	PM428, *dcr1Δ::kanMX*
PM1035	PM428, *clr4Δ::kanMX*
PM1037	PM428, *dcr1-R1R2::kanMX*
PM1058	PM428, *seb1+::kanMX*
PM1060	PM428, *seb1-R442G::hygMX*
PM1063	PM428, *seb1I-524V::hygMX*
PM1064	PM428, *seb1-R442G, I524V::hygMX*
PM1075	PM428, *seb1-G76S, I524V::hygMX*
PM1077	PM428, *seb1-G76S, R442G, I524V::hygMX*
PM1085	PM428, *seb1-G76S::hygMX*
PM1103	PM428, *seb1-1 (A45G, T132A, G226A, T1194C, T1260A, A1324G, A1570G)*::hygMX*
PM1114	PM428, *seb1-G76S, R442G::hygMX*
PM1121	PM428, *dcr1-R1R2::kanMX, seb1-1 (A45G, T132A, G226A, T1194C, T1260A, A1324G, A1570G)*::hygMX*
PM1200	PM251, *seb1-1 (A45G, T132A, G226A, T1194C, T1260A, A1324G, A1570G)*::hygMX*
PM1316	PM06, *seb1-1::natMX*
PM1339	PM06, *dcr1-R1R2::hygMX, seb1-1::natMX*
PM1355	PM06, *clr4Δ::kanMX, seb1::CBP-2XFLAG hygMX*
PM1357	PM1403, *dcr1Δ::natMX*
PM1360	PM06, *clr3Δ::kanMX*
PM1362	PM06, *seb1-1::natMX, clr3Δ::kanMX*
PM1364	PM06, *dcr1-R1R2::hygMX, clr3Δ::kanMX*
PM1382	PM1025, *clr3Δ::hygMX*

PM1386	PM06, *clr3::4myc hygMX*
PM1388	PM1025, *clr3::4myc hygMX*
PM1390	PM06, *seb1-1::CBP-2XFLAG kanMX, clr3::4myc hygMX*
PM1392	*M(h-), smt-0, ade6-M210, leu1-32, ura4-D18, mit1-K587A::kanMX, dcr1-R1R2::hygMX*
PM1394	*M(h-), smt-0, ade6-M210, leu1-32, ura4-D18, mit1Δ::kanMX, dcr1-R1R2::hygMX*
PM1396	*P(h+), ura4-DS/E, ade6-M210, leu1-32, imr1L(NcoI)::ura4, otr1R(SphI)::ade6, clr1Δ::kanMX, dcr1-R1R2::hygMX*
PM1398	*M(h-), smt-0, ade6-M210, leu1-32, ura4-D18, chp2Δ::hygMX, dcr1-R1R2::kanMX*
PM1400	*M(h-), smt-0, ade6-M210, leu1-32, ura4-D18, clr3-D232N::natMX, dcr1-R1R2::hygMX*
PM1402	*can1::4UAS-ade6+, ade6-M210, ura4-D18, leu1-32*
PM1403	*can1::4UAS-ade6+, ade6-M210, ura4-D18, leu1-32, clr4::hygMX-GBD-ΔCD*
PM1404	PM1403, *clr3Δ::kanMX*
PM1405	PM1403, *seb1-1::natMX*
PM1407	*P(h+), ura4-DS/E, ade6-M210, leu1-32, imr1L(NcoI)::ura4, otr1R(SphI)::ade6, clr1Δ::kanMX, seb1-1::natMX*
PM2043	PM06, *clr1::13myc hygMX*
PM2046	PM06, *mit1::13myc hygMX*
PM2048	PM1025, *clr1::13myc hygMX*
PM2050	PM1025, *mit1::13myc hygMX*
PM2053	PM1316, *chp2::7myc kanMX*
PM2055	PM1316, *clr1::13myc hygMX*
PM2057	PM1316, *mit1::13myc hygMX*

'*padh1+*' = *adh1+* promoter (for sequence information see supplementary table 3)

'ter' = terminator (for sequence information see supplementary table 3)

'B-boxes' = synthetic boundary element (for sequence information see supplementary table 3)

'Fragment 1' = a fragment derived from *dh* repeats (for sequence information see supplementary table 3)

*Numbers indicate positions of mutations (bp) in the predicted spliced coding sequence of *seb1+*

[#] From Karl Ekwall

Table 2. List of primers used in this study

Primer Name	Sequence	Locus (orientation)
P581	CAGCAATATCGTACTCCTGAA	*ura4+* (forward)
P582	ATGCTGAGAAAGTCTTTGCTG	*ura4+* (reverse)
P1044	CCATCACCACTTTCATCTCC	*dg* (forward)
P1045	CAGGATACCTAGACGCACAA	*dg* (reverse)
P62	TTTAAAGCTTCACTACCATCGAAA	*dh* (forward)
P63	TGCCAACAGTTTTTCCAACTT	*dh* (reverse)
P638	AACCCTCAGCTTTGGGTCTT	*act1+* (forward)
P639	TTTGCATACGATCGGCAATA	*act1+* (reverse)
P1174	TTCGACTGCAGGTTGAGAGTT	*snR30* (forward)
P1176	TGCAAGGATCCAGAGATCATG	*snR30* (reverse)
P2224	TATAGGTACCTTACTGTCATTAGGATATGCT	Fragment 1 riboprobe-sense (forward)
P2225	TATACCCGGGATACAATGATTCCTCTCATCTCG	Fragment 1 riboprobe-sense (reverse)
P2203	TATAGGTACCATACAATGATTCCTCTCATCTCG	Fragment 1 riboprobe-antisense (forward)
P2204	TATACCCGGGTTACTGTCATTAGGATATGCT	Fragment 1 riboprobe-antisense (reverse)
P2596	CCAATTAAATTAACGCATATTAATG	*ade6-can1* junction (forward)
P2597	TCTATCGATCTCTGCAATTTG	*ade6-can1* junction (reverse)
P2532	CGCTCTGACGACGAATGATA	*clr4+* (forward)
P2533	TCAAGTTTGGAAGGGTTTCG	*clr4+* (reverse)
P2536	CGGTAGACACAGCGACTTCA	*rik1+* (forward)
P2537	CCTCGTCCCAATAAATCGAA	*rik1+* (reverse)
P2540	TTTTGACGGGGCTAATGAAG	*raf1+* (forward)
P2541	CCTCACTGAACCCTCCGTAA	*raf1+* (reverse)
P2544	TTACCCGAGCAACCGTTTAG	*raf2+* (forward)
P2545	TGAGCAATAACGCTGCAAAC	*raf2+* (reverse)
P2550	ATCACATATCCGGCTTCCAG	*cul4+* (forward)
P2551	GTTCCTTATTGCCCAGTGGA	*cul4+* (reverse)
P2782	TATTTTGCGTCCATGGTTGA	*clr1+* (forward)
P2783	TGTTGCACCTGTAGCTTTGG	*clr1+* (reverse)
P2786	CAAGATCCGTCCCTTCGTTA	*clr2+* (forward)
P2787	TTATTGGGATTACCGGTGGA	*clr2+* (reverse)
P2790	CATGCAGAACCCCATAAACC	*clr3+* (forward)
P2791	AGCCATTTGCGTACCATTTC	*clr3+* (reverse)
P2794	TCATGGCTAGCCGGTATTTC	*mit1+* (forward)
P2795	AACCACGCCAAGAAACAAAG	*mit1+* (reverse)
P2798	AAGGGTACGATGACCCTTCC	*chp2+* (forward)
P2799	TACGATTTGCTGCATTCCTG	*chp2+* (reverse)

For the list of tiling primer sets for centromeric H3K9Me2 ChIP, please refer to Braun *et al.* 2011

Table 3. List of chromosome coordinates of different fragments used in this study

Fragment	Chromosome	Chromosome coordinate
padh1+	3	1590559..1591323
terminator	1	2274985..2275583
B-boxes	N/A	Synthetic boundary element*
Fragment 1	1	Reverse complement (3787059..3789869)
Control Fragment	1	Complement (3787059..3789869)

*B-boxes sequence:
TGTTCGTAGCAACGTAATAATCGAAAGTAGCAGGACTCGAACCATTCGCAAA
TCGAACCGATCAAAAGTAGAACC

Table 4. List of plasmids used in this study

BHM#	Former name	Description	Marker
1982	pDM78	Chp2-7myc	G418
1983	pDM131	Seb1-TAP	HygB
1984	pDM132	Seb1-CBP-2XFLAG	G418
1985	pDM133	Nab3-TAP	HygB
1986	pDM134	Nab3-CBP-2XFLAG	G418
1987	pDM135	Rpb7-TAP	HygB
1988	pDM136	Rpb7-CBP-2XFLAG	G418
1989	pDM163	Seb1-1-CBP-2XFLAG	G418
1990	pDM167	Seb1-TAP	Nat
1991	pDM168	*seb1-1*	Nat
1992	pDM171	*rpb7ED*	Nat
1993	pDM172	Rik1-CBP-2XFLAG	G418
1994	pDM173	Seb1-1-TAP	HygB
1995	pDM176	Seb1-CBP-2XFLAG	HygB
1996	pDM178	Rik1-CBP-2XFLAG	HygB
1997	pDM179	*clr4Δ*	HygB
1998	pDM184	*seb1-1*	G418
1999	pDM189	Clr3-4myc	HygB
2000	pDM190	Clr1-13myc	HygB
2001	pDM191	Mit1-13myc	HygB

Chapter IV: A Model for Pericentromeric Transcript Recognition by Competing RNA-Processing Pathways in Fission Yeast

Diana B. Marina, Margot Rowley and Hiten Madhani

Author contributions:

Diana Marina performed all experiments and wrote this chapter. Margot Rowley performed the genetic screen. Hiten Madhani supervised this work.

INTRODUCTION

In the fission yeast *S. pombe,* transcription of pericentromeric *dg* and *dh* repeats by RNA Polymerase II (PolII) is required to trigger the RNAi-dependent pathway of heterochromatin assembly (Djupedal et al., 2005; Kato et al., 2005). These non-coding pericentromeric transcripts are processed into small interfering RNAs (siRNAs) by the combined action of Dicer (Dcr1) and RNA-dependent RNA polymerase complex (RDRC) (Lejeune & Allshire, 2011; Verdel, Vavasseur, Le Gorrec, & Touat-Todeschini, 2009). The siRNAs are loaded onto an Argonaute protein (Ago1) (Verdel et al., 2004), which in turn recruits Clr4, the sole H3K9 methyltransferase in *S. pombe,* to nucleate heterochromatin at pericentromeric repeats (Bayne et al., 2010; Nakayama, Rice, Strahl, Allis, & Grewal, 2001; Zhang, Mosch, Fischle, & Grewal, 2008).

In *S. cerevisiae*, which lacks RNAi and classical heterochromatin, several species of non-coding RNA transcripts are processed by a unique RNA-processing machinery involving the nuclear exosome and the TRAMP (Trf4-Air1-Mtr4 Polyadenylation) complex (Houseley, LaCava, & Tollervey, 2006; LaCava et al., 2005). The nuclear exosome is a multi-unit protein complex that plays a crucial role in processing stable RNA species such as rRNAs, tRNAs and snoRNAs as well as in degrading unstable RNAs such as cryptic unstable transcripts (CUTs) (Houseley et al., 2006). The nuclear exosome interacts with the TRAMP complex that contains non-canonical poly(A) polymerases (Trf4/5), a zinc-knuckle protein (Air1) and a nuclear cofactor of the exosome (Mtr4) (LaCava et al., 2005) . The TRAMP complex has been shown to polyadenylate both stable and unstable RNA transcripts for processing or degradation by the nuclear exosome (Vanacova et al., 2005; Wyers et al., 2005).

Intriguingly, in *S. pombe,* several lines of evidence indicate that RNAi and TRAMP-nuclear exosome machineries compete to process or degrade pericentromeric transcripts. First, a study has shown that cells lacking Cid14, the *S. pombe* homolog of Trf4/5 (the non-canonical poly(A) polymerases of TRAMP), have decreased heterochromatic silencing without having major changes in the levels of H3K9Me, a conserved hallmark of heterochromatin (Buhler, Haas, Gygi, & Moazed, 2007). Additionally, *cid14Δ* mutant has increased levels of transcripts originating from the *ura4+* heterochromatic reporter gene (Buhler et al., 2007). These findings led the authors to propose that Cid14 is involved in co-

transcriptional gene silencing by targeting heterochromatic transcripts to the nuclear exosome for degradation (Buhler et al., 2007). A follow-up study revealed that in cells lacking Cid14, Ago1 is overloaded with small RNAs originating from rRNAs, which are the normal substrates for the TRAMP-nuclear exosome pathway (Buhler, Spies, Bartel, & Moazed, 2008). The authors concluded that mutations in the TRAMP-nuclear exosome pathway cause aberrant entry of several abundant RNA species into the RNAi pathway, thereby preventing RNAi from acting on its proper RNA substrates, i.e. the pericentromeric *dg* and *dh* transcripts (Buhler et al., 2008).

The competition model between these 2 distinct RNA-processing pathways raises an unanswered question about substrate recognition: How are pericentromeric transcripts recognized and targeted to each RNA-processing pathway? While the mechanism regulating pericentromeric transcript recognition is largely unknown, it has been suggested that a polyadenylation signal might influence the fate of a given RNA transcript (Thon, 2008). Interestingly, in a genetic screen performed to search for additional factors involved in heterochromatic silencing, we identified 2 polyadenylation-related factors whose gene deletions have opposite phenotypes in heterochromatic silencing. We found that *pab2Δ* mutant has an increase in heterochromatic silencing while deletion of *SPBC29A10.09c* causes loss of heterochromatic silencing. Previous studies revealed that Pab2 plays a major role in the maturation of snoRNAs. More specifically, Pab2 binds to the poly(A) tails of pre-snoRNAs and it promotes

poly(A) trimming of the pre-snoRNAs by recruiting the nuclear exosome (Lemay et al., 2010). These studies also show that Pab2 is physically associated with the nuclear exosome (Lemay et al., 2010). *SPBC29A10.09c* is a gene that is predicted to encode a CAF1 family deadenylase (www.pombase.org). We named this previously uncharacterized gene, *dfs1+* (<u>d</u>eadenylase <u>f</u>or <u>s</u>ilencing 1).

Based on the silencing phenotypes of these 2 mutants, we propose a model for how pericentromeric transcripts are recognized and targeted to the RNAi machinery or to the TRAMP-nuclear exosome pathway (Figure 1). In this model, polyadenylation of pericentromeric transcripts serves as a signal recognition for Pab2, which in turn targets these transcripts to the TRAMP-nuclear exosome pathway for degradation. In cells lacking Pab2, less pericentromeric transcripts are targeted to the TRAMP-nuclear exosome pathway. This allows more transcripts to be processed by the RNAi machinery, which leads to increased heterochromatic silencing. Additionally, this model predicts that deadenylation of pericentromeric transcripts by Dfs1 is required for processing of these transcripts by the RNAi machinery. Silencing is lost in *dfs1Δ* mutant presumably because less pericentromeric transcripts are processed by RNAi. Here we describe several experimental results that support this model. First, by measuring the levels of pericentromeric *dg* and *dh* transcripts in the single and double mutants of RNAi and Pab2, we demonstrate that Pab2 acts in parallel to the RNAi pathway in the processing of *dg* and *dh* transcripts. Second, we show that Pab2 is physically associated with pericentromeric *dg* and *dh*

transcripts. Finally, we demonstrate that polyadenylation of pericentromeric transcripts is inhibitory to heterochromatic silencing.

RESULTS AND DISCUSSION

Development of a weak heterochromatic silencing reporter strain for use in a genetic screen

In order to search for both silencing and anti-silencing factors in our genetic screen, we utilized a weak heterochromatic silencing reporter strain that was developed in a systematic study that analyzed the activities of *dg* and *dh* fragments (described in details in Chapter II). This reporter strain harbors a unique artificial construct inserted near the endogenous *ura4+* gene (Figure 2). This construct consists of the strong *adh1+* promoter that drives the transcription of a 200-bp fragment (named '*dhR5L4*') derived from the pericentromeric *dh* repeat. In the construct, a bidirectional terminator is inserted downstream of the *dhR5L4* fragment in order to ensure proper transcription termination of this fragment. This construct also contains *REIII*, an RNAi-independent sequence element from the mating-type locus, which has been shown to act synergistically with fragments derived from pericentromeric *dg* and *dh* repeats in inducing heterochromatic silencing (described in details in Chapter II).

Insertion of the entire construct downstream of the endogenous *ura4+* locus causes weak silencing of the *ura4+* gene as indicated by growth of a few

colonies on media containing 5-FOA, a drug that kills cells that express *ura4+*

gene (Figure 3). We crossed this reporter strain to the *Bioneer* deletion collection

that contains over 3000 strains (Kim et al., 2010), each with a deletion of a non-

essential gene (Figure 4). After sporulation, we selected progenies that contain

both the reporter construct and the gene deletion. Furthermore, we grew these

progenies on media containing 5-FOA to look for gene deletions that cause an

increase or a decrease of heterochromatic silencing of the *ura4+* reporter gene.

Identification of polyadenylation-related factors that are involved in

heterochromatic silencing

In this genetic screen, we identified 2 interesting hits that are related to

polyadenylation. The deletions of these polyadenylation-related genes have

opposite effects on heterochromatic silencing. Heterochromatic silencing is

increased in cells lacking Pab2, a poly(A)-binding protein, as indicated by the

increase of growth of the mutant on media containing 5-FOA (Figure 5). The

increase of silencing observed in *pab2Δ* cells corresponds to 17-fold reduction of

the *ura4+* transcript level as measured in an RT-qPCR assay (Figure 6).

Additionally, *pab2Δ* mutation leads to a 30-fold increase of H3K9Me2 level at the

ura4+ locus as measured in a chromatin immunoprecipitation (ChIP) experiment

(Figure 7). The increase of silencing in *pab2Δ* cells requires functional RNAi as

indicated by the complete loss of silencing when *dcr1+* is deleted (Figure 8). On

the other hand, our screen identified that *dfs1Δ* mutant can no longer grow on 5-

FOA media indicating that deletion of *dfs1+* (*SPBC29A10.09c*), a putative CAF1

deadenylase, disrupts heterochromatic silencing (Figure 5). The loss of silencing in *dfs1Δ* cells corresponds to a 3-fold increase of *ura4+* transcript level in the mutant when compared to its level in the wild-type strain (Figure 9).

A model for pericentromeric transcript recognition regulated by polyadenylation

The 2 polyadenylation-related hits that came out of our screen led to a model for how pericentromeric transcripts are targeted to the 2 competing RNA-processing pathways (Figure 1). In this model, Pab2 plays an anti-silencing role in targeting pericentromeric transcripts to the TRAMP-nuclear exosome pathway for degradation while Dfs1 is required to deadenylate these transcripts and directs them to the RNAi pathway. Pab2 has been shown to bind to the poly(A) tails of snoRNA transcripts and direct them to the TRAMP-nuclear exosome pathway for their 3'-end processing (Lemay et al., 2010). Since pericentromeric *dg* and *dh* transcripts are polyadenylated (Djupedal et al., 2005), we hypothesize that these polyadenylated transcripts are also bound by Pab2, which in turn targets them to the TRAMP-nuclear exosome pathway for degradation. Dfs1 is a putative deadenylase that belongs to the CAF1 family. The CAF1 family deadenylase has been shown to interact with Argonaute proteins in microRNA-mediated silencing in mammalian cells (Fabian et al., 2009; Piao, Zhang, Wu, & Belasco, 2010). We postulate that Dfs1 deadenylates pericentromeric transcripts and that the deadenylation targets the transcripts to the RNAi pathway for processing into siRNAs. The rest of this chapter describes several experiments conducted to test this model.

Pab2 and RNAi process pericentromeric transcripts in parallel pathways

Our model predicts that Pab2 acts in parallel to the RNAi pathway in

processing pericentromeric transcripts. To test this, we measured the levels of *dg*

and *dh* transcripts in the *pab2Δ dcr1Δ* double mutant and compared them to the

levels in the corresponding single mutants by RT-qPCR. Consistent with previous

reports (Volpe et al., 2002), we found that the levels of *dg* and *dh* transcripts are

increased in the *dcr1Δ* mutant by 167-fold and 12-fold, respectively (Figure 10).

The *pab2Δ* mutant also has increased levels of *dg* and *dh* transcripts (27-fold

and 4-fold, respectively), albeit lower than the fold differences observed in the

dcr1Δ mutant (Figure 10). Interestingly, the *pab2Δ dcr1Δ* double mutation further

increases the levels of these transcripts. We observed 228-fold increase of *dg*

transcript level and 22-fold increase of *dh* transcript level in the double mutant

(Figure 10). Consistent with the competition model, these results demonstrate

the role of Pab2 in the processing of *dg* and *dh* transcripts that is parallel to the

RNAi pathway.

Pab2 is physically associated with pericentromeric transcripts

Previous studies have demonstrated that pericentromeric transcripts are

polyadenylated although the poly(A) polymerase(s) responsible for it are

currently unknown. Our model predicts that Pab2 binds to the poly(A) tails of

pericentromeric transcripts. To test this, we performed an RNA

immunoprecipitation (RIP) experiment. In this experiment, we tagged Pab2

endogenously with an N-terminus 2XFLAG tag. Extracts from formaldehyde-crosslinked cells were subjected to anti-FLAG immunoprecipitation and the associated RNAs were quantified by RT-qPCR. Consistent with previous report (Lemay et al., 2010), we found that Pab2 is associated with a snoRNA but not with *srp7+* RNA, a non-coding cytoplasmic RNA (Figure 11). Interestingly, supportive of our model, we found that Pab2 is strongly associated with the pericentromeric *dg* transcripts (Figure 11).

<u>Addition of polypurine but not polythymine to the 3' end of a pericentromeric fragment inhibits heterochromatic silencing</u>

Our model predicts that Pab2 binds the poly(A) tails of pericentromeric transcripts and targets them to the nuclear exosome for degradation. This led to the hypothesis that polyadenylation of pericentromeric transcripts is inhibitory to heterochromatic silencing. To test this hypothesis, we added 30 adenine residues to the 3' end of the 200-bp *dhR5L4* fragment that is part of the reporter construct (Figure 12). Interestingly, we found that the *dhR5L4* fragment can no longer confer silencing of the *ura4+* reporter gene when the poly(A) tail is added to its 3' end (Figure 12). To test if addition of other nucleotides to the 3' end of *dhR5L4* fragment results in the same phenotype, we added 30 thymine or guanine residues to the 3' end of *dhR5L4*. Interestingly, while poly(G) tail addition to *dhR5L4* also abolishes silencing conferred by this fragment, poly(T) tail addition has no effect (Figure 12). Therefore, we conclude that adding polypurine tails to pericentromeric transcripts is inhibitory to heterochromatic silencing. This

finding is also consistent with our model.

CONCLUSIONS AND FUTURE DIRECTIONS

In this chapter, we describe a model for pericentromeric transcript recognition by 2 competing RNA-processing pathways: RNAi and TRAMP-nuclear exosome. This model was inspired by the 2 polyadenylation-related gene hits that came out of a genetic screen. In this model we propose that the poly(A) tails of pericentromeric transcripts serve as recognition signals for targeting to the TRAMP-nuclear exosome pathway. We propose that Pab2, a poly(A)-binding protein, binds these poly(A) tails and targets the transcripts for degradation by the nuclear exosome. We also hypothesize that Dfs1, a putative CAF1 deadenylase, is a silencing factor that deadenylates pericentromeric transcripts and directs them to the RNAi pathway for processing. More experiments are needed to test this hypothesis. For example, to confirm the deadenylase activity of Dfs1, we need to perform a Northern blot analysis to measure the length of poly(A) tails of pericentromeric transcripts in the wild-type and *dfs1Δ* mutant background. We also need to test if Dfs1 is physically associated with pericentromeric transcripts. Additionally, we still need to confirm that Pab2 acts in the TRAMP-nuclear exosome pathway. Measuring the pericentromeric transcript levels in the *pab2Δ cid14Δ* double mutant and comparing them to the levels in the corresponding single mutants should be informative.

MATERIALS AND METHODS

Strain Construction and Growth Conditions

Strains were constructed by lithium acetate transformation of plasmid DNA
containing 500 bp of targeting homology. Strains were grown in YS medium (5
g/liter Difco yeast extract + 250 mg/liter each of L-histidine, L-leucine, adenine,
uracil, and L-lysine and 3% glucose) at 30°C unless noted otherwise.

Genetic Screen

The screen was performed by crossing the *ura4+* reporter strain harboring
dhR5L4 fragment to the commercially available *Bioneer* deletion collection of *S.
pombe.* The Synthetic Genetic Array (SGA) screening method was employed as
described previously (Tong et al., 2001).

Silencing Assays

The strains were grown overnight to saturation and diluted to OD_{600} of 1 at the
highest dilution. Serial dilutions were performed with dilution factor of 5 and cells
were grown on non-selective and 5-FOA (2 grams/liter of 5-fluoroorotic acid)
containing media at 30°C for 2-3 days.

Chromatin Immunoprecipitation

The ChIP assays were performed as described previously (Rougemaille,
Shankar, Braun, Rowley, & Madhani, 2008) except for a few minor changes: 1.
Cells were lysed by bead beating 7 times for 1 min each with 2 min rests on ice.

2. Chromatin fraction was sonicated 20 times for 30 s each with 1-min rest in between cycles using a Bioruptor®. 3. Ab1220 (Abcam) antibody was used for H3K9Me2 ChIP. 4. Protein A Dynabeads were used instead of Sepharose beads.

Reverse Transcription quantitative Polymerase Chain Reaction (RT-qPCR)

RNA extraction was performed as described previously (Rougemaille et al., 2008). Five μg of total RNA was treated with 2 U of Turbo DNase I (Ambion) and used in each reverse transcription reaction with 2.5 U of AMV RT (Promega) and strand-specific primers or random 9-mer. The reverse transcription reaction was performed at 42°C for 2 hours. The cDNA samples were analyzed by quantitative PCR using SYBR Green (Invitrogen).

RNA Immunoprecipitation

250 ml cultures were grown to OD_{600} of 3-4. Cells were crosslinked by adding 0.25% of formaldehyde. Cell pellets were resuspended in RIPA buffer (1% NP-40, 0.5% sodium deoxycholate, 0.1% SDS, 150 mM NaCl, 50 mM Tris-HCl pH 8.0, 2 mM EDTA) supplemented with 1 mM PMSF and 40 U/ml of RNase inhibitor (New England Biolabs). Cell lysis was accomplished mechanically using a ball mill (Retsch). Frozen pellets were lysed for 5 cycles (3 minutes per cycle) at 15 Hz. 60 μl of 50% resuspension of Anti-Flag M2 agarose beads (Sigma) were added into each immunoprecipitation (IP) sample. All IP samples were incubated for 2 hours at 4°C with constant nutation. The IP beads were washed 2 times with low salt buffer (150 mM NaCl, 10 mM Tris-HCl pH 7.5, 0.5% Triton X-

100) and 3 times with high salt buffer (1 M NaCl, 10 mM Tris-HCl pH 7.5, 0.5%

Triton X-100). Each wash was for 10 minutes. After washing, crosslinks were

reversed by incubation at 70°C for 45 minutes in reverse buffer (10 mM Tris-HCl

pH 6.8, 5 mM EDTA, 10 mM DTT, 1% SDS) and subjected to treatment with 40

μg of proteinase K. RNA extraction was performed by adding sodium acetate

(final concentration 0.3 M) and 1X volume of phenol-chloroform followed by

ethanol precipitation. DNase treatment and RT-qPCR were performed as

described above.

Primers used in quantitative PCR following ChIP, RT and RIP experiments

For *ura4+* locus: P581 (5'-CAGCAATATCGTACTCCTGAA-3') and P582 (5'-

ATGCTGAGAAAGTCTTTGCTG-3')

For *act1+* locus: P638 (5'-AACCCTCAGCTTTGGGTCTT-3') and P639 (5'-

TTTGCATACGATCGGCAATA-3')

For *dg*: P1044 (5'-CCATCACCACTTTCATCTCC-3') and P1045 (5'-

CAGGATACCTAGACGCACAA)

For *dh:* P62 (5'- TTTAAAGCTTCACTACCATCGAAA-3') and P63 (5'-

TGCCAACAGTTTTTCCAACTT-3')

For *snR30:* P1174 (5'-TTCGACTGCAGGTTGAGAGTT-3') and P1176 (5'-

TGCAAGGATCCAGAGATCATG-3')

For *srp7+*: P2257 (5'- ATGGCTTGGTCGAAGTGTTT-3') and P2258 (5'-

AAGACCCGGTAGTGATGTGC-3'

FIGURE LEGENDS

Figure 1: A model for pericentromeric transcript recognition by RNAi and TRAMP-nuclear exosome pathways.

Figure 2: Schematic of the heterochromatic silencing reporter construct used in the genetic screen. The construct consists of the *adh1+* promoter driving transcription of a 200-bp *dhR5L4* fragment, a bidirectional terminator ('term'), the *REIII* element, B-boxes boundary element ('B') and a resistant drug marker ('natR'). The entire construct was inserted downstream of the endogenous *ura4+* gene.

Figure 3: The *dhR5L4* fragment induces weak silencing of the reporter *ura4+* gene when inserted in the reporter construct. Silencing assays of the reporter strain used in the genetic screen. Cells were plated on non-selective YS media (N/S) and YS media with 5-FOA (5-FOA).

Figure 4: Schematic of the SGA screen. The screen was performed by crossing the reporter strain described in Figure 2 to the *S. pombe Bioneer* deletion collection. After sporulation, progenies containing the reporter gene and the gene deletion were selected by plating on media containing appropriate drug markers. The effect of each gene deletion on heterochromatic silencing was assayed by scoring the growth of each cross progeny on media containing 5-FOA.

Figure 5: *pab2Δ* mutant has increased heterochromatic silencing while *dfs1Δ* mutant lost heterochromatic silencing. Silencing assays of *pab2Δ* and *dfs1Δ* mutants. Cells were plated on non-selective YS media (N/S) and YS media with 5-FOA (5-FOA).

Figure 6: *pab2Δ* mutation decreases *ura4+* transcript level. RT-qPCR analysis of *ura4+* transcript levels (normalized to *act1+* transcript levels) in the wild-type and *pab2Δ* strains. Shown are mean values relative to the wt strain ± SD of three parallel RT reactions of one representative experiment.

Figure 7: *pab2Δ* mutant has increased level of H3K9Me at the *ura4+* locus. ChIP analysis of H3K9Me2 levels at *ura4+* locus (normalized to H3K9Me2 levels at *act1+* locus) in the wild-type and *pab2Δ* strains. Shown are mean values relative to the wt strain ± SD of three parallel IP samples of one representative experiment.

Figure 8: Heterochromatic silencing in *pab2Δ* mutant requires functional RNAi. Silencing assays of *pab2Δ* single mutant and *pab2Δ dcr1Δ* double mutant. Cells were plated on non-selective YS media (N/S) and YS media with 5-FOA (5-FOA).

Figure 9: *dfs1Δ* mutation increases *ura4+* transcript level. RT-qPCR analysis of *ura4+* transcript levels (normalized to *act1+* transcript levels) in the wild-type and

dfs1Δ strains. Shown are mean values relative to the wt strain ± SD of three parallel RT reactions of one representative experiment.

Figure 10: Pab2 processes pericentromeric transcripts in parallel to the RNAi pathway. RT-qPCR analysis of *dg* and *dh* transcript levels (normalized to *act1+* transcript levels) in the wild-type strain and in the strains with single and double combinations of *dcr1Δ* and *pab2Δ* mutations. Shown are mean values relative to the wt strain ± SD of three parallel RT reactions of one representative experiment.

Figure 11: Pab2 is physically associated with the pericentromeric transcripts. RIP experiments measuring the enrichment of 2XFLAG-Pab2 at *dg, srp7+* transcripts and *snR30* snoRNA. Shown are mean values relative to the untagged strain ± SD of three parallel IP samples of one representative experiment.

Figure 12: Addition of polypurine to the 3' end of pericentromeric transcripts is inhibitory to heterochromatic silencing. Silencing assays of reporter strains with the original *dhR5L4* fragment and the modified versions of *dhR5L4* fragment with addition of polyadenine, polyguanine or polythymine to its 3' end. Cells were plated on non-selective YS media (N/S) and YS media with 5-FOA (5-FOA).

REFERENCES

Bayne, E. H., White, S. A., Kagansky, A., Bijos, D. A., Sanchez-Pulido, L., Hoe, K. L., . . . Allshire, R. C. (2010). Stc1: a critical link between RNAi and chromatin modification required for heterochromatin integrity. *Cell, 140*(5), 666-677. doi: S0092-8674(10)00073-5 [pii]
10.1016/j.cell.2010.01.038

Buhler, M., Haas, W., Gygi, S. P., & Moazed, D. (2007). RNAi-dependent and - independent RNA turnover mechanisms contribute to heterochromatic gene silencing. *Cell, 129*(4), 707-721. doi: S0092-8674(07)00454-0 [pii]
10.1016/j.cell.2007.03.038

Buhler, M., Spies, N., Bartel, D. P., & Moazed, D. (2008). TRAMP-mediated RNA surveillance prevents spurious entry of RNAs into the Schizosaccharomyces pombe siRNA pathway. *Nat Struct Mol Biol, 15*(10), 1015-1023. doi: nsmb.1481 [pii]
10.1038/nsmb.1481

Djupedal, I., Portoso, M., Spahr, H., Bonilla, C., Gustafsson, C. M., Allshire, R. C., & Ekwall, K. (2005). RNA Pol II subunit Rpb7 promotes centromeric transcription and RNAi-directed chromatin silencing. *Genes Dev, 19*(19), 2301-2306. doi: 19/19/2301 [pii]
10.1101/gad.344205

Fabian, M. R., Mathonnet, G., Sundermeier, T., Mathys, H., Zipprich, J. T., Svitkin, Y. V., . . . Sonenberg, N. (2009). Mammalian miRNA RISC recruits CAF1 and PABP to affect PABP-dependent deadenylation. [Research Support, N.I.H., Extramural
Research Support, Non-U.S. Gov't]. *Mol Cell, 35*(6), 868-880. doi: 10.1016/j.molcel.2009.08.004

Houseley, J., LaCava, J., & Tollervey, D. (2006). RNA-quality control by the exosome. [Review]. *Nat Rev Mol Cell Biol, 7*(7), 529-539. doi: 10.1038/nrm1964

Kato, H., Goto, D. B., Martienssen, R. A., Urano, T., Furukawa, K., & Murakami, Y. (2005). RNA polymerase II is required for RNAi-dependent heterochromatin assembly. *Science, 309*(5733), 467-469. doi: 1114955 [pii]
10.1126/science.1114955

Kim, D. U., Hayles, J., Kim, D., Wood, V., Park, H. O., Won, M., . . . Hoe, K. L. (2010). Analysis of a genome-wide set of gene deletions in the fission yeast Schizosaccharomyces pombe. *Nat Biotechnol, 28*(6), 617-623. doi: nbt.1628 [pii]
10.1038/nbt.1628

LaCava, J., Houseley, J., Saveanu, C., Petfalski, E., Thompson, E., Jacquier, A., & Tollervey, D. (2005). RNA degradation by the exosome is promoted by a nuclear polyadenylation complex. [Research Support, Non-U.S. Gov't]. *Cell, 121*(5), 713-724. doi: 10.1016/j.cell.2005.04.029

Lejeune, E., & Allshire, R. C. (2011). Common ground: small RNA programming and chromatin modifications. *Curr Opin Cell Biol, 23*(3), 258-265. doi: S0955-0674(11)00022-6 [pii]

10.1016/j.ceb.2011.03.005

Lemay, J. F., D'Amours, A., Lemieux, C., Lackner, D. H., St-Sauveur, V. G., Bahler, J., & Bachand, F. (2010). The nuclear poly(A)-binding protein interacts with the exosome to promote synthesis of noncoding small nucleolar RNAs. [Research Support, Non-U.S. Gov't]. *Mol Cell, 37*(1), 34-45. doi: 10.1016/j.molcel.2009.12.019

Nakayama, J., Rice, J. C., Strahl, B. D., Allis, C. D., & Grewal, S. I. (2001). Role of histone H3 lysine 9 methylation in epigenetic control of heterochromatin assembly. *Science, 292*(5514), 110-113.

Piao, X., Zhang, X., Wu, L., & Belasco, J. G. (2010). CCR4-NOT deadenylates mRNA associated with RNA-induced silencing complexes in human cells. [Research Support, N.I.H., Extramural

Research Support, Non-U.S. Gov't]. *Mol Cell Biol, 30*(6), 1486-1494. doi: 10.1128/MCB.01481-09

Rougemaille, M., Shankar, S., Braun, S., Rowley, M., & Madhani, H. D. (2008). Ers1, a rapidly diverging protein essential for RNA interference-dependent heterochromatic silencing in Schizosaccharomyces pombe. *J Biol Chem, 283*(38), 25770-25773.

Thon, G. (2008). Competing to destroy: a fight between two RNA-degradation systems. [Comment

News]. *Nat Struct Mol Biol, 15*(10), 1001-1002. doi: 10.1038/nsmb1008-1001

Tong, A. H., Evangelista, M., Parsons, A. B., Xu, H., Bader, G. D., Page, N., . . . Boone, C. (2001). Systematic genetic analysis with ordered arrays of yeast deletion mutants. [Research Support, Non-U.S. Gov't]. *Science, 294*(5550), 2364-2368. doi: 10.1126/science.1065810

Vanacova, S., Wolf, J., Martin, G., Blank, D., Dettwiler, S., Friedlein, A., . . . Keller, W. (2005). A new yeast poly(A) polymerase complex involved in RNA quality control. [Research Support, Non-U.S. Gov't]. *PLoS Biol, 3*(6), e189. doi: 10.1371/journal.pbio.0030189

Verdel, A., Jia, S., Gerber, S., Sugiyama, T., Gygi, S., Grewal, S. I., & Moazed, D. (2004). RNAi-mediated targeting of heterochromatin by the RITS complex. *Science, 303*(5658), 672-676. doi: 10.1126/science.1093686

1093686 [pii]

Verdel, A., Vavasseur, A., Le Gorrec, M., & Touat-Todeschini, L. (2009). Common themes in siRNA-mediated epigenetic silencing pathways. *Int J Dev Biol, 53*(2-3), 245-257. doi: 082691av [pii]

10.1387/ijdb.082691av

Volpe, T. A., Kidner, C., Hall, I. M., Teng, G., Grewal, S. I., & Martienssen, R. A. (2002). Regulation of heterochromatic silencing and histone H3 lysine-9 methylation by RNAi. *Science, 297*(5588), 1833-1837. doi: 10.1126/science.1074973

1074973 [pii]

Wyers, F., Rougemaille, M., Badis, G., Rousselle, J. C., Dufour, M. E., Boulay, J., . . . Jacquier, A. (2005). Cryptic pol II transcripts are degraded by a nuclear quality control pathway involving a new poly(A) polymerase. [Research Support, Non-U.S. Gov't]. *Cell, 121*(5), 725-737. doi: 10.1016/j.cell.2005.04.030

Zhang, K., Mosch, K., Fischle, W., & Grewal, S. I. (2008). Roles of the Clr4 methyltransferase complex in nucleation, spreading and maintenance of heterochromatin. *Nat Struct Mol Biol, 15*(4), 381-388. doi: nsmb.1406 [pii] 10.1038/nsmb.1406

Figure 1

Figure 2

Figure 3

N/S   5-FOA

REIII

REIII+dhR5L4

Figure 4

Figure 5

	N/S	5-FOA
REIII		
REIII+dhR5L4		
pab2Δ		
pab2Δ		
pab2Δ		
dfs1Δ		

Figure 6

RT-qPCR chart showing ura4+/act1+ levels for wt and pab2Δ strains.

Figure 7

H3K9Me2 ChIP
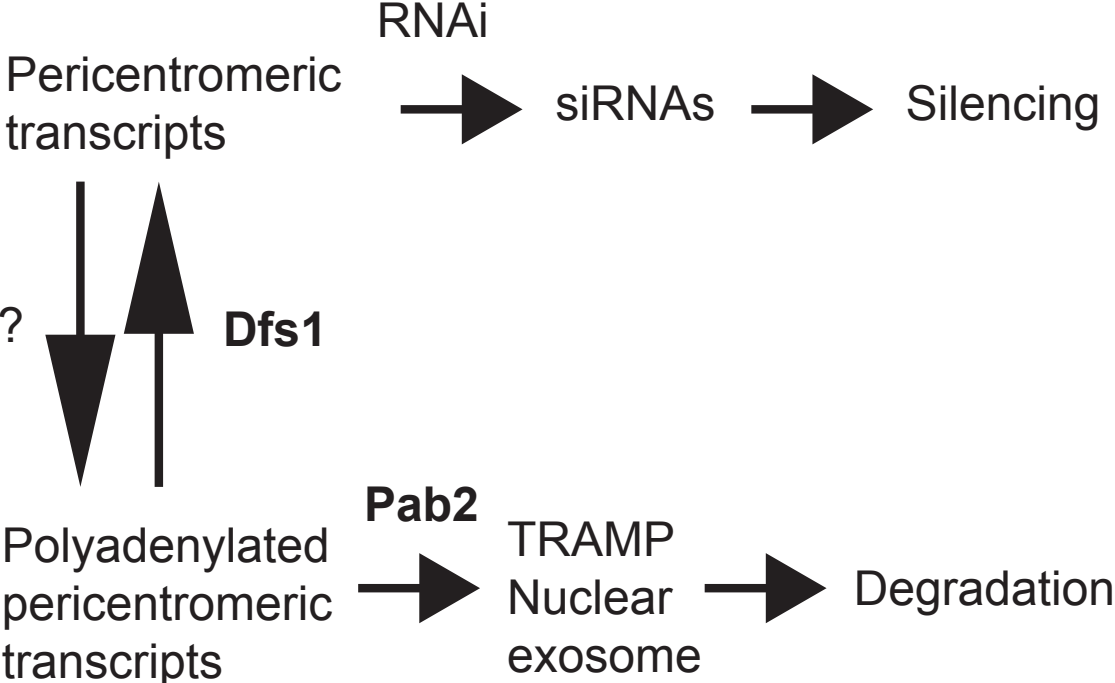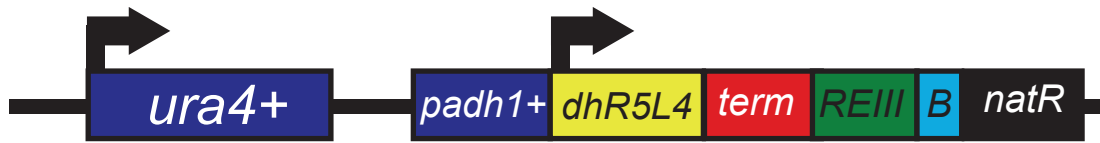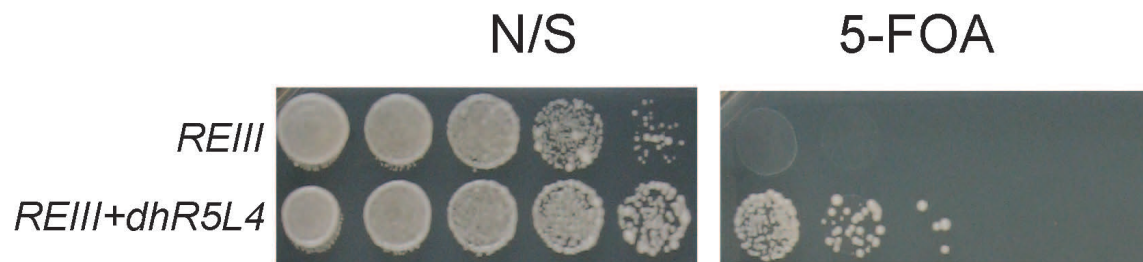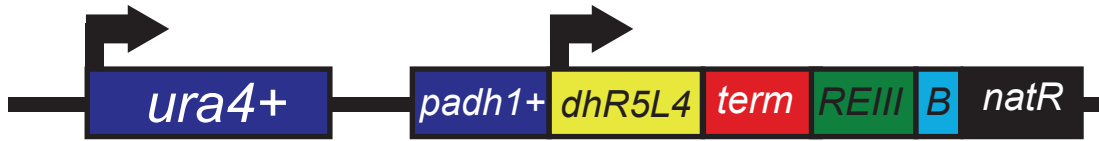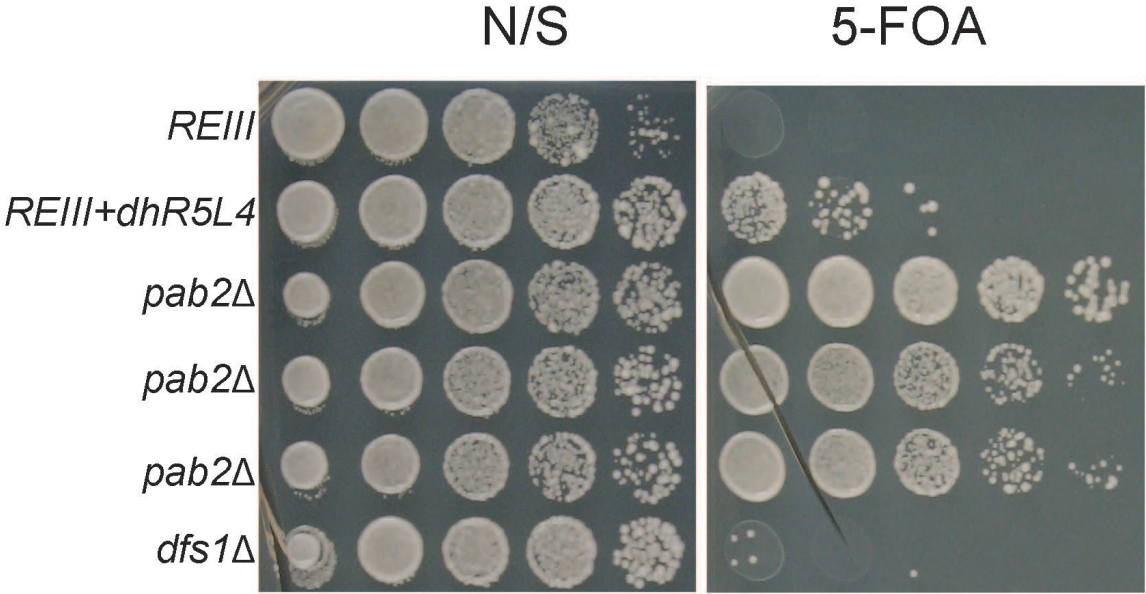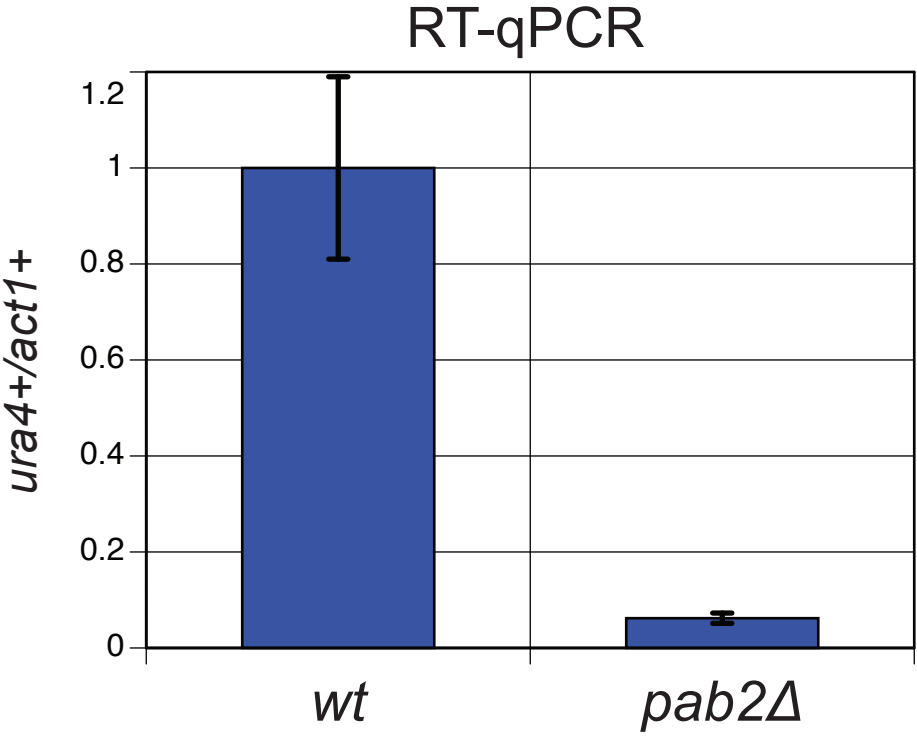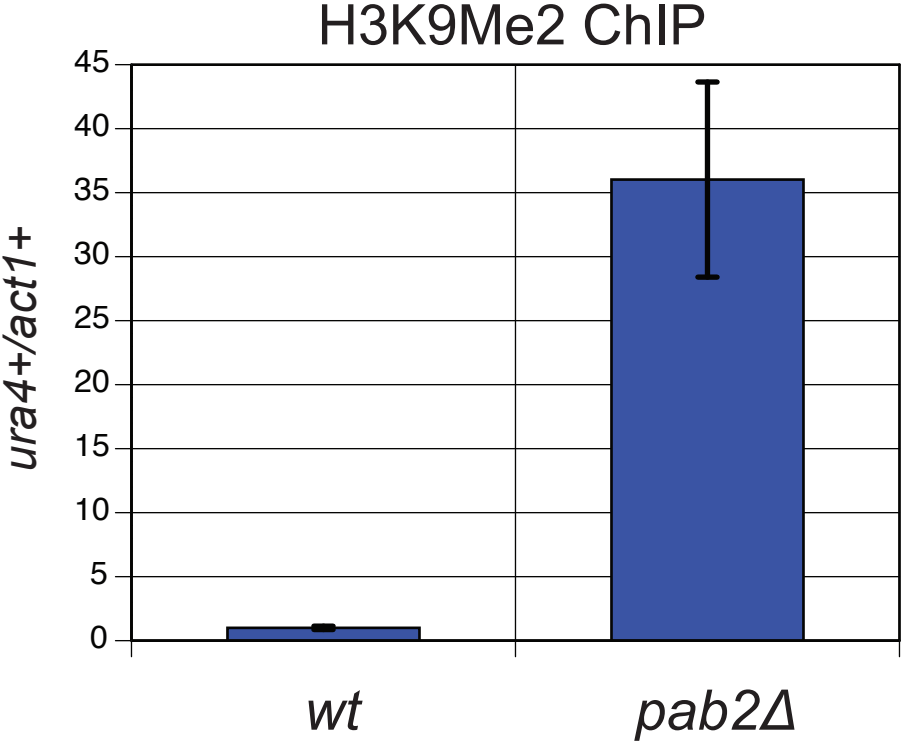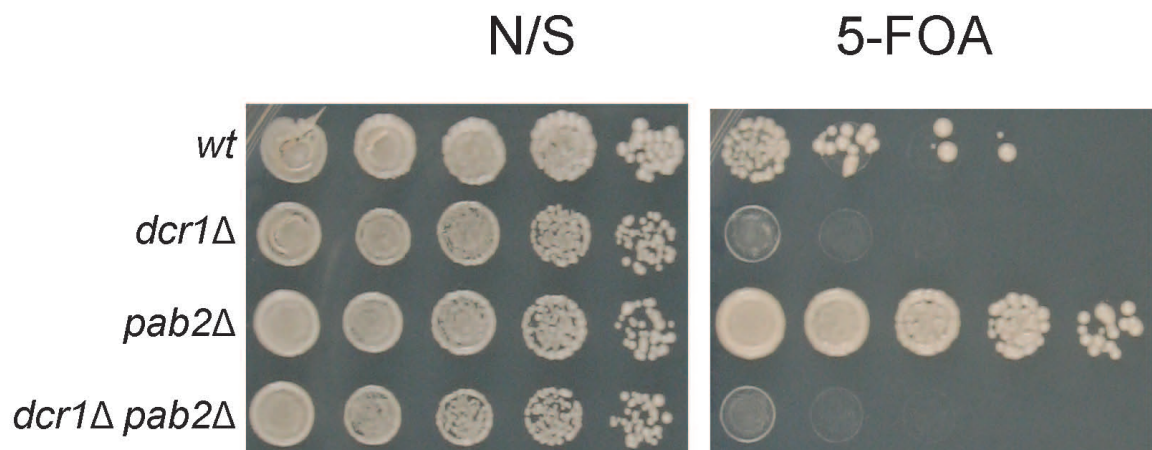
Figure 8
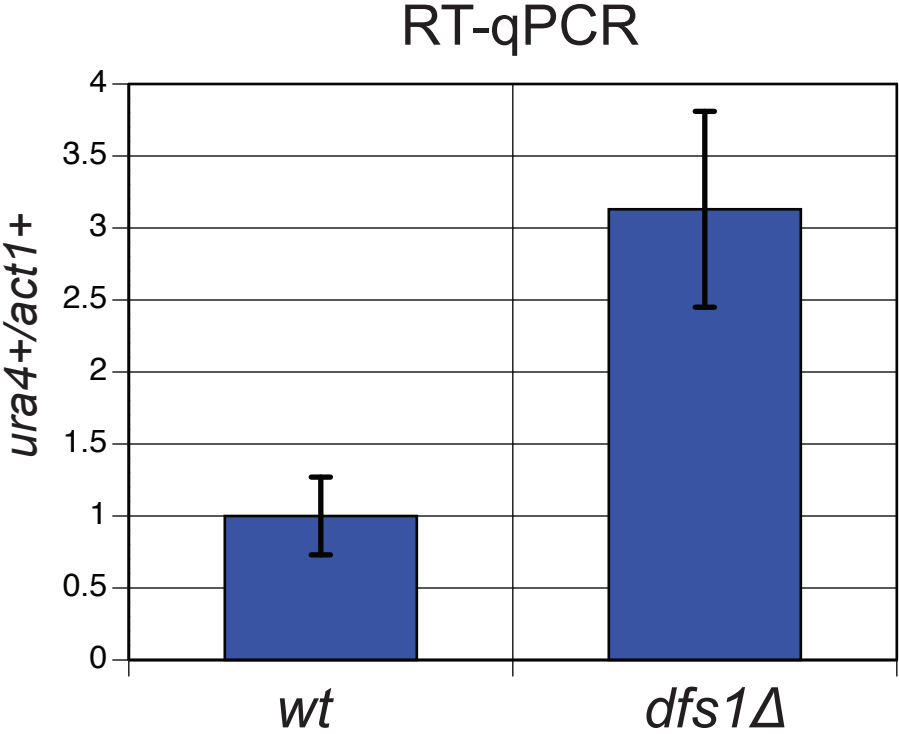
Figure 9

RT-qPCR

Figure 10

RT-qPCR
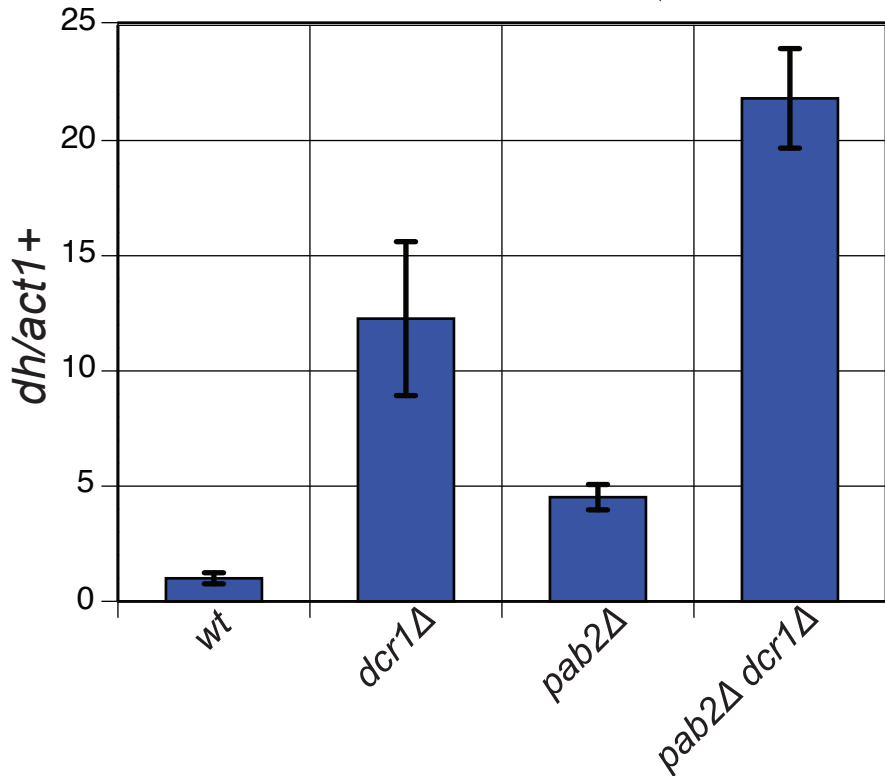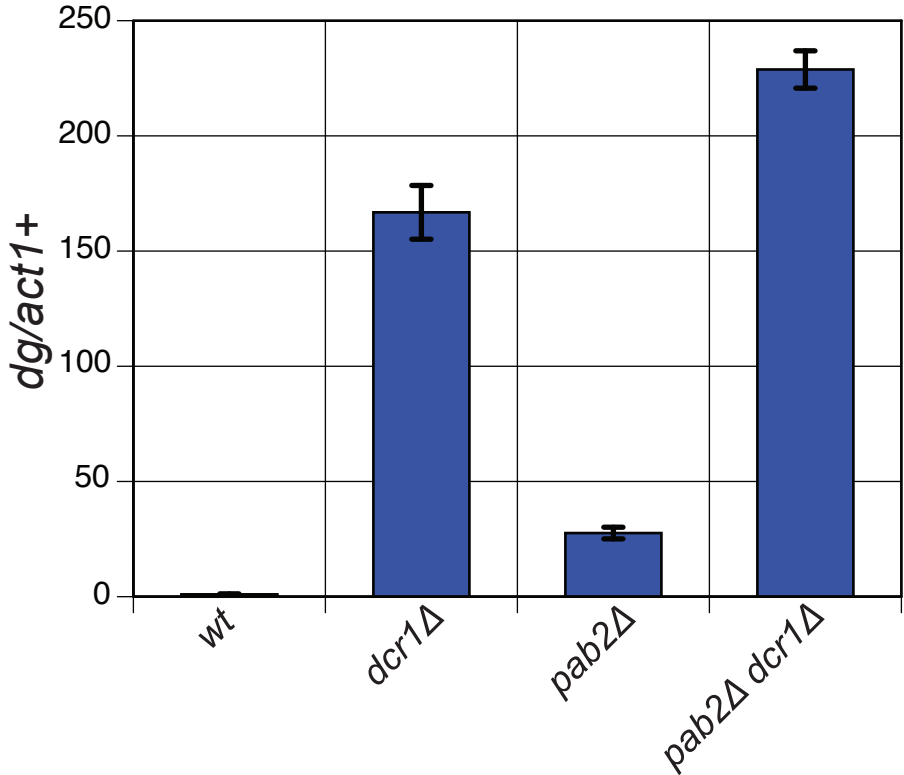
Figure 11
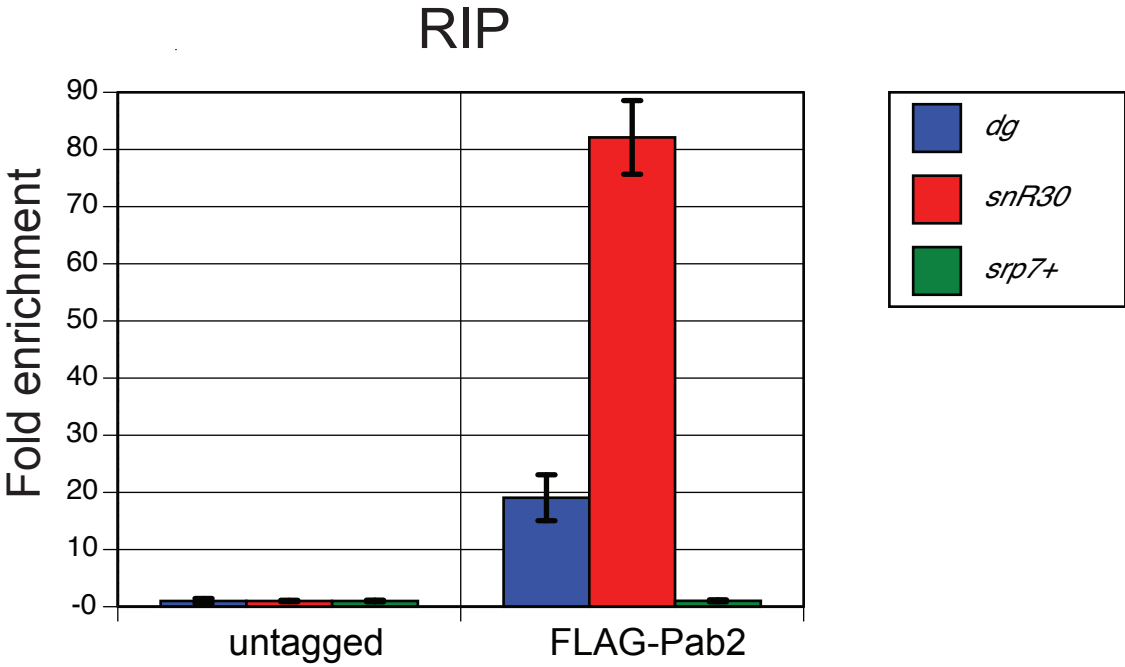
Figure 12
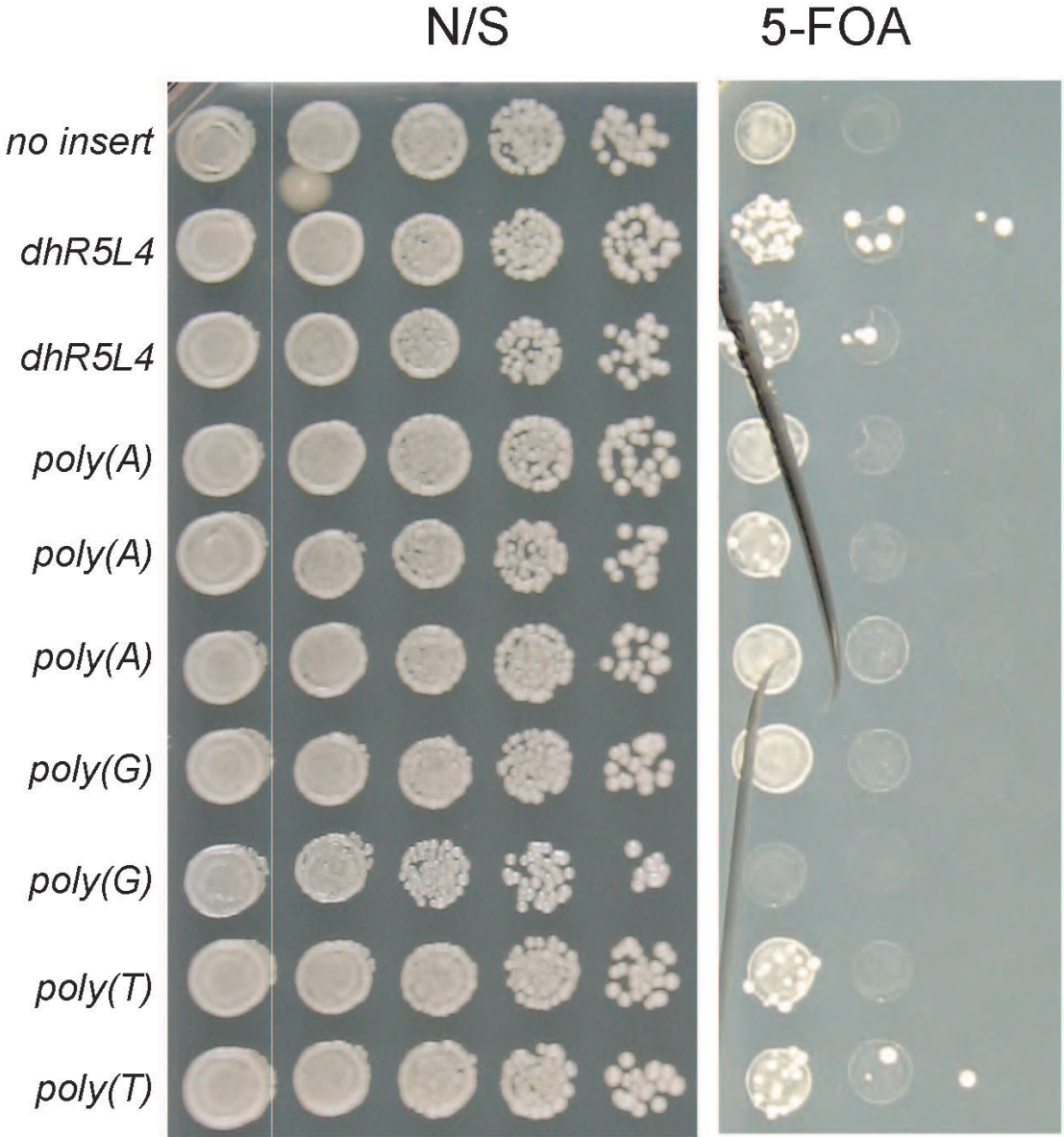
Table 1. List of *S. pombe* strains used in this study.

Strain name	Genotype
PM1129	PM06, *ura4::padh1+*-ter-*REIII*-Bboxes-*natMX*
PM1130	PM06, *ura4::padh1+-dhR5L4*-ter-*REIII*-Bboxes-*natMX*
PM2090	PM1130, *pab2Δ::hygMX*
PM2091	PM1130, *dfs1Δ:kanMX*
PM2092	PM1130, *dcr1Δ:kanMX*
PM2093	PM1130, *pab2Δ:hygMX dcr1Δ:kanMX*
PM2071/PM1132	PM06, *ura4::padh1+-3XdhR5L4*-ter-*REIII*-Bboxes-*natMX*
PM2094	PM1132 , *dfs1Δ:kanMX*
PM06	*S. pombe* wild type strain 972 *M(h-)*
PM251[#]/PM1205	*P(h+), ura4-DS/E, ade6-210, leu1-32, imr1L(NcoI)::ura4+, otr1R(SphI)::ade6+*
PM2095	PM251, *kanMX-2XFLAG::pab2+*
PM2096	PM06, *ura4::padh1+-dhR5L4-30A*-ter-*REIII*-Bboxes-*natMX*
PM2097	PM06, *ura4::padh1+-dhR5L4-30T*-ter-*REIII*-Bboxes-*natMX*
PM2098	PM06, *ura4::padh1+-dhR5L4-30G*-ter-*REIII*-Bboxes-*natMX*

[#] From Karl Ekwall

'ter' = terminator (for sequence information see table 2)

'B-boxes' = synthetic boundary element (for sequence information see table 2)

Table 2. List of chromosome coordinates of different fragments used in this study

Fragment	Chromosome	Chromosome coordinate
padh1+	3	1590559..1591323
terminator	1	2274985..2275583
B-boxes	N/A	Synthetic boundary element*
REIII	2	Mating type locus (13409..15415)
dhR5L4	1	Reverse complement(3787037..3787236)

*B-boxes sequence:
TGTTCGTAGCAACGTAATAATCGAAAGTAGCAGGACTCGAACCATTCGCAAA
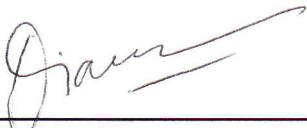TCGAACCGATCAAAAGTAGAACC

Table 3. List of plasmids used in this study

BHM#	Former name	Type of reporter	Fragment inserted	Used in PM Strains
1932	pDM06	*ura4::padh1+-ter-REIII-*Bboxes-*natMX*	None	PM1129
1954	pDM47	*ura4::padh1+-ter-REIII-*Bboxes-*natMX*	*dhR5L4*	PM1130
1959	pDM138	*ura4::padh1+-ter-REIII-*Bboxes-*natMX*	*3XdhR5L4*	PM2071/ PM1132
1970	pDM164	*kanMX 2XFLAG::pab2+*	N/A	PM2095
1971	pDM169	*ura4::padh1+-ter-REIII-*Bboxes-*natMX*	*dhR5L4+30A*	PM2096
1972	pDM174	*ura4::padh1+-ter-REIII-*Bboxes-*natMX*	*dhR5L4+30G*	PM2098
1973	pDM175	*ura4::padh1+-ter-REIII-*Bboxes-*natMX*	*dhR5L4+30T*	PM2097

Publishing Agreement

It is the policy of the University to encourage the distribution of all theses, dissertations, and manuscripts. Copies of all UCSF theses, dissertations, and manuscripts will be routed to the library via the Graduate Division. The library will make all theses, dissertations, and manuscripts accessible to the public and will preserve these to the best of their abilities, in perpetuity.

I hereby grant permission to the Graduate Division of the University of California, San Francisco to release copies of my thesis, dissertation, or manuscript to the Campus Library to provide access and preservation, in whole or in part, in perpetuity.

_____   12/20/2012
Author Signature   Date